**Structural and Functional Neuroimaging of Individuals with Prenatal Exposure to Addictive Substances**

A Dissertation
Presented to
The Academic Faculty

By

Priya Santhanam

In Partial Fulfillment
of the Requirements for the Degree
Doctor of Philosophy in
Biomedical Engineering

Georgia Institute of Technology

December 2009

**Structural and Functional Neuroimaging of Individuals with Prenatal Exposure to Addictive Substances**

Approved by:

Dr. Xiaoping Hu, Advisor
Department of Biomedical Engineering
*Georgia Institute of Technology*

Dr. John Oshinski
Department of Biomedical Engineering
*Georgia Institute of Technology*

Dr. Shella Keilholz
Department of Biomedical Engineering
*Georgia Institute of Technology*

Dr. Claire Coles
Department of Psychiatry and Behavioral
Sciences
*Emory University*

Dr. Stephan Hamann
Department of Psychology
*Emory University*

Date Approved: October 15, 2009

To my father, for who am I but his daughter

## ACKNOWLEDGEMENTS

There are several people who made this thesis work possible. First and foremost, I would like to thank my advisor for the past five years, Xiaoping Hu, for all his assistance and support. He took a chance on a non-engineer, and gave me the opportunity to choose among projects in the lab, even ones that were more technically oriented. Thanks in great part to the collaborative environment he has nurtured in the lab, I have also had the opportunity to work with several fellow students and post-docs. These are the people who really formed my expertise in the field, and this work would not have been possible without them.

I owe a great deal of my success to Zhihao Li, who taught me practically everything I know about image analysis. He has always been present to guide me and give advice, and has also been a great collaborator, giving extremely helpful feedback and lending a hand to my writing. Though English is not his first language, he has really taught me a lot about how to be a better scientific writer, and for that I am so very grateful. Additionally, I must thank Longchuan Li, Xiangchuan Chen, and Andy James for all their help and feedback through especially the last two years of my thesis work. In particular, Longchuan taught me DTI techniques, Xiangchuan provided study design and analysis tips, and Andy was helpful with proofreading. Finally, I would be remiss not to mention the old triumvirate (Scott Peltier, Steve LaConte, and Keith Heberlein) for their mentoring in my first years in the lab. Scott in particular introduced me to conducting imaging studies and helped me take the lead on the PAE study when I first joined the lab. Steve provided very helpful feedback for my first abstracts and presentations for the imaging community and ensured that I had "all the answers." Keith was a great resource for that most challenging MR course and for acclimation to the ins and outs of the BITC.

On a personal level, I have had an excellent support system during my time in graduate school. Firstly, my parents have always been very loving and supportive of my decision to pursue a PhD, just as they have served as role models in all of my academic pursuits. My brother Parthi (the scientist trapped in an engineer's body) has also been very supportive and, though younger than me, taught me a great deal about how to think critically and how to be a better scientist overall. My fellow-student support group (Swathi, Rekha, Abbey, and Laveeta) has balanced out the stress of grad school with lots of fun and great friendship that will surely outlast this common experience. Another friend whose bond has grown stronger with me through our shared grad school experience is Stephanie. She has lent a non-judgmental, ever-present ear to me, and made even the hardest times in grad school more bearable with her support. Finally, I thank Jason for his unwavering support of me day-to-day through this long journey. He has taught me that, no matter what may come my way personally or professionally, "everything is going to be ok."

# TABLE OF CONTENTS

# LIST OF TABLES

## LIST OF FIGURES

x

# LIST OF ABBREVIATIONS

AD          axial diffusivity

ANOVA       analysis of variance

BOLD        blood oxygen level dependent

CC          corpus callosum

DARTEL      diffeomorphic anatomical registration through exponentiated lie algebra

DMN         default mode network

DTI         diffusion tensor imaging

EPI         echo planar imaging

FA          fractional anisotropy

FAS         fetal alcohol syndrome

FASD        fetal alcohol spectrum disorder

fMRI        functional magnetic resonance imaging

FOV         field of view

FWHM        full-width half maximum

GSR         global signal regression

HIPS        horizontal interparietal sulcus

IRF         impulse response function

M1          primary motor cortex

MD          mean diffusivity

MPFC        medial prefrontal cortex

MPRAGE      magnetization prepared rapid gradient echo

MTL         medial temporal lobe

PAE         prenatal alcohol exposure

| PCC | posterior cingulate cortex |
| --- | --- |
| PCE | prenatal cocaine exposure |
| RD | radial diffusivity |
| ROI | region of interest |
| S1 | primary sensory cortex |
| SES | socio-economic status |
| SMA | supplementary motor area |
| SMG | supramarginal gyrus |
| TBSS | tract-based spatial statistics |
| TE | echo time |
| TFCE | threshold-free cluster enhancement |
| TI | inversion time |
| TR | repetition time |
| VBM | voxel based morphometry |
| VMPFC | ventral medial prefrontal cortex |

# SUMMARY

Although the hazards of prenatal exposure to addictive substances have been documented for decades, it continues to be a prevalent social and health concern today. Alcohol and cocaine are two commonly abused substances during pregnancy, often leading to behavioral and cognitive disorders in exposed children. At present, the relationship between teratogenic effects of prenatal alcohol exposure (PAE) and prenatal cocaine exposure (PCE) on the brain and observed behavioral outcomes is still unclear. A primary reason for this incomplete understanding is the lack of information regarding neuronal functioning in these populations. Functional MRI, which measures real-time brain activation in response to certain stimuli, can be utilized to bridge the gap between known structural damage and observed behavioral outcomes.

This thesis aims to examine structural and functional alterations in PAE and PCE populations as compared to unexposed, socio-economic status-matched populations. As the PAE population is highly affected by structural dysmorphology, the applicability of a newly developed diffeomorphic image registration method to this population is examined. Additionally, task-positive and task-negative functional connectivity and activity are investigated in the PAE population, and related to underlying structural alterations. Neural correlates of global arousal and emotional regulation are investigated in the PCE population, as these behavioral outcomes are most notable. Similarly, functional connectivity and activation in task-positive and task-negative networks, as well as correlated structural measures, are examined in the PCE population.

The diffeomorphic image registration algorithm was found to improve both structural and functional image registration for the PAE population. In the examination of specific deficits in

arithmetic processing, poorer performance in the PAE group was attributed to a multi-level effect produced by altered structural and functional connectivity and functional activity in calculation and default mode networks. Baseline arousal levels were found to be higher in adolescents with PCE as compared to healthy controls (by altered default mode network functioning); emotional regulation also appeared to be affected in the PCE group by a prefrontal-amygdala structural and functional disconnect.

The findings of this thesis give insights into the relationship between task-positive and task-negative duality and cognitive impairment, and contribute to a more comprehensive understanding of the spectrum of clinical disorders caused by prenatal exposure to alcohol and cocaine.

**CHAPTER 1**

**Introduction**

The hazards of prenatal exposure to addictive substances have been documented for decades, yet it continues to be a prevalent social and health concern today. Alcohol and cocaine are two commonly abused substances during pregnancy, leading often to behavioral and cognitive disorders in exposed children. Prenatal alcohol exposure (PAE) and prenatal cocaine exposure (PCE) cause specific neurocognitive and behavioral deficits that persist into adolescence and adulthood. Identification of specific structural and functional regions affected by prenatal exposure contributes to a better understanding of underlying mechanisms. Currently the relationship between teratogenic effects of PAE and PCE on the brain and observed behavioral outcomes is still unclear. A primary reason for this incomplete understanding is the lack of information regarding functional brain ability in the populations. Functional MRI, which measures real-time brain activation in response to certain stimuli, can be utilized to bridge the gap between structural and behavioral data in PAE individuals by elucidating patterns of neuronal activation during specific task-positive and task-negative states.

This thesis aims to examine structural and functional alterations in prenatal alcohol exposed and prenatal cocaine exposed populations. As the PAE population is highly affected by structural dysmorphology, spatial normalization of images from this population has proved challenging. In the present thesis, the applicability of a newly developed diffeomorphic image registration method is examined. Additionally, task-positive and task-negative functional connectivity and activity are investigated in the PAE population, as well as correlation of functional deficits with underlying structural alterations. Neural correlates of

1

global arousal and emotional regulation are investigated in the PCE population, as these behavioral outcomes are most notable. Similarly, functional connectivity and activation in task-positive and task-negative networks, as well as related structural measures, are examined in the PCE population. With the accomplishment of these aims, a more comprehensive understanding of the spectrum of clinical disorders caused by prenatal exposure to alcohol and cocaine can be formed.

**Structural and Functional Neuroimaging of Adults with Prenatal Alcohol Exposure**

**CHAPTER 2**

**Improved Inter-Subject Structural and Functional Registration Using DARTEL in**

**Individuals Prenatally Exposed to Alcohol**

**2.1 Background**

2.1.1   Prenatal Alcohol Exposure and Structural Brain Damage

The most severe form of prenatal alcohol exposure (PAE) results in a disorder known as fetal alcohol syndrome (FAS). Microcephaly, or reduced head/brain size, is one of the primary indicators used in clinical diagnosis of FAS (Smith and Eckardt, 1991). Structural abnormalities are also observed in specific cortical and subcortical regions as a result of PAE. One of the most highly affected areas of the brain in PAE individuals is the corpus callosum (CC). Gross anatomical and imaging studies have revealed that the CC can experience thinning or shrinkage upon alcohol exposure (Riley and McGee, 2005; Roebuck et al., 1998; Spadoni et al., 2007), and even agenesis in extreme cases (Archibald et al., 2001). Studies of CC morphology have revealed high variability in size and location of the structure (Bookstein et al., 2001) as well as spatial shifts in the inferior and anterior directions within the brain (Sowell et al., 2001). Bookstein, et al. has shown that variability in CC size and location can even be used as a classifier of PAE (2002). DTI studies have also reported CC alterations, including decreased fractional anisotropy and increased mean diffusivity, particularly in the posterior CC regions (Li et al., 2009; Ma et al., 2005; Wozniak et al., 2009).

### 2.1.2 <u>Current Image Registration Methods</u>

The vast majority of studies on structural abnormality in PAE populations have utilized high-resolution magnetic resonance imaging (MRI) in their analysis. Three popular approaches for examining exposure effects on macro- and microstructure are region of interest (ROI)-based volumetric analysis, voxel-based morphometry (VBM), and diffusion tensor imaging (DTI). Volumetric analyses involves slice-by-slice anatomical delineation of specific brain regions, VBM is performed by segmentation and voxel-wise comparison of homologous regions, and DTI analysis specifically assesses white matter integrity. While ROI-based analysis can be done in native space, it requires neuroanatomical expertise and is comparatively time-consuming; more common are the VBM and DTI approaches, which require image co-registration. In order to compare structural differences between subjects and, more relevantly, between groups of subjects, images are generally registered to a common space using anatomical landmarks as guides. On account of the multifaceted structural damage induced by PAE specifically, image registration problems have been a roadblock in the detailed analysis of structural and functional data from this population (Bookheimer and Sowell, 2005). MR images from the PAE population therefore may benefit from a more customizable registration method.

### 2.1.3 <u>DARTEL: Diffeomorphic Anatomical Registration Through Exponentiated Lie Algebra</u>

*2.1.3.1 Concept*

The DARTEL (Diffeomorphic Anatomical Registration Through Exponentiated Lie Algebra) tool from SPM has been recently developed in hopes of improving image registration in

healthy and affected populations by creating an average space template from the individual images.  Briefly, DARTEL is an algorithm for diffeomorphic image registration, which uses large-deformation functions to preserve local topology (Ashburner, 2007b). Large deformations can achieve local optimization due to the use of greater degrees of freedom in the estimation. Deformations are parameterized by a single flow field (considered to be constant in time), allowing for generation of true inverse (one-to-one mapping) transformations. Ashburner cites high local optimization and regularization (similarity) as achievable with DARTEL (2007b). As the aim of most structural MR image registration algorithms to common space is global optimization as opposed to local, DARTEL may improve registration in the PAE population given known local-level damage.

*2.1.3.2 Applications to Date*

Since DARTEL was made available only recently, there are few studies that have implemented and/or compared it with other registration techniques. One study used the medial temporal lobe (MTL) of healthy individuals as a sample region to compare various registration techniques, including standard VBM, ROI, and DARTEL (Yassa and Stark, 2009). The authors compared smoothness of average images among 20 subjects, and found a combination of ROI segmentation and deformation to be optimal. However, of the automated techniques considered, DARTEL was found to produce to least variability (blurring) between subjects in the MTL region. It was noted that improved localization of the MTL likely also pertains to other brain sub-regions. Another study examined the ability of DARTEL to improve co-registration of the hippocampus in patients with depression (Bergouignan et al., 2009). Given the assumption from meta-analyses of reduced hippocampal volume in subjects with depression, the authors compared standard VBM techniques to DARTEL. Results showed significant differences in the depressed group could

6

be noted using the DARTEL method but not by standard VBM. Recently, Klein, et al. performed a comparative study of 14 registration algorithms, including DARTEL (Klein et al., 2009). Using eight different measures of error, the authors ranked DARTEL as a method with relatively high inter-subject whole brain overlap. Furthermore, they note that registration method performance did not appear to depend on the population or labeling used, meaning DARTEL could be versatile enough for use on clinical populations.

### 2.1.3.3 Potential for Functional Image Registration

Although thus far DARTEL has only been applied to improving structural image registration, it could also potentially improve spatial normalization of functional images from different subjects (Ashburner, 2007a, b). Since DARTEL uses only structural information for deformation, if greater overlap is found between functional overlays, it can be inferred that spatial normalization has been improved. In healthy subjects, this improved overlap can be measured by examining the sensitivity of voxel-wise statistics (Ardekani, 2004). For clinical populations, functional activation differences between groups could be compared among registration methods and these differences correlated with behavioral or structural measures known to be associated with the condition.

### 2.1.4  Aims

The present study aims to apply the DARTEL technique to the structural analysis of the CC, which is known to be highly affected by PAE, and compare with a tradition VBM (tVBM) technique. Given prior studies showing reduced volume and spatial shifts of the CC in individuals with PAE, we hypothesize that DARTEL will result in less variability in size and location upon alignment to a common space. Furthermore, DARTEL will be compared with

current functional MRI (fMRI) techniques for alignment of anatomical and functional datasets from the PAE population. Functional activation will be examined in control and PAE individuals using a bimanual vibrotactile stimulation task.  This task requires the subject to detect a tactile stimulation in one hand and respond with the other hand, thus invoking interhemispheric transmission along the corpus callosum. Given previous studies using similar tasks and known alterations in corpus callosum in the PAE population (Fabri et al., 2005), activation is anticipated to be higher in the PAE group, particularly in primary sensory/motor (S1/M1), supplementary motor (SMA), and supramarginal gyrus (SMG) areas (Muetzel et al., 2008; Wahl and Ziemann, 2008). Improved functional overlay registration is anticipated with DARTEL, demonstrated by greater differences (size and number of significant difference clusters) between groups. Furthermore, correlation between the magnitude of functional activation differences and exposure-related characteristics is expected to be significant using the DARTEL method as opposed to the tVBM method. Characteristics known to be associated with PAE include dysmorphic score (Fernhoff et al., 1980), brain size, and FA of certain CC subregions. FA of posterior CC regions (isthmus and splenium) were chosen for correlation analysis, given previously reported reduced FA in these regions in this PAE cohort (Li et al., 2009) and their known contribution to interhemispheric transfer of tactile information (Fabri et al., 2005).

**2.2 Methods**

2.2.1   Participants

Participants were recruited from a longitudinal study started in the 1980s (Smith et al., 1986), comprising a low-income, predominantly African-American urban population. At the time of imaging, participants were between 18-24 years old. Participants were divided into

8

two groups: 1) prenatally exposed to alcohol and positive for dysmorphia and 2) healthy socio-economic status matched controls. The number of subjects used in the study are as follows: anatomical run: control n=18, PAE n=23; functional run: control n=18; PAE n=14. Additionally, a non-dysmorphic PAE group was imaged but not used in this study. Demographics information for all three groups in the cohort is given in Table 2.1. A subset of subjects from Table 2.1 was used in the present study. All participants were evaluated using a dysmorphia checklist (Fernhoff et al., 1980; Smith et al., 1986), where characteristics associated with the disorder are listed and weighted based on their saliency for the diagnosis (e.g., hypoplastic philtrum is a "3" while anteverted nares is a "1"). The 30 items on the checklist were assessed either by a pediatric dysmophologist or a nurse trained and supervised by a dysmorphologist who were blind to the participant's exposure status. The weightings of items checked are summed to yield a dysmorphology index. The checklist has been evaluated repeatedly as part of other longitudinal research studies from birth to adolescence with individuals prenatally exposed to alcohol receiving higher total scores in comparison to non-exposed controls (Blackston, 2004; Fernhoff et al., 1980). The criterion used to define the dysmorphic group was that the participant score had to be one standard deviation above the group mean at any one of three testing points (birth, age 7, mid-adolescence). Potential participants who were left-handed, had some risk during the MRI procedure (e.g., due to pregnancy or metal in the body) or who were uncomfortable with the procedure (e.g., claustrophobia) were not imaged.

9

Table 2.1. Demographic and Prenatal Exposure for Participants (n=96) by Exposure Group. a: If data for a variable are not available for some participants, the n used for the analysis is noted next to the variable name; b: WASI IQ obtained at current testing; c: Post hoc comparisons completed with Tukey HSD test.

| Variable | Group Control (n= 29)[a] | NonDys (n= 34)[a] | Dys (n= 33)[a] | Statistic | Significance |
|---|---|---|---|---|---|
| Gender – % male | 44.8 | 20.6 | 51.5 | $x^2_{(2)}$=7.455 | p=.024 |
| Ethnicity – % African-American | 100 | 97.1 | 100 | $x^2_{(2)}$=1.843 | n.s. |
| Age at imaging, M (SD) | 22.6 (1.8) | 22.9 (1.7) | 23.0 (2.0) | $F_{(2,93)}$=.294 | n.s. |
| Monthly income – $ in past 30 days, M (SD) n=94 | 1199 (1675) | 624 (419) | 1088 (1037) | $F_{(2,91)}$=2.358 | n.s. |
| Education completed – years, M (SD) n=95 | 12.2 (1.6) | 11.6 (1.5) | 12.0 (1.5) | $F_{(2,92)}$=.949 | n.s. |
| Full-scale IQ[b], M (SD) n=95 | 84 (8.6) | 80 (11.4) | 78 (11.6) | $F_{(2,92)}$=2.747 | p=.069 |
| Dysmorphia rating at adult visit, M (SD) n=95 | 3.4 (3.3) | 4.2 (3.6) | 9.4 (7.4) | $F_{(2,92)}$=12.712 | p=.000; Dysm>Control, Etoh[c] |
| Current alcohol use by participant (oz/AA/wk) n=95 | 1.2 (2.7) | 1.2 (1.7) | 1.1 (1.8) | $F_{(2,92)}$=.011 | n.s. |
| Amount of alcohol exposure during pregnancy – AA per week, M (SD) | 0 (0) | 7.7 (13.4) | 13.8 (13.3) | $F_{(2,93)}$=11.741 | p=.000; Control < Dysm, Etoh[c] |
| Cigarettes during pregnancy – % using | 34.5 | 61.8 | 84.8 | $x^2_{(2)}$=16.532 | p=.000 |
| Marijuana during pregnancy – % using | 17.2 | 35.3 | 27.3 | $x^2_{(2)}$=2.584 | n.s. |
| Cocaine during pregnancy – % using n=92 | 0 | 17.6 | 6.9 | $x^2_{(2)}$=6.312 | p=.043 |

<u>Experimental Design</u>

Tactile stimulation was applied using MRI-compatible piezo-electric buzzers (www.piezo.com) controlled through an analog output board (www.ni.com) using a MATLAB control script (www.mathworks.com). Stimuli were triggered from the scanner using a TTL line to achieve time-locking of events. A buzzer was placed on each hand, and a button box (www.curdes.com) was used to collect responses in Presentation (www.neurobs.com). The scan consisted of 24 trials (10sec inter-stimulus interval, left/right balanced); upon feeling the vibrotactile stimulus on their left hand, participants were asked to press a button with their right hand.

2.2.2   <u>Image Acquisition</u>

All acquisition was performed on a 3T Siemens Trio scanner (Siemens Medical Solutions, Erlangen, Germany). For the anatomical scan, the parameters were as follows: TR/TI/TE of 2600ms/900ms/3.93ms, flip angle of 8°, field of vie w of 256 × 224 × 176 mm3, matrix of 256 × 224 × 176, corresponding to an isotropic resolution of 1 mm. For the functional scan, an EPI-BOLD sequence was used to acquire 120 axial images (30, 4mm thick slices) in each run, with an in-plane resolution of 3.44 mm×3.44 mm. Sequence parameters were TR/TE/FA/FOV of 2000ms/35ms/90º/22 cm.

11

### 2.2.3  Image Analysis

*2.2.3.1 Structural Data*

The tVBM technique used was standard non-linear registration in SPM5 (http://www.fil.ion.ucl.ac.uk/spm/, 09/2009), which includes the following steps: skull stripping, affine registration, segmentation, bias correction, and spatial normalization to MNI space. For the DARTEL method, the input were affine registered, skull-stripped brains; the DARTEL toolbox provided for SPM8b was used, consisting of the following steps: 1) creating a template that is the average of all subjects in the study in a customized space; 2) generating warping functions for each individual between native space and template space; 3) applying warping functions to each subject to create structural image in customized average space. Details on the methodology used in DARTEL can be found in the manual (2007a) provided by Ashburner.

Following registration of all images to either standard or customized space, the CC was masked at one mid-sagittal slice (Figure 2.1). Standard deviation of the CC region was calculated voxel-by-voxel between all pairs of subjects within group, averaged over entire CC region, and compared between the two methods and between the two groups, respectively, by F-test. Additionally, to measure displacement, the center of mass for the CC cluster was found in each individual and compared with average CC image center of mass. As no directional displacement trend was seen, the absolute value of displacement was used as the measure. Paired t-test was used to compare displacement in anterior-posterior and superior-inferior directions between the two methods and the two groups, respectively. Given known alterations to specific subareas of the CC, the mid-sagittal slice CC image was then divided into subregions (Figure 2.2) using a previously implemented method {Li, 2009

12

#31}, and variability and displacement were determined for each subregion as well. Again,

variability was measured between methods and between groups by F-test, while

displacement was measured by paired t-test.

tVBM



extract
corpus callosum

Underlay = mean Control image
Overlay (blue) = mean PAE image

DARTEL
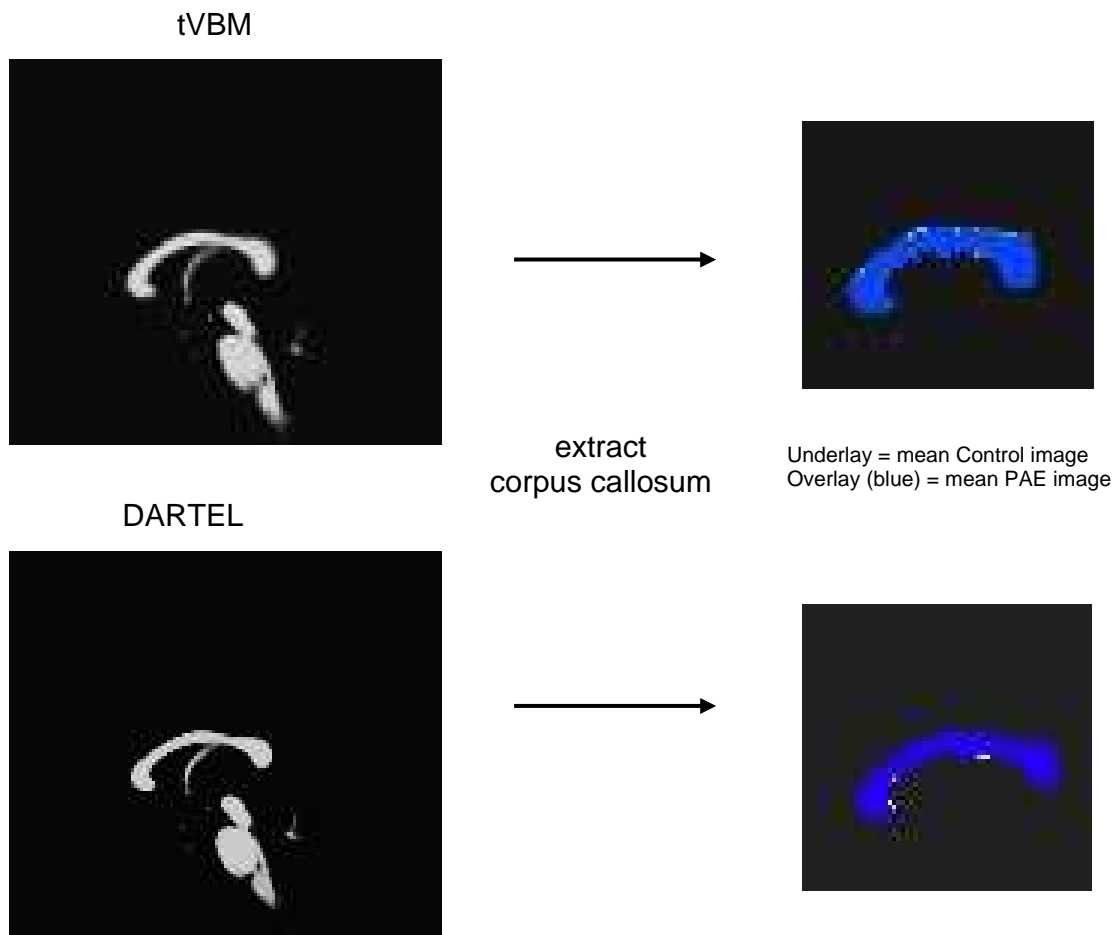


**Figure 2.1.** Corpus callosum extraction for each individual and overlap between control and PAE mean images for each registration technique.
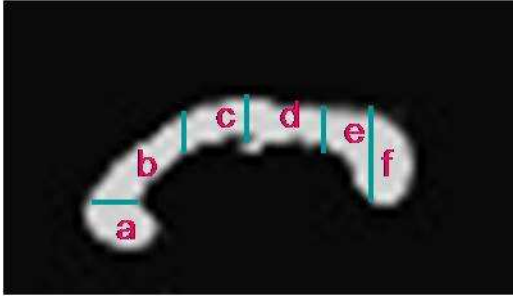
**Figure 2.2.** Segmentation of corpus callosum into six subregions: a) genu; b) rostral body; c) anterior midbody; d) posterior midbody; e) isthmus; and f) splenium.

*2.2.3.2 Functional Data*

For the functional data run, preprocessing was performed in AFNI (http://afni.nimh.nih.gov/afni/, 09/2009) and included slice-timing correction, motion correction, and spatial smoothing (using a 5mm FWHM). Given the event-related stimulus function, the impulse response function (IRF) was estimated for each voxel. The IRF was then convolved with the stimulus time series to yield the estimated response. Activation maps were generated by a multiple linear regression analysis evaluating the goodness of the fit. To correct for multiple comparisons, a voxel-wise threshold of $p<0.05$ and cluster threshold of 5 contiguous voxels were applied, corresponding to a family-wise error rate of $alpha<0.01$ by Monte Carlo simulation.

Functional data was warped to either Talairach space (using automatic Talairach transformation command provided by AFNI) or to the customized space created by the DARTEL toolbox (using the gray matter template and its associated transformation matrix for warping from native space). Difference maps were then generated to compare between the two exposure groups, using a voxel-wise threshold of $p<0.01$ and cluster threshold of 4 contiguous voxels.

14

To determine whether difference maps generated by Talairach warping or DARTEL are more representative of the alcohol exposure effect, exposure-related measures were correlated with the magnitude of activation at a region of significant difference (SMA) between the two groups by the DARTEL method. The average intensity over the SMA region (masked from significant difference map in DARTEL method) was found for each individual. The same mask was used for all subjects in each registration method, respectively, such that the comparison was between the SMA of each subject after warping to customized space and the SMA of each subject after warping to Talairach space. Intensity over this ROI was correlated (using Pearson's correlation in the SPSS software: www.spss.com) with measures known to be related to PAE in these individuals specifically: dysmorphic score, brain size, and FA of the isthmus and splenium (control n=12, PAE n=12). Statistical information on these characteristics for the subjects used in this study is listed in Table 2.2.

**Table 2.2.** Statistical information for exposure-related characteristics. All comparisons are by unpaired t-test; *significantly different between exposure group.

| Variable | Group | | Significance (p-value) |
|---|---|---|---|
| | Control | PAE | |
| Dysmorphic score | 0 (0) | 4.83 (1.43) | p=0.025 |
| Brain size (voxels) | 24859.08 (805.85) | 20885.91 (846.02) | p=0.003 |
| FA isthmus | 0.6676 (0.023) | 0.5880 (0.025) | p=0.029 |
| FA splenium | 0.8143 (0.013) | 0.7780 (0.016) | p=0.036 |

**2.3 Results**

2.3.1   <u>Structural Image Registration</u>

Variability in location and size of the CC, as measured by standard deviation in the overall CC region, was significantly lower between registered images from DARTEL method versus tVBM technique (Figure 2.3a). Additionally, variability was marginally significantly higher in the PAE group as compared to control group by tVBM, while the difference became significant by DARTEL. On the subregional level (Figure 2.3b), significant differences between groups were more detectable with DARTEL (all subregions of the CC versus only genu, rostral body, and isthmus with tVBM).

Anterior-posterior and inferior-superior displacement of the overall CC was lower in registered images from DARTEL method as compared to tVBM (Figure 2.4a). Overall CC displacement in both directions was marginally significantly higher in dysmorphic PAE group for traditional method, but comparable using DARTEL. By tVBM, the splenium was significantly more displaced in the A-P direction (Figure 2.4b), while the genu and splenium were displaced in the I-S direction (Figure 2.4c), in the PAE group. With the DARTEL method, however, no significant differences in displacement were seen. Additionally, no directional trend in displacement was noted (results not shown).
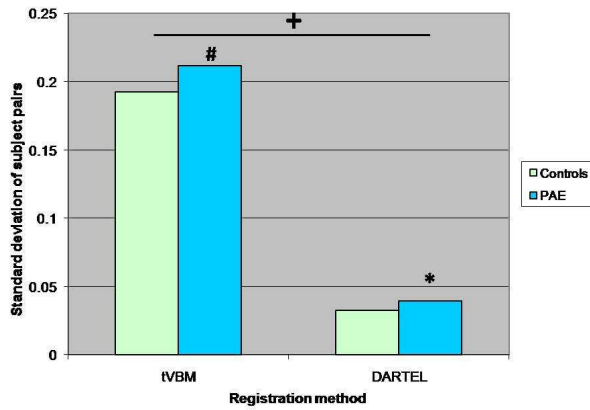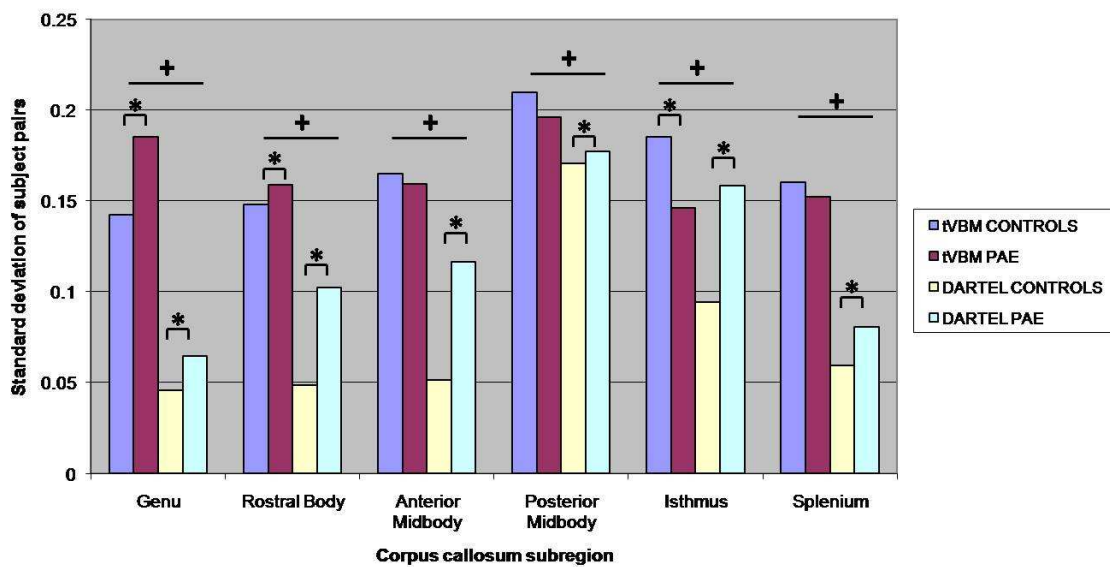
**Figure 2.3.** Standard deviation of all subjects a) over whole corpus callosum; and b) by corpus callosum subregion. + significant difference between registration methods; * significant difference between exposure groups (p<0.05); # marginally significantly different between exposure groups (p<0.10).
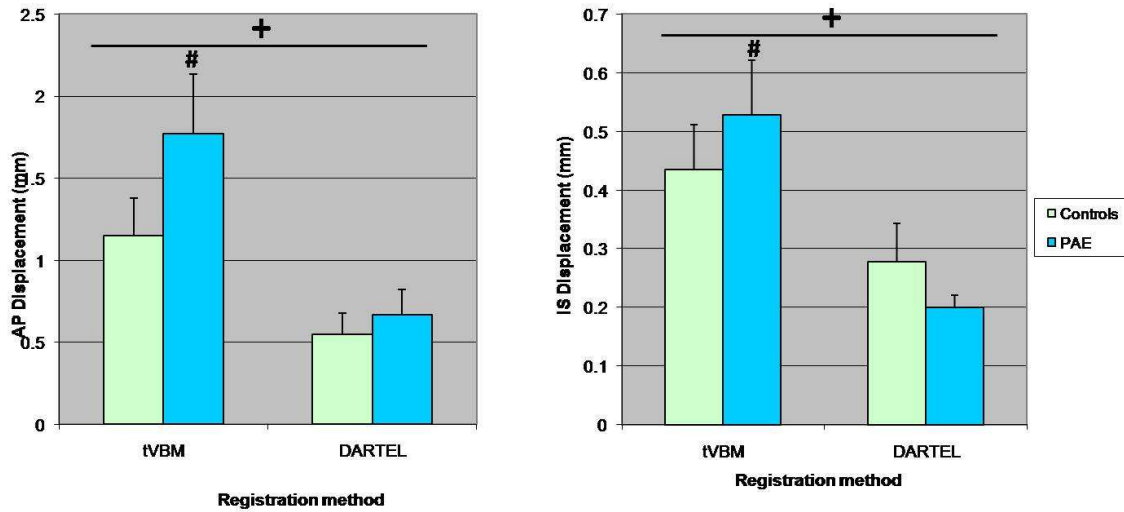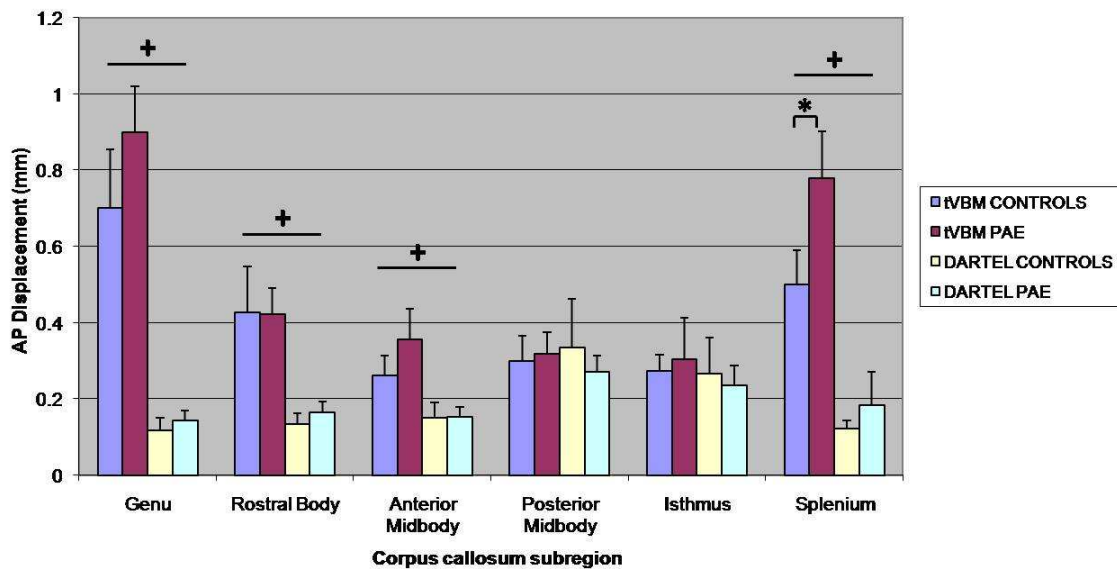
**Figure 2.4.** Anterior-posterior and inferior-superior displacement a) of whole corpus callosum; b) A-P by subregion; c) I-S by subregion. + significant difference between registration methods; * significant difference between exposure groups (p<0.05); # marginally significantly different between exposure groups (p<0.10).

**c)**
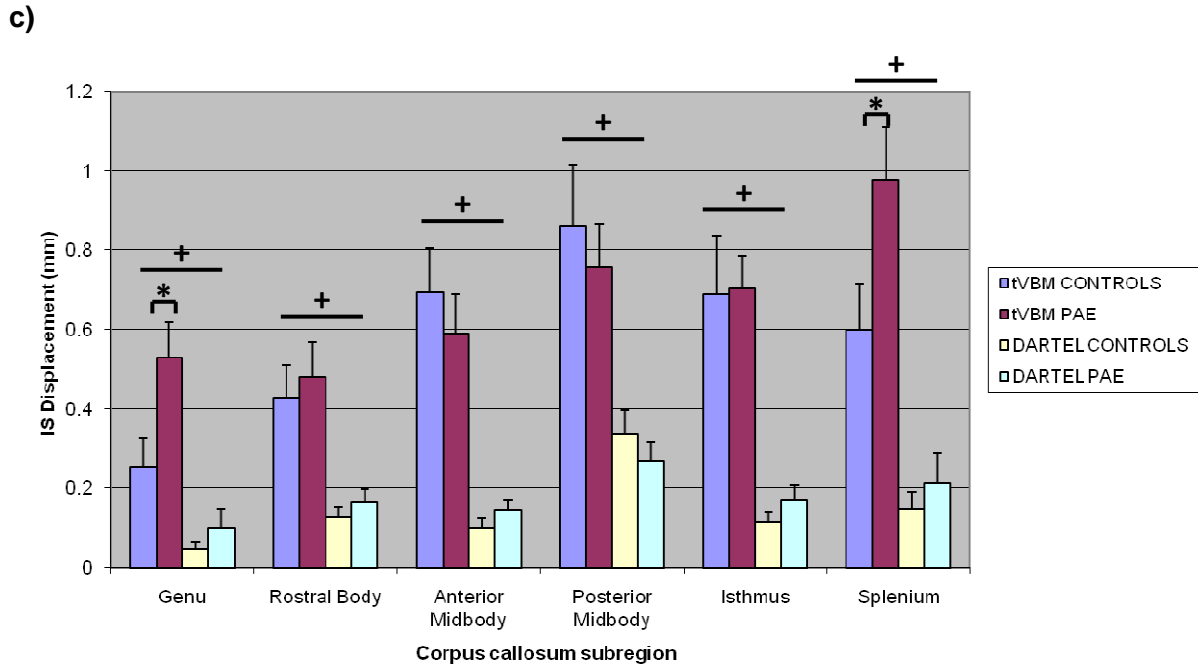


**Figure 2.4.** continued

### 2.3.2 <u>Functional Image Registration</u>

Activation maps created by Talairach transform indicate significant activation in bilateral SMG, bilateral S1/M1, and SMA regions (Figure 2.5). Homologous regions can be indentified in activation maps created from DARTEL template warping (Figure 2.6). Difference maps between groups indicate higher activation in the PAE group as compared to the control group by both methods (Figure 2.7). More differences are notable by the DARTEL warp method than Talairach, with significant clusters located in the regions identified in Figures 2.5 and 2.6. The difference cluster at the SMA (identified by pink circle in Figure 2.7) was used for subsequent correlation analysis. Positive correlation with

dysmorphic score and negative correlation with brain size and splenium FA were significant,

while negative correlation with isthmus FA was not significant (Table 2.3).
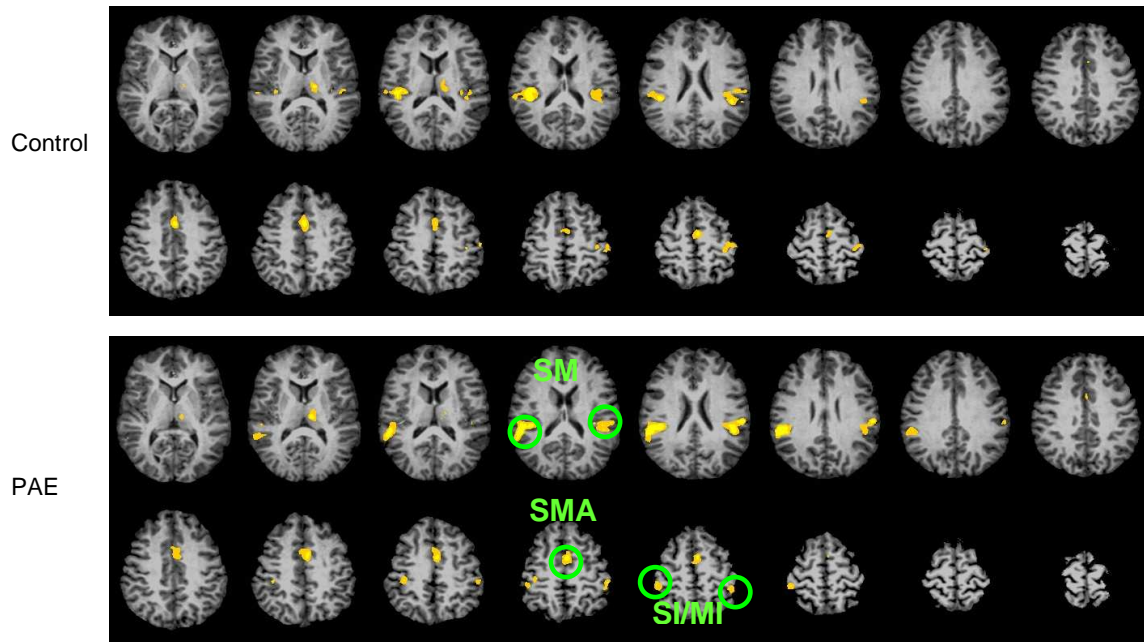


**Figure 2.5.** Activation maps using standard Talairach space as template for functional data warping; circles indicate bilateral SMA, S1/M1, and SMG activation in control and PAE groups. Voxel-wise threshold was p<0.05 with cluster threshold of 5 contiguous voxels.

المنارة للاستشارات

www.manaraa.com
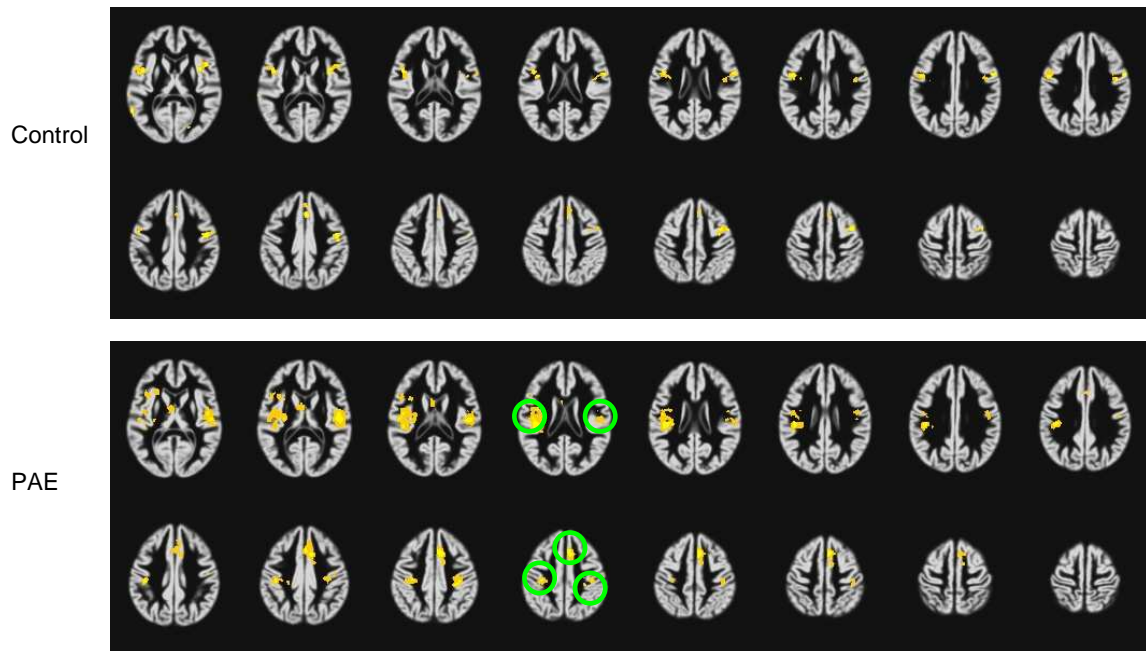
**Figure 2.6.** Activation maps using DARTEL customized templatefor functional data warping; circles indicate bilateral SMA, S1/M1, and SMG activation in control and PAE groups (homologous regions to those circled in Figure 2.5). Voxel-wise threshold was p<0.05 with cluster threshold of 5 contiguous voxels.
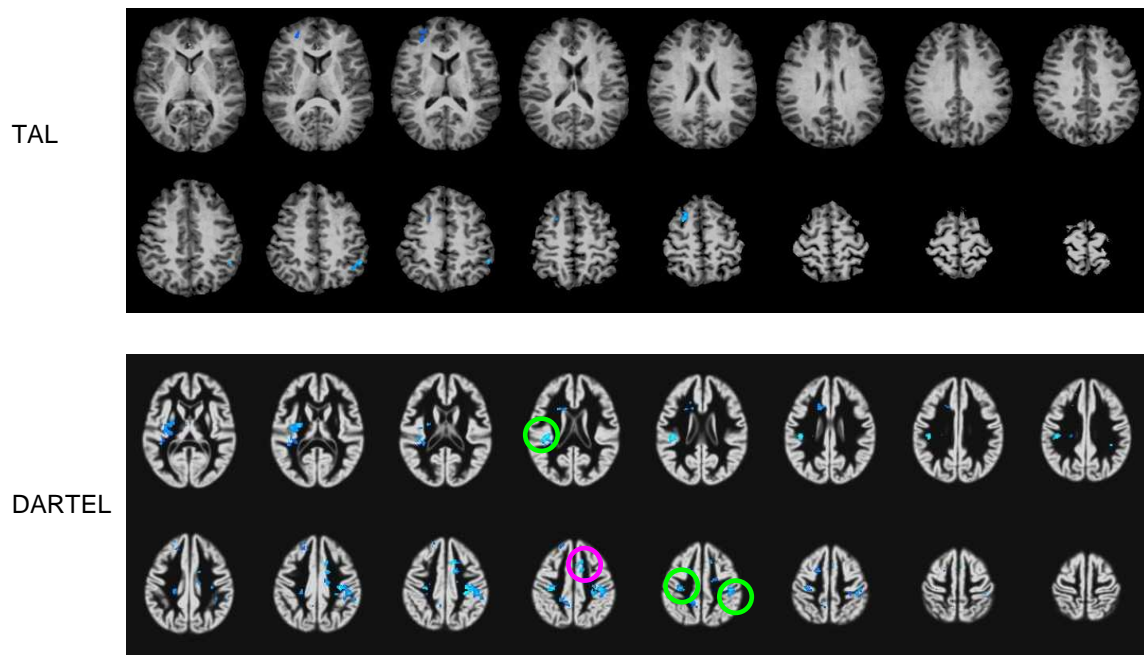
**Figure 2.7.** Difference maps (Control-PAE) for both Talairach (TAL) and DARTEL registration methods. SMA difference cluster circled in red; signal intensity was masked over this region and used in subsequent exposure-related correlation analysis. Voxel-wise threshold was p<0.01 with cluster threshold of 4 contiguous voxels.

**Table 2.3.** Pearson's correlation results (r and p-values) relating Talairach (TAL) and DARTEL registration methods to exposure-related measures. *significant correlation (p<0.05).

| Registration method | Exposure-related measure correlation: r (p-value) | | | |
|---|---|---|---|---|
| | **Dysmorphic score** | **Brain size** | **FA isthmus** | **FA splenium** |
| TAL | -0.018 (0.935) | 0.266 (0.209) | 0.329 (0.116) | -0.329 (0.116) |
| DARTEL | 0.448 (0.028*) | -0.500 (0.013*) | -0.221 (0.300) | -0.439 (0.032*) |

المنارة للاستشارات

www.manaraa.com

**2.4 Discussion**

2.4.1    Summary

DARTEL was able to improve spatial normalization of both structural and functional images from the PAE population. Significant decreases in variability (location and size) and displacement of the CC were seen in both groups using DARTEL as compared to tVBM. Differences in variability between controls and PAE subjects were seen in more subregions of the CC by DARTEL, while fewer differences between groups were noted in displacement. Additionally, functional difference maps comparing groups had more detectable regional differences when aligned to DARTEL customized space as compared to standard normalization to Talairach space.

2.4.2    Context in Current Literature

*2.4.2.1 Structural Image Registration*

As previously mentioned, a few studies have reported a high variability in location and size of the CC in individuals with fetal alcohol spectrum disorder (FASD). Since standard registration methods use anatomical landmarks near the CC region (e.g., anterior and posterior commissures), alignment between subjects from the PAE group is particularly challenging. DARTEL is shown in this study to reduce the variability in size and location of the CC in both healthy controls and individuals with PAE. Improved alignment within the control group would be expected based on validation from the original DARTEL manuscript (Ashburner, 2007b), and is not surprising in the PAE group either given the high whole-brain similarity achievable between images using DARTEL. On the subregional level, differences

23

in variability between groups were more detectable with DARTEL, seen in all subregions as compared to only in three (genu, rostral body, and isthmus) with tVBM. Bookstein, et al. has examined CC morphology in individuals with FAS using Procrustes analysis methods, which examine specifically differences in shape (2002; 2001); while the authors concluded variability was overall higher in the FAS group (not localized to any one CC subregion), they also reported on average a thinner isthmus, thicker genu, and "differently shaped" splenium in the FAS group. Registration from Cartesian space to "shape" space was performed by a neuroanatomist on each individual using anatomical landmarks. While this is not a standard VBM technique, it did not reveal as many mid-CC regional deformations as the DARTEL method in this study. The reason for this discrepancy is unclear; it is possible our population has more CC differences or that the registration performed in these other studies was biased against the CC mid-region, as the anatomical landmarks used did not span the entire CC.

Multiple studies have reported spatial shifts in the CC in individuals with PAE (Riley et al., 1995; Sowell et al., 2001; Spadoni et al., 2007). Recently, Sowell, et al. specifically identified CC displacement in the anterior and inferior directions in individuals with FAS (2001). The authors employed VBM following registration to ICBM-standard space. In the present study, no directional shift trends were seen with either method when considering the whole CC. On the subregional level, tVBM revealed A-P shifts in the splenium, and I-S shifts in the genu and splenium, which were absent using the DARTEL method. While these results suggest that CC displacement may not be as significant in PAE groups as previous studies have shown, the discrepancy between studies is difficult to interpret. The findings in the study by Sowell, et al. may be due to misalignment of the CC to standard space, or the present study cohort may simply differ a great deal from theirs. Though the authors stipulate that they also measured displacement in native space as a control for standardized registration, these

24

measurements may be skewed by age differences between subjects (age range was 8-25 yrs). More systematic studies of CC directional displacement need to be performed in order to establish a more direct causal link to PAE.

Another possible reason for DARTEL yielding fewer differences between groups in displacement is that high regularization may have made the CC image more similar between subjects, but not necessarily more representative of their real position in space. Increased image similarity is evident in the present study by decreased variability and displacement in both groups by DARTEL (versus tVBM). One limitation listed by Ashburner is that diffeomorphisms focus on local optimization, perhaps at the expense of ROI-level representation (2007b). However, general CC variability does not appear to be affected thus by DARTEL, so it is unclear the contribution of this confound to the results of the present study. Regardless, despite this limitation, DARTEL can still have significant applications to functional datasets, because the warping does not directly affect functional data.

*2.4.2.2 Functional Image Registration*

Studies of interhemispheric information transfer in individuals with PAE have revealed increased activation and longer reaction times (Dodge et al., 2009; Roebuck-Spencer et al., 2004); these alterations are thought to result from CC damage, which can hinder efficient transfer between hemispheres (Lum et al., 2009; Wahl and Ziemann, 2008). As the functional task in the present study examines interhemispheric transfer, increased bilateral activation of sensory and motor-related regions was expected in subjects with PAE. When used to align functional overlays from multiple subjects, DARTEL improved functional image registration as compared to the tVBM method. This was demonstrated by larger differences in sensory and motor-related regions between groups, in terms of size and number of

25

significant difference clusters in group subtraction maps. Furthermore, the intensity of the SMA cluster from the difference map was found to positively correlate with dysmorphic score, and negatively correlate with brain size and FA of the splenium. Thus it is possible that studies of the PAE population would benefit from alignment to a customized space (e.g, DARTEL method) rather than a standardized common space.

### 2.4.3   Limitations

It should be noted that since DARTEL warping applies only to structural data, the differences in functional overlays are a product of different transformation functions and not related to pre-processing steps. All pre-processing was the same for both registration types, including spatial smoothing with a 5 FWHM kernel. Traditionally, smoothing is applied to functional data in order to off-set misalignment to common space, which likely contributed in both registration methods to greater correspondence between functional images from different subjects. On the other hand, spatial smoothing may have hindered resolution of smaller activation clusters, in either method. It would be interesting to note the differences between groups using non-blurred functional data, and the effect of DARTEL versus tVBM on functional maps.

### 2.4.4   Future Considerations

The results of this study suggest that DARTEL improves both structural and functional image registration in individuals with PAE. Since inter-subject registration is especially problematic in this population, identification of new methods could allow for more accurate group comparison. Comparative study of DARTEL with several other registration methods has shown that while it is highly ranked, it is not necessarily the most appropriate method

available. Due to the specific microstructural alterations caused by PAE, further examination of these alternative registration methods as applied to the PAE population could yield even greater group comparison accuracy. Furthermore, as very recent VBM and DTI studies have revealed other cortical regions structurally affected by PAE, including temporal-occipital areas and cerebellum (Lebel et al., 2008; Wozniak et al., 2009), it would be interesting to note the effect of DARTEL on these group differences. If customized templates can be shown to improve overall brain image registration in the PAE population, on the global and local levels, as well as improve functional overlay normalization, their implementation could aid in more precise localization of PAE-related structural and functional damage.

## 2.5 References

Archibald SL, Fennema-Notestine C, Gamst A, Riley EP, Mattson SN, Jernigan TL (2001) Brain dysmorphology in individuals with severe prenatal alcohol exposure. Dev Med Child Neurol 43(3):148-54.

Ardekani BA, Bachman, A.H., Strother, S., Fujibayashi, Y., Yonekura, Y., (2004) Impact of inter-subject image registration on group analysis of fMRI data. Int. Congr. Ser., Elsevier 1265:49-59.

Ashburner J (2007a) DARTEL guide, in *http://www.fil.ion.ucl.ac.uk/~john/misc/dartel_guide.pdf*. Accessed 09/2009.

Ashburner J (2007b) A fast diffeomorphic image registration algorithm. Neuroimage 38(1):95-113.

Bergouignan L, Chupin M, Czechowska Y, Kinkingnehun S, Lemogne C, Le Bastard G, Lepage M, Garnero L, Colliot O, Fossati P (2009) Can voxel based morphometry, manual segmentation and automated segmentation equally detect hippocampal volume differences in acute depression? Neuroimage 45(1):29-37.

Blackston RD, Coles, C. D., Kable, J.A., & Seitz, R. (2004) Reliability and validity of the Dysmorphia Checklist: Relating severity of dysmorphia to cognitive and behavioral outcomes in children with prenatal alcohol exposure. Paper presented at the American Society of Human Genetics Annual Meeting, Toronto, Canada.

27

Bookheimer SY, Sowell ER (2005) Brain imaging in FAS: commentary on the article by Malisza et al. Pediatr Res 58(6):1148-9.

Bookstein FL, Sampson PD, Connor PD, Streissguth AP (2002) Midline corpus callosum is a neuroanatomical focus of fetal alcohol damage. Anat Rec 269(3):162-74.

Bookstein FL, Sampson PD, Streissguth AP, Connor PD (2001) Geometric morphometrics of corpus callosum and subcortical structures in the fetal-alcohol-affected brain. Teratology 64(1):4-32.

Dodge NC, Jacobson JL, Molteno CD, Meintjes EM, Bangalore S, Diwadkar V, Hoyme EH, Robinson LK, Khaole N, Avison MJ, Jacobson SW (2009) Prenatal alcohol exposure and interhemispheric transfer of tactile information: Detroit and Cape Town findings. Alcohol Clin Exp Res 33(9):1628-37.

Fabri M, Del Pesce M, Paggi A, Polonara G, Bartolini M, Salvolini U, Manzoni T (2005) Contribution of posterior corpus callosum to the interhemispheric transfer of tactile information. Brain Res Cogn Brain Res 24(1):73-80.

Fernhoff PM, Smith IE, Falek A (1980) Dysmorphia Checklist. Document available through the Maternal Substance Abuse and Child Development Project, Department of Psychiatry and Behavioral Sciences, Emory University School of Medicine.

Klein A, Andersson J, Ardekani BA, Ashburner J, Avants B, Chiang MC, Christensen GE, Collins DL, Gee J, Hellier P, Song JH, Jenkinson M, Lepage C, Rueckert D, Thompson P, Vercauteren T, Woods RP, Mann JJ, Parsey RV (2009) Evaluation of 14 nonlinear deformation algorithms applied to human brain MRI registration. Neuroimage 46(3):786-802.

Lebel C, Rasmussen C, Wyper K, Walker L, Andrew G, Yager J, Beaulieu C (2008) Brain diffusion abnormalities in children with fetal alcohol spectrum disorder. Alcohol Clin Exp Res 32(10):1732-40.

Li L, Coles CD, Lynch ME, Hu X (2009) Voxelwise and skeleton-based region of interest analysis of fetal alcohol syndrome and fetal alcohol spectrum disorders in young adults. Hum Brain Mapp 30(10):3265-74.

Lum C, McAndrews MP, Holodny AI, McManus KA, Crawley A, Chakraborty S, Mikulis DJ (2009) Investigating Agenesis of the Corpus Callosum Using Functional MRI: A Study Examining Interhemispheric Coordination of Motor Control. J Neuroimaging.

Ma X, Coles CD, Lynch ME, Laconte SM, Zurkiya O, Wang D, Hu X (2005) Evaluation of corpus callosum anisotropy in young adults with fetal alcohol syndrome according to diffusion tensor imaging. Alcohol Clin Exp Res 29(7):1214-22.

Muetzel RL, Collins PF, Mueller BA, A MS, Lim KO, Luciana M (2008) The development of corpus callosum microstructure and associations with bimanual task performance in healthy adolescents. Neuroimage 39(4):1918-25.

Riley EP, Mattson SN, Sowell ER, Jernigan TL, Sobel DF, Jones KL (1995) Abnormalities of the corpus callosum in children prenatally exposed to alcohol. Alcohol Clin Exp Res 19(5):1198-202.

Riley EP, McGee CL (2005) Fetal alcohol spectrum disorders: an overview with emphasis on changes in brain and behavior. Exp Biol Med (Maywood) 230(6):357-65.

Roebuck-Spencer TM, Mattson SN, Marion SD, Brown WS, Riley EP (2004) Bimanual coordination in alcohol-exposed children: role of the corpus callosum. J Int Neuropsychol Soc 10(4):536-48.

Roebuck TM, Mattson SN, Riley EP (1998) A review of the neuroanatomical findings in children with fetal alcohol syndrome or prenatal exposure to alcohol. Alcohol Clin Exp Res 22(2):339-44.

Smith IE, Coles CD, Lancaster J, Fernhoff PM, Falek A (1986) The effect of volume and duration of prenatal ethanol exposure on neonatal physical and behavioral development. Neurobehav Toxicol Teratol 8(4):375-81.

Smith KJ, Eckardt MJ (1991) The effects of prenatal alcohol on the central nervous system. Recent Dev Alcohol 9:151-64.

Sowell ER, Mattson SN, Thompson PM, Jernigan TL, Riley EP, Toga AW (2001) Mapping callosal morphology and cognitive correlates: effects of heavy prenatal alcohol exposure. Neurology 57(2):235-44.

Spadoni AD, McGee CL, Fryer SL, Riley EP (2007) Neuroimaging and fetal alcohol spectrum disorders. Neurosci Biobehav Rev 31(2):239-45.

Wahl M, Ziemann U (2008) The human motor corpus callosum. Rev Neurosci 19(6):451-66.

Wozniak JR, Muetzel RL, Mueller BA, McGee CL, Freerks MA, Ward EE, Nelson ML, Chang PN, Lim KO (2009) Microstructural Corpus Callosum Anomalies in Children With Prenatal Alcohol Exposure: An Extension of Previous Diffusion Tensor Imaging Findings. Alcohol Clin Exp Res.

Yassa MA, Stark CE (2009) A quantitative evaluation of cross-participant registration techniques for MRI studies of the medial temporal lobe. Neuroimage 44(2):319-27.

**CHAPTER 3**

**Effects of Prenatal Alcohol Exposure on Arithmetic Functioning: an fMRI Study**

## 3.1 Background

### 3.1.1 Prenatal Alcohol Exposure and Behavioral Deficits

The hazards of prenatal alcohol exposure (PAE) have been documented for decades, yet it continues to be a prevalent social and health concern today. It has been estimated that approximately 1 of 500 infants in the United States is born affected by such exposure (Abel, 1995). The teratogenic results for offspring of maternal alcohol consumption during pregnancy are referred to as fetal alcohol spectrum disorders, the most severe of which is fetal alcohol syndrome (FAS). Currently, FAS is clinically characterized by facial dysmorphia, diminished growth, and neurodevelopmental disorders including microcephaly (Jones and Smith, 1973). However, diagnosis of FAS can be challenging since there is no one presenting symptom and often behavioral outcomes appear similar to those associated with other neurocognitive disorders (Coles, 2001; Coles et al., 1997; Nash et al., 2006). Structural and functional effects are reported in individuals exposed prenatally who lack the physical dysmorphia associated with FAS (Mattson et al., 1998).

Behavioral problems in individuals with a range of PAE have been observed for decades and are reported to include both neurocognitive deficits as well as social and adaptive dysfunction (Mattson and Riley, 1998). In general, individuals with FAS have lower IQ, often accompanied by impaired visuo-spatial, attentional, memory recall, and/or language skills

(Coles et al., 1997; Conry, 1990; Mattson and Riley, 1998; Olson et al., 1998; Streissguth et al., 1994b). Developmental dyscalculia, the reduced ability to understand and/or apply core mathematical processes due to teratogenic damage, is also widely reported to be associated with prenatal alcohol exposure (Goldschmidt et al., 1996; Streissguth et al., 1994b; Streissguth et al., 1989), perhaps even more often than global and verbal deficits (Streissguth et al., 1994b). In adolescents, math-related deficits range from longer response interval for mental math calculations to an inability to do basic addition and subtraction (Streissguth et al., 1994a). Additionally, a study in adults found dysfunction in a number of math skills including the ability to estimate efficiently (Kopera-Frye et al., 1996). Since math processing appears to be a specific deficit associated with prenatal alcohol exposure, the underlying neurocognitive correlates of this arithmetic processing impairment warrant the closer examination that can be provided through functional neuroimaging.

### 3.1.2   Neural Correlates of Dyscalculia

Neural correlates of developmental and clinical dyscalculia have been extensively documented and can serve as a guide to the current investigation. Several studies have reported systematic activation of bilateral parietal, frontal, and precentral cortices during arithmetic calculation (Fehr et al., 2007; Kazui et al., 2000; Menon et al., 2000; Zhang et al., 2005). Lesion studies and examinations of clinical populations indicate that bilateral parietal and frontal regions are responsible for clinical dyscalculia (Dehaene et al., 2004; Menon et al., 2000). Dehaene, et al. (2003) point specifically to the horizontal interparietal sulcus (HIPS) as a region activated for various types of arithmetic calculation, and Cantlon et al. (2006) have confirmed that the intraparietal sulcus (IPS) is activated in both children and adults during both symbolic and nonsymbolic tests of numerosity. It has further been suggested that medial frontal and bilateral parietal regions are specifically related to the

31

nonverbal, spatial aspects of math processing with other areas of the brain subsuming the verbal (symbolic) functions (Fehr et al., 2007; Hubbard, 2005; Kong et al., 2005). To date, no study has examined the effect of PAE on activation in these brain regions in the context of dyscalculia.

### 3.1.3   Potential Confound

A potential methodological confound in functional neuroimaging of individuals affected by PAE is head size differences. Reduced subregion and overall brain size have been widely reported in alcohol-affected individuals (Riley et al., 2004; Sowell et al., 2001) and is especially prevalent in those with FAS (Archibald et al., 2001). The microcephaly common to affected individuals has the potential to distort results of imaging studies if not taken into account during activation analysis. Previous studies of this clinical group have not addressed this issue formally although it has been acknowledged that normal spatial transformation may affect interpretation of results (Bookheimer and Sowell, 2005).

### 3.1.4   Aims

In the present study we used functional MRI (fMRI) to examine the effects of prenatal alcohol exposure on brain activation during performance of a subtraction task. Previous studies have demonstrated successful use of BOLD signal as an indicator of arithmetic functioning and deficiency (Cantlon et al., 2006; Delazer et al., 2003; Fehr et al., 2007; Kong et al., 2005). Expected outcomes included a significant difference between physically affected (dysmorphic) PAE and control groups in task performance and brain activation patterns in those regions previously associated with general arithmetic calculation and specifically subtraction. In order to deal with the problem of potentially confounding head

size differences, we identified regions of interest on an individual basis, and normalized activation volumes based on the size of the identified subregion.

A second focus of the study was to examine the extent to which alcohol-exposed individuals with and without dysmorphic features would demonstrate similar patterns of activation in comparison to socio-economic status-matched, nonexposed controls. If neurodevelopment is equally affected in nondysmorphic individuals, we would anticipate a similar pattern of dysfunction in nondysmorphic, PAE individuals as that seen in the more physically affected dysmorphic group. However, since we hypothesize that there is a relationship between severity of physical effects of PAE and the functional deficit associated with dyscalculia, we expect that exposed but non-dysmorphic individuals should show no deficits or should be intermediate in performance between those with dysmorphic features and nonexposed controls.

## 3.2 Methods

### 3.2.1  Participants

Participants were 54 young adults, age 20-26, whose prenatal exposure to alcohol was quantified prenatally through maternal report. All were recruited from a longitudinal cohort, derived from a predominantly African-American, low socio-economic status population first identified between 1979 and 1986 when their mothers applied for prenatal care (Smith et al., 1986). From this cohort, three groups were selected for participation in the current study and recontacted. These included individuals who were: 1) Exposed to alcohol prenatally and exhibiting physical signs of such exposure, specifically facial dysmorphia (n=19); 2) Exposed, without dysmorphia (n=18), but with ability scores (i.e., IQ < 83) consistent with

33

mean scores in Group 1; and 3) Unexposed controls from the same low SES population (n=17). The mean ounces of absolute alcohol consumption per week during pregnancy for the dysmorphic and non-dysmorphic groups were 13.5 (sd=15.9) and 10.4 (sd=18), respectively. Demographics information for the cohort is given in Table 2.1. A subset of subjects from Table 2.1 was used in the present study. Potential participants who were left handed, had some risk during the MRI procedure (e.g., due to pregnancy or metal fragments) or who were uncomfortable with the procedure (e.g., claustrophobia) were not imaged.

Participants had been seen during adolescence (Coles et al., 2002) and when recontacted as adults, gave informed consent to continue to participate in the research. To protect the confidentiality of their mothers, who had originally given informed consent, no information about exposure group status or maternal substance use was provided. The informed consent procedure was consistent with the Declaration of Helsinki and was approved by the School of Medicine's Institutional Review Board. Study personnel provided transportation to and from the University research site for data collection and imaging. Experimental procedures, including neuropsychological testing and functional neuroimaging, were carried out by staff blind to group status. Participants were reimbursed for their time and effort.

### 3.2.2  Experimental Design

The experimental paradigm, used previously by Connor (personal communication, 2004) with adults affected by alcohol exposure, allowed the evaluation of subtraction performance while using a letter-matching task to control for baseline cognitive and motor activity. The task was presented in blocks, alternating between the letter-matching control task (10 consecutive presentations) and a subtraction task (10 consecutive presentations). Although

problems were repeated across blocks, the order of the problems was randomized. Five

blocks of each type of task were presented, with instructions stating either "Name the letter"

or "Subtract from 11" being shown before each block. Both tasks had a similar visual

presentation (Figure 3.1). Participants were asked to choose between the two letters or

numbers on the bottom half of the screen by pressing the left or right button on a button

response box (http://www.curdes.com, 09/2009). Paradigm presentation and response

collection, including accuracy and reaction time, were done using E-prime

(http://www.pstnet.com, 09/2009). It should be noted that the subtraction task was of a type

that requires estimation (Klahr, 1973) of quantity and the technique known as "borrowing,"

(McCarthy and Warrington, 1987) rendering it "complex" rather than "simple" by the

standards of previous studies of arithmetic operation correlates (Fehr et al., 2007; Kong et

al., 2005).
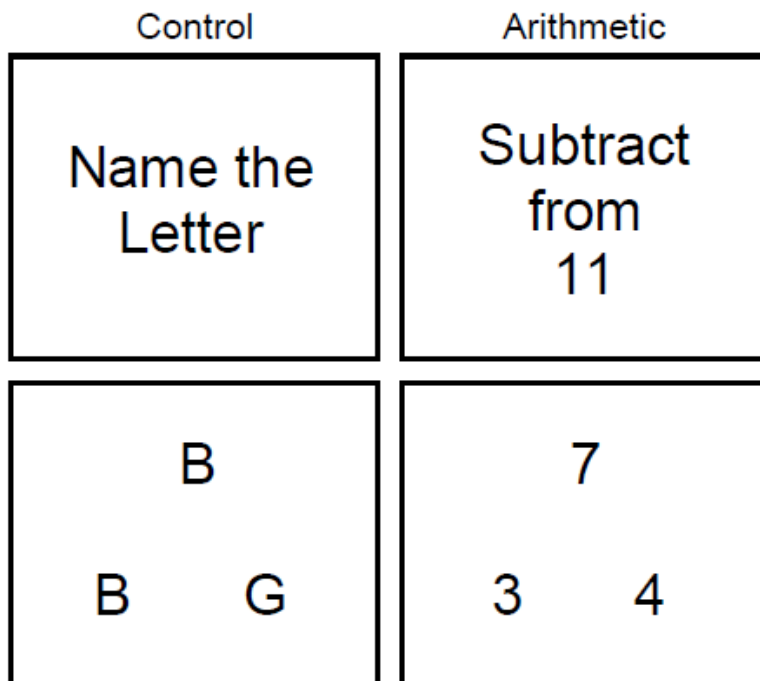
**Figure 3.1.** Example of stimulus paradigm.

3.2.3    Image Acquisition

All fMRI data was acquired on a 3T Siemens Trio scanner (Siemens Medical, Erlangen, Germany). The arithmetic study was only one of several functional paradigms implemented, with a total scan time of 39:59 min. For the arithmetic task, single-shot T2*-weighted EPI images were acquired, consisting of 34 contiguous axial slices of with 3mm slice thickness. Pulse sequence parameters, designed to minimize susceptibility to signal loss, were TR/TE/FA/FOV of 3000ms/32ms/90º/22cm. The scan time was 5:06 min, with 102 time points collected. High-resolution, T1-weighted, three-dimensional (3D) anatomical images were also acquired with a 3D MPRAGE (magnetization prepared rapid gradient echo) sequence for all participants. The scan protocol, optimized at 3T, used TR/TI/TE of 2600ms/900ms/3.93ms, flip angle of 8°, field of vie w of 256 × 224 × 176 mm3, matrix of 256 × 224 × 176, corresponding to an isotropic resolution of 1 mm. Scan time was 7:18 min.

3.2.4    Image Analysis

AFNI (http://afni.nimh.nih.gov, 09/2009) was used to perform imaging data analysis. After the data preprocessing steps (slice timing correction, volume registration, signal normalization to percent change, and 5mm FWHM Gaussian blur), 3D+time fMRI datasets for each individual were submitted to a multiple regression analysis. Using the letter task as baseline, the main regressor was generated by convolving the boxcar stimulation functions with a standard impulse response function ($y=t^b \times \exp(-t/c)$, where b and c are constants) (Cohen, 1997). In order to achieve a better modeling of the motion-related signal variation, the rigid body head motion parameters (x, y, z displacements and roll, pitch, yaw rotations) were included as 6 additional regressors as well. The outcome of this multiple regression

36

analysis included statistical parametric maps, which show voxels with a significant task effect (partial F-statistic), and regression coefficients, which are least squares estimates of the linear model and are proportional to the BOLD (blood oxygenation level-dependent) signal increase level in the arithmetic task from the letter task (baseline). For each group, the statistical parametric maps of individuals were averaged after transforming the dataset into the Talairach space (Talairach and Tournoux, 1988) and normalizing the F values into Z-scores. Voxels that followed the general linear model of letter task baseline and arithmetic block activation were considered to reflect the so-called "arithmetic effect." Thresholded activation maps of this arithmetic effect, averaged from individual datasets, are shown for PAE and control groups in Figure 3.2. Voxel-wise group t-test maps were also created to determine activation difference between control and both exposure groups (Figure 3.3). To account for multiple comparisons, voxel-wise thresholding ($p < 0.05$ for Figure 2; $p < 0.01$ for Figure 3.3) with cluster thresholding of 4 contiguous voxels was applied. Monte Carlo simulation revealed that these thresholds corresponded to a false-positive discovery rate (alpha) of less than 1% for Figure 3.2 and less than 0.1% for Figure 3.3.

In order to quantitatively compare brain activities between groups, we defined regions of interests (ROI) in the Talairach space based on an atlas provided by AFNI. ROIs were chosen based on activation maps of arithmetic effect for the sample as a whole (regions with higher activation in the arithmetic task versus control task). The following brain areas were identified: left and right superior and inferior parietal regions, superior frontal, medial frontal, middle frontal, and inferior frontal gyri. It was noted that all these ROIs were also implicated in previous studies of arithmetic processing. ROI associated functional activation volumes and corresponding regression coefficients were then calculated in native space for each individual. The location and extent of each ROI was defined anatomically in native space by applying the inverse nonlinear warping from the Talairach transformation onto the

37

ROI mask and using the functional dataset as a template. Activation extent (number of active voxels) was subsequently determined for each ROI and then normalized to the voxel size of the entire ROI for each individual. Normalized activation volumes were compared between exposure groups by t-test. Additionally, the unthresholded regression coefficient was calculated for each ROI in native space, converted to percent BOLD signal change, and compared between exposure groups by t-test.

## 3.3 Results

### 3.3.1  <u>Task Performance</u>

Using "number correct" as the outcome measure, there was a significant difference in performance on the arithmetic task between control subjects and dysmorphic PAE subjects (Table 3.1), with lower accuracy in the dysmorphic group. When participants gave no response (so-called "skips"), it was counted as an incorrect response in determining accuracy. Participants who skipped more than 50% of arithmetic responses were excluded from analysis (n=2), and of the remaining participants, the number of skips was comparable among groups. Accuracy was at or near 100% on the letter-matching control task for all groups, and there was not a significant difference in reaction time for either task between any of the groups.

38

**Table 3.1.** Accuracy on the arithmetic task for each exposure group, determined as percent of questions correctly answered (out of 60) and including skipped questions as incorrect. SEM = standard error of mean. *indicates significantly different from control group.

| Exposure group | Accuracy (%) ± SEM | p-value |
| --- | --- | --- |
| Control | 72.6 ± 3.8 | |
| Non-Dys | 65.3 ± 4.2 | 0.104 |
| Dys | 60.1 ± 4.4 | 0.022* |

### 3.3.2   fMRI Results

Figure 3.2 shows the arithmetic effect (arithmetic task minus control task) in selected slices for each group. Specifically, robust activation is seen in bilateral parietal lobe, medial frontal gyrus, and bilateral middle frontal gyrus in the control group, while activation in the exposed individuals is sparser and primarily on the right side of the middle frontal and parietal regions. Figure 3.2 also indicates more overall activation in the control group as compared to the two PAE groups. Regions of interest (ROI), listed in Table 3.2, were identified based on these activation maps. Selected slices from group difference maps of arithmetic effect-related activation are shown in Figure 3.3. Greater activation in controls as compared to non-dysmorphic PAE in the middle frontal and parietal regions is notable in Figure 3.3A. Figure 3.3B shows significantly more activation in control subjects as compared to dysmorphic PAE subjects in bilateral parietal, middle frontal, and medial frontal gyri.

Activation volumes and percent signal change for each ROI are indicated in Table 3.2. To verify that activation differences were reflective of impairment and not lack of task engagement, activation was also examined excluding subjects performing below chance

(50%) on the arithmetic task (ExLS: n=17 for non-dysmorphic PAE group; n=13 for dysmorphic PAE group). None in the control group scored below chance. Left and right superior and right inferior parietal regions and medial frontal gyrus showed an exposure-dependent response, with the dysmorphic PAE group having the lowest amount of activation. Furthermore, dysmorphic PAE subjects had significantly less ($p < 0.05$) activation as compared to the control group in all of these regions except the right superior parietal area. When low-scoring subjects were excluded, the same ROIs remained significantly different from controls, and no other ROIs had significantly different activation volumes. The percent BOLD signal change is also indicated in Table 3.2 for each ROI. Average percent signal change trended in the same direction as activation volumes (correlation with average activation volume was $r = 0.97$), with marginally significant differences ($p < 0.10$) between the control and dysmorphic groups in the right inferior parietal and medial frontal gyri. With the exclusion of the low-scoring subjects, these ROI differences were still marginally significant. No significant correlation was found between task performances and either activation volume or percent signal change ($r < 0.5$ for all groups and all ROIs).
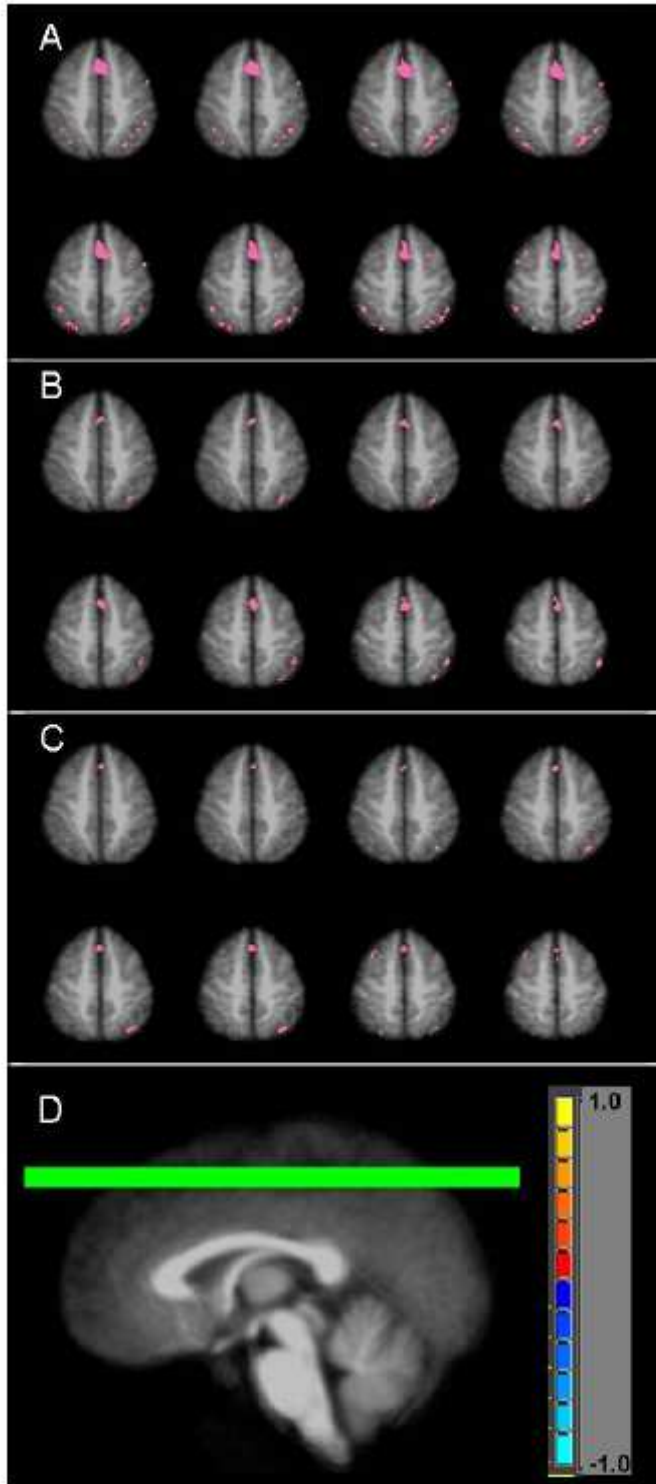
**Figure 3.2.** Arithmetic effect for (A) controls, (B) non-dysmorphic PAE, and (C) dysmorphic PAE groups. (D) indicates location of chosen axial slices (z= +46 to +53).
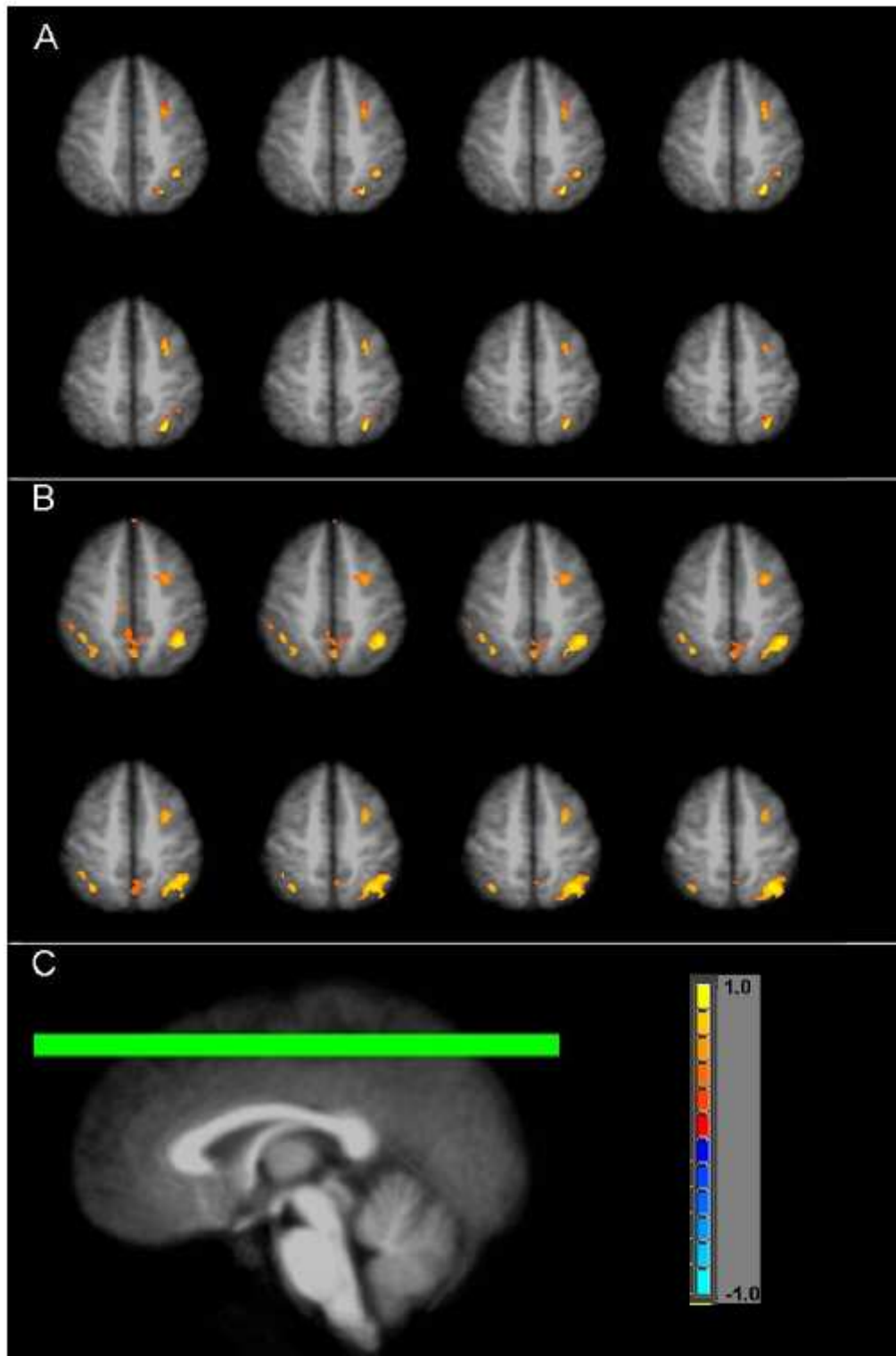
**Figure 3.3.** Subtraction map of the arithmetic effect in control subjects minus arithmetic effect in the (A) non-dysmorphic PAE subjects or (B) dysmorphic PAE subjects. (C) indicates location of chosen axial slices (z= +46 to +53).

Table 3.2. Comparison of average activation volume and percent signal change in selected regions of interest. a: TAL coordinate is center coordinate in Talairach space for each ROI; b: ExLS indicates exposure group excluding low-scoring subjects (below chance); *indicates significantly different from control group (p<0.05); +indicates marginally significant difference from control group (p<0.10).

| Region of Interest | | TAL Coordinate[a] [x, y, z] | Brodmann Area | Normalized Cluster Volume | | | | | Percent Signal Change | | | | |
|---|---|---|---|---|---|---|---|---|---|---|---|---|---|
| | | | | Control | Non-Dys | Non-Dys (ExLS)[b] | Dys | Dys (ExLS)[b] | Control | Non-Dys | Non-Dys (ExLS)[b] | Dys | Dys (ExLS)[b] |
| Superior parietal | L | [27,57,53] | 7 | 25.1 | 18.7 | 18.7 | 16.1* | 15.4* | 0.30 | 0.24 | 0.24 | 0.22 | 0.20 |
| | R | [-27,57,53] | 7 | 19.3 | 15.8 | 15.9 | 15.1 | 16.7 | 0.23 | 0.17 | 0.17 | 0.16 | 0.16 |
| Inferior parietal | L | [48,41,39] | 7, 40 | 11.8 | 12.2 | 11.4 | 8.23 | 5.74 | 0.12 | 0.12 | 0.11 | 0.09 | 0.07 |
| | R | [-48,41,39] | 7, 40 | 11.3 | 10.9 | 12.4 | 6.75* | 7.27* | 0.10 | 0.11 | 0.12 | 0.06+ | 0.05+ |
| Superior frontal | | [±19,-40,27] | 9 | 8.83 | 8.23 | 8.36 | 9.01 | 8.85 | 0.09 | 0.09 | 0.09 | 0.09 | 0.08 |
| Medial frontal | | [±9,-24,35] | 6, 9 | 7.16 | 7.12 | 7.37 | 4.64* | 4.34* | 0.07 | 0.07 | 0.08 | 0.05+ | 0.04+ |
| Middle frontal | | [±37,-29,26] | 9 | 18.1 | 15.3 | 15.7 | 16.7 | 16.6 | 0.20 | 0.16 | 0.17 | 0.16 | 0.14 |
| Inferior frontal | | [±44,-24,2] | 47 | 9.31 | 10.3 | 10.8 | 9.00 | 7.80 | 0.10 | 0.09 | 0.10 | 0.11 | 0.07 |

**3.4 Discussion**

3.4.1  <u>Summary</u>

Given that prenatal alcohol exposure has been reported to cause deficits in arithmetic processing, we expected an exposure-dependent response in task performance and in brain regions previously associated with arithmetic calculation, with significantly different activation patterns between the dysmorphic PAE group and controls. As predicted, in the present study, dysmorphic PAE individuals showed significantly diminished ability to perform a subtraction task while activation differences were noted in regions known to be associated with arithmetic processing. Activation in the left superior parietal regions, right inferior parietal region, and medial frontal gyrus during the task reflected an exposure-dependent response, with dysmorphic PAE individuals having significantly less activity. It should be noted that excluding those subjects with task performance below chance level still resulted in less activation in the dysmorphic PAE group in the same ROIs which verifies that reduced activation volume was reflective of exposure-based deficit as opposed to lack of engagement in the task. In general, the non-dysmorphic PAE group had both intermediate activation and task performance although they were not significantly different in performance from either group. Furthermore, the trend of less activation in exposed groups than controls by volume measure was also reflected in percent signal change.

It should be noted that the control group had greater activation volume in all ROIs as compared to the dysmorphic PAE group, with the exception of superior frontal gyrus, though the difference was not always significant. Additionally, activation was not significantly impaired in the non-dysmorphic group, and was actually comparable or higher as compared with controls in the inferior parietal region and medial/inferior frontal gyri. While activation

44

volume differences may appear sizeable for some ROIs, they were not always significant. This lack of significance may be due to the considerable inter-subject variability within each group. We also note that while percent signal change correlated with activation volume in this study, it was only marginally statistically significant between groups. The finding of poorer performance on the subtraction task by alcohol-affected individuals is consistent with previous reports that PAE is associated with diminished arithmetic processing in children and adolescents. As noted in the introduction, a number of studies have reported such effects. Streissguth, et al. (1994b; 1989) showed significant effects in children asked to perform arithmetic-based tasks at several stages of academic development. This longitudinal study additionally noted that 91% of the PAE children who showed arithmetic deficiency at 7 years of age, continued to show deficits at 14 years of age as opposed to only 45% in the control group (Streissguth et al., 1994b).

### 3.4.2   Context in Current Literature

This fMRI study found significant differences in activation in bilateral parietal regions as well as the medial frontal region, which are known to be associated with arithmetic processing (Dehaene et al., 2004; Dehaene et al., 2003; Menon et al., 2000). Recently, Fehr, et al. (2007) used fMRI to comprehensively identify brain areas related to a number of simple arithmetic operation (e.g., addition, subtraction, etc). One specific finding was that, among other regions, medial frontal and bilateral inferior parietal regions were significantly more activated during a "complex" subtraction task as compared to a "simple" arithmetic task. Kong, et al. (2005) also recently examined the neural correlates associated with simple and complex arithmetic operations using fMRI. Complex subtraction was defined by the authors as involving "borrowing," using tasks similar to those in the present study. They too found involvement of medial frontal gyrus, among other regions, for the complex arithmetic tasks.

45

Furthermore, left superior and right inferior parietal cortices were identified as the two subregions of the parietal lobe specifically associated with subtraction. It was further shown that all regions recruited in performing addition tasks were also required for subtraction. The association of these two subregions with subtraction calculation specifically supports our finding that the dysmorphic PAE group has less activation during the subtraction task in the left superior and right inferior parietal cortices. In the current study, differences in activation in these regions could reflect a deficiency on the part of the dysmorphic PAE group in recruiting the neuronal arithmetic network. Specifically, bilateral parietal region differences could indicate dyscalculia or the inability to perform the subtraction itself, while medial frontal gyrus differences could signify poor recruitment of a region needed for complexity ("borrowing"). This component is believed to be involved in the working memory aspect of the task (Hampson et al., 2006). Dysmorphic alcohol-affected individuals may therefore have neuronal recruitment problems in both the regions activated by all types of arithmetic function and those unique to subtraction operation calculation. Such a deficiency could also account for the poorer task performance by the dysmorphic group.

There have been few other studies that utilize fMRI to examine neurocognitive deficits associated with PAE. Malisza, et al. (2005) reported functional differences in brain regions in individuals with fetal alcohol spectrum disorder (FASD) during a spatial working memory task. In both children and adults, the authors found increased activation in FASD individuals in inferior-middle frontal lobe and greater activation in control individuals in superior frontal and parietal lobes. Additionally, adults had less overall activation as compared to children and FASD groups had lower activation overall versus controls.

Another very recent fMRI study on FASD children (Meintjes et al., Abstract #232, Organization for Human Brain Mapping, Chicago, IL, USA, 2007) reported increased activity in controls as compared to FASD in the left HIPS and left superior frontal region during an

exact addition task. The children also performed a proximity judgment task, in which increased activation in controls in left and right HIPS and frontal areas was noted, along with greater activation in FASD in the anterior cingulate and left angular gyrus. As the task in the present study mirrors exact addition more than proximity judgment, our findings are consistent with the report that FASD children have diminished neuronal activation.

### 3.4.3   <u>Limitations</u>

The control and PAE groups in this study were not IQ-matched, raising the question of whether task performance was influenced by IQ differences. However, it should be noted that while both PAE groups had significantly lower IQ as compared to the controls, only the dysmorphic PAE group had significantly poorer task performance. Furthermore, a study of learning deficits in this cohort (Howell, et al., 2006) revealed that while PAE groups specifically demonstrated arithmetic deficits, a low-IQ "special-education" contrast group had deficits in reading and spelling in addition to arithmetic. This finding suggests that the contrast group may have global damage more closely tied to their low IQ whereas the PAE groups have specific problems with math resulting from exposure.

As noted in the Results section, while the dysmorphic PAE group performed more poorly overall on the subtraction task, no correlation was found between this behavioral performance and activation. The use of different strategies by different subjects (e.g., rote memorization, counting) is a possible explanation for the general lack of association between activation and task performance. However, several studies have shown activation patterns in the parietal lobe varying with arithmetic competency (Delazer et al., 2003; Fehr et al., 2007; Grabner et al., 2007), including degree of automaticity and efficient functioning

47

with task (Ischebeck et al., 2006) and these results suggest that further research is needed to evaluate the relationship between performance and activation.

### 3.4.4   New methods

As we have noted, one challenge when using the fMRI method on a prenatally alcohol exposed population is the smaller head size that results from perturbed neurodevelopment and characterizes this group. In the present study, for example, whole brain size was found to be significantly different between both PAE groups and the control group (p=0.0048 for non-dysmorphic and p=0.0007 for dysmorphic). Bookheimer and Sowell (2005) point out that because of microcephaly, apparent increases in activation volume in the FASD population could be a result of structural abnormality or improper image registration. Therefore, studies in which anatomical images are normalized to common space may be distorting the activation differences. In this study, we wished to control for this potential methodological issue. We verified that whole brain activation differences between non-dysmorphic and dysmorphic PAE groups and controls were not significant when normalized to whole brain anatomical size (p=0.35 and p=0.39, respectively). Therefore, for our activation volume measurements, we utilized a warping method in which regions of interest were chosen by Talairach atlas in common space and their masks were warped with the inverse matrix back into original space for each individual. The activation volumes in each ROI were then normalized to the size of the whole ROI for each individual. In this way the regions of interest analyzed were uniquely sized and standardized for each individual, making the number of active voxels in the region more accurate.

### 3.4.5   <u>Future Considerations</u>

The behavioral and imaging results of this study suggest that prenatal alcohol exposure is associated with diminished arithmetic processing capabilities and that such deficits are the result of functional damage to regions known to be associated with mathematical calculation. Specifically, the dysmorphic PAE group appears to have marked impairment in recruiting neurons from bilateral parietal and medial frontal regions for arithmetic processing. Given prior characterization of the neural correlates of arithmetic operations, more heavily exposed alcohol-affected individuals may have difficulty with both the operation itself and its complexity. Furthermore, that the non-dysmorphic PAE group did not have significant activation or performance problems implies a range of responses to the teratogenic exposure that require further study to delineate. Overall, the findings of this study further support the direct relationship between prenatal alcohol exposure and functional brain damage, specifically elucidating a neurological basis for observed arithmetic deficit.

A next step in understanding the relationship between structural damage induced by PAE exposure and its effects on the functional brain activation is to obtain a more direct correlation between performance and brain activity for cognitive tasks. Using a simpler task could decrease the high variance in activation measures and elucidate a quantifiable relationship between arithmetic calculation and neuronal activation in alcohol affected and exposed individuals. It should also be noted that since the brain regions affected in the present study are associated specifically with subtraction, a paradigm consisting of several different arithmetic operations could elucidate the extent of dyscalculia in the affected population.

## 3.5 References

Abel EL (1995) An update on incidence of FAS: FAS is not an equal opportunity birth defect. Neurotoxicol Teratol 17(4):437-43.

Archibald SL, Fennema-Notestine C, Gamst A, Riley EP, Mattson SN, Jernigan TL (2001) Brain dysmorphology in individuals with severe prenatal alcohol exposure. Dev Med Child Neurol 43(3):148-54.

Bookheimer SY, Sowell ER (2005) Brain imaging in FAS: commentary on the article by Malisza et al. Pediatr Res 58(6):1148-9.

Cantlon JF, Brannon EM, Carter EJ, Pelphrey KA (2006) Functional imaging of numerical processing in adults and 4-y-old children. PLoS Biol 4(5):e125.

Cohen MS (1997) Parametric analysis of fMRI data using linear systems methods. Neuroimage 6(2):93-103.

Coles CD (2001) Fetal alcohol exposure and attention: moving beyond ADHD. Alcohol Res Health 25(3):199-203.

Coles CD, Brown RT, Smith IE, Platzman KA, Erickson S, Falek A (1991) Effects of prenatal alcohol exposure at school age. I. Physical and cognitive development. Neurotoxicol Teratol 13(4):357-67.

Coles CD, Platzman KA, Lynch ME, Freides D (2002) Auditory and visual sustained attention in adolescents prenatally exposed to alcohol. Alcohol Clin Exp Res 26(2):263-71.

Coles CD, Platzman KA, Raskind-Hood CL, Brown RT, Falek A, Smith IE (1997) A comparison of children affected by prenatal alcohol exposure and attention deficit, hyperactivity disorder. Alcohol Clin Exp Res 21(1):150-61.

Conry J (1990) Neuropsychological deficits in fetal alcohol syndrome and fetal alcohol effects. Alcohol Clin Exp Res 14(5):650-5.

Dehaene S, Molko N, Cohen L, Wilson AJ (2004) Arithmetic and the brain. Curr Opin Neurobiol 14(2):218-24.

Dehaene S, Piazza M, Pinel P, Cohen L (2003) Three parietal circuits for number processing. Cognitive Neuropsychology 20(3/4/5/6):487-506.

Delazer M, Domahs F, Bartha L, Brenneis C, Lochy A, Trieb T, Benke T (2003) Learning complex arithmetic--an fMRI study. Brain Res Cogn Brain Res 18(1):76-88.

Fehr T, Code C, Herrmann M (2007) Common brain regions underlying different arithmetic operations as revealed by conjunct fMRI-BOLD activation. Brain Res 1172:93-102.

Fernhoff PM, Smith IE, Falek A (1980) Dysmorphia Checklist. Document available through the Maternal Substance Abuse and Child Development Project, Department of Psychiatry and Behavioral Sciences, Emory University School of Medicine.

Goldschmidt L, Richardson GA, Stoffer DS, Geva D, Day NL (1996) Prenatal alcohol exposure and academic achievement at age six: a nonlinear fit. Alcohol Clin Exp Res 20(4):763-70.

Grabner RH, Ansari D, Reishofer G, Stern E, Ebner F, Neuper C (2007) Individual differences in mathematical competence predict parietal brain activation during mental calculation. Neuroimage 38(2):346-56.

Hampson M, Driesen NR, Skudlarski P, Gore JC, Constable RT (2006) Brain connectivity related to working memory performance. J Neurosci 26(51):13338-43.

Howell, KK, Lynch, ME, Platzman, KA, Smith, GH, Coles, CD (2006) Prenatal alcohol exposure and ability, academic achievement, and school functioning in adolescence: a longitudinal follow-up. J Pediatr Psychol 31(1): 116-26.

Hubbard TL (2005) Representational momentum and related displacements in spatial memory: A review of the findings. Psychon Bull Rev 12(5):822-51.

Ischebeck A, Zamarian L, Siedentopf C, Koppelstatter F, Benke T, Felber S, Delazer M (2006) How specifically do we learn? Imaging the learning of multiplication and subtraction. Neuroimage 30(4):1365-75.

Jones KL, Smith DW (1973) Recognition of the fetal alcohol syndrome in early infancy. Lancet 2(7836):999-1001.

51

Kazui H, Kitagaki H, Mori E (2000) Cortical activation during retrieval of arithmetical facts and actual calculation: a functional magnetic resonance imaging study. Psychiatry Clin Neurosci 54(4):479-85.

Klahr D (1973) *Quantification processes.* Academic Press, Inc., 111 Fifth Ave., New York, New York 10003.

Kong J, Wang C, Kwong K, Vangel M, Chua E, Gollub R (2005) The neural substrate of arithmetic operations and procedure complexity. Brain Res Cogn Brain Res 22(3):397-405.

Kopera-Frye K, Dehaene S, Streissguth AP (1996) Impairments of number processing induced by prenatal alcohol exposure. Neuropsychologia 34(12):1187-96.

Malisza KL, Allman AA, Shiloff D, Jakobson L, Longstaffe S, Chudley AE (2005) Evaluation of spatial working memory function in children and adults with fetal alcohol spectrum disorders: a functional magnetic resonance imaging study. Pediatr Res 58(6):1150-7.

Mattson SN, Riley EP (1998) A review of the neurobehavioral deficits in children with fetal alcohol syndrome or prenatal exposure to alcohol. Alcohol Clin Exp Res 22(2):279-94.

Mattson SN, Riley EP, Gramling L, Delis DC, Jones KL (1998) Neuropsychological comparison of alcohol-exposed children with or without physical features of fetal alcohol syndrome. Neuropsychology 12(1):146-53.

McCarthy RA, Warrington E (1987) *Cognitive mechanism in normal and impaired number processing, in: G. Deloche, X. Seron (Eds.), Mathematical Disabilities: Cognitive Neuropsychological Perspective.*

Menon V, Rivera SM, White CD, Glover GH, Reiss AL (2000) Dissociating prefrontal and parietal cortex activation during arithmetic processing. Neuroimage 12(4):357-65.

Nash K, Rovet J, Greenbaum R, Fantus E, Nulman I, Koren G (2006) Identifying the behavioural phenotype in Fetal Alcohol Spectrum Disorder: sensitivity, specificity and screening potential. Arch Womens Ment Health 9(4):181-6.

Olson HC, Feldman JJ, Streissguth AP, Sampson PD, Bookstein FL (1998) Neuropsychological deficits in adolescents with fetal alcohol syndrome: clinical findings. Alcohol Clin Exp Res 22(9):1998-2012.

Riley EP, McGee CL, Sowell ER (2004) Teratogenic effects of alcohol: a decade of brain imaging. Am J Med Genet C Semin Med Genet 127(1):35-41.

Smith IE, Coles CD, Lancaster J, Fernhoff PM, Falek A (1986) The effect of volume and duration of prenatal ethanol exposure on neonatal physical and behavioral development. Neurobehav Toxicol Teratol 8(4):375-81.

Sowell ER, Thompson PM, Mattson SN, Tessner KD, Jernigan TL, Riley EP, Toga AW (2001) Voxel-based morphometric analyses of the brain in children and adolescents prenatally exposed to alcohol. Neuroreport 12(3):515-23.

Spadoni AD, McGee CL, Fryer SL, Riley EP (2007) Neuroimaging and fetal alcohol spectrum disorders. Neurosci Biobehav Rev 31(2):239-45.

Streissguth AP, Barr HM, Olson HC, Sampson PD, Bookstein FL, Burgess DM (1994a) Drinking during pregnancy decreases word attack and arithmetic scores on standardized tests: adolescent data from a population-based prospective study. Alcohol Clin Exp Res 18(2):248-54.

Streissguth AP, Barr HM, Sampson PD, Bookstein FL (1994b) Prenatal alcohol and offspring development: the first fourteen years. Drug Alcohol Depend 36(2):89-99.

Streissguth AP, Bookstein FL, Sampson PD, Barr HM (1989) Neurobehavioral effects of prenatal alcohol: Part III. PLS analyses of neuropsychologic tests. Neurotoxicol Teratol 11(5):493-507.

Talairach J, Tournoux P (1988) Co-planar stereotaxic atlas of the human brain. New York: Thieme Medical Publishers, Inc.

Zhang YT, Zhang Q, Zhang J, Li W (2005) Laterality of brain areas associated with arithmetic calculations revealed by functional magnetic resonance imaging. Chin Med J (Engl) 118(8):633-8.

**CHAPTER 4**

**Default Mode Network Dysfunction in Adults with Prenatal Alcohol Exposure**

**4.1 Background**

4.1.1 <u>Prenatal Alcohol Exposure and Cognitive Neuroimaging</u>

Neurocognitive deficits as well as social and adaptive dysfunction have been observed in individuals with prenatal alcohol exposure (PAE) (Guerri et al., 2009; Mattson and Riley, 1998). In general, adolescents with PAE have lower IQ, often accompanied by impaired visuo-spatial, attentional, verbal learning, and memory abilities (Coles et al., 1997; Conry, 1990; Mattson et al., 1998; Olson et al., 1998). While behavioral studies have documented deficiencies in individuals with PAE, the underlying neuronal causes of the outcomes are still not well understood. There are only a few functional neuroimaging studies on the PAE population, all of which focus on the task-positive activation patterns created by the blood-oxygen level dependent (BOLD) response in functional MRI (fMRI). Malisza, et al. (2005) reported functional differences in brain regions in both children and adults with fetal alcohol spectrum disorder (FASD) during a spatial working memory task, and a separate study of verbal learning in children with heavy PAE found exposed children had altered patterns of activation during a paired association task (Sowell et al., 2007). A recent study from our group (Santhanam et al., 2009) investigated arithmetic processing and found less activation in dysmorphic PAE individuals in calculation-associated regions. Though these studies do reveal brain regions associated with specific cognitive dysfunction, they do not examine the possibility of contribution from a global underlying attentional modulation effect.

### 4.1.2 Default Mode Network

*4.1.2.1 Concept*

Recent discovery of consistent regions that are more active during resting periods than during cognitive demand has led to the characterization of a so-called "default mode network" (DMN) in the brain (Greicius et al., 2003b). Comprised of the medial prefrontal cortex (MPFC), posterior cingulate cortex (PCC), precuneus, inferior parietal cortices, and medial temporal regions, the network has been shown to exhibit reduced activation in the presence of high cognitive demand (Golland et al., 2008; Greicius et al., 2003b; Margulies et al., 2007). Multiple studies have shown that DMN deactivation increases with increased task difficulty (McKiernan et al., 2006; Singh and Fawcett, 2008), and that activity persists during simple sensory tasks, in which good task performance is achievable with little attentional resources (Greicius et al., 2003b; Wilson et al., 2008). Attention lapse, marked by longer reaction time and lower accuracy on an attentional control task, has been associated with less task-induced deactivation of the DMN (Weissman et al., 2006). Thus patters of task-related DMN activity are thought to reflect an attentional modulation unrelated to the specific task being performed (Broyd et al., 2009).

*4.1.2.2 Interference Hypothesis*

Recently, Sonuga-Barke and Castellanos, et al. hypothesized that the attenuation of DMN activity during cognitive demand is a point of dysfunction in those prone to attentional lapse (2007). Their "default mode interference hypothesis" posits that as attention to a cognitive task lessens, DMN deactivation also lessens, such that DMN activity is persistent in the

55

task-active state and thus interferes with task performance. Task-induced DMN deactivation has been studied in several populations with dysfunctions of attention, including schizophrenia, Alzheimer's disease, normal aging, and autism spectrum disorder (Kennedy et al., 2006; Persson et al., 2007; Pomarol-Clotet et al., 2008; Rombouts et al., 2005). While PAE is known to have cognitive task-related attentional problems, such as increased distractibility and longer reaction times (Shaywitz et al., 1981; Simmons et al., 2002; Streissguth et al., 1986), it is unclear whether these outcomes contribute to the general cognitive deficits seen in the population. Patterns of task-related deactivation in PAE could reveal whether attentional modulation is contributing to poorer task performance.

### 4.1.3  Aims

Previously (Chapter 3), we identified arithmetic processing dysfunction in PAE by reduced task performance and activation in arithmetic processing centers (Santhanam et al., 2009). In the present study, we examined deactivation of the DMN during the arithmetic task (using a letter-matching task as baseline). Given known attentional problems and the lower task performance and activation reported in the prior study, we expected less deactivation in the DMN in affected groups as compared to control groups. Additionally, given known white matter alterations in several areas of the brain caused by PAE, we examined structural and functional connectivity of the DMN by diffusion tensor imaging (DTI) and resting state fMRI signal correlation, respectively. We expected reduced white matter integrity and synchronization between the medial prefrontal cortex and posterior cingulate in the groups with PAE as compared to controls. Furthermore, as the underlying DMN structure has been shown to reflect its functional connectivity (Greicius et al., 2009; van den Heuvel et al., 2008), we expected a correlative relationship between the DTI and resting state correlation measures across all groups.

56

**4.2 Methods**

4.2.1   Participants

Participants were young adults recruited from a longitudinal cohort, derived from a predominantly African-American, low socio-economic status (SES) population, first identified in the prenatal period between 1979 and 1986 (Smith et al., 1986). All participants were aged 18-24 at the time of participation. Participants were part of a longitudinal study with large-scale follow-ups at birth, 7 years, mid-adolescence, and young adulthood. Participants (and guardians, if necessary) gave informed consent to continue to participate in the research when recontacted as adults. From the longitudinal cohort, three groups were selected for participation in the current study based on prenatal maternal reports of alcohol use in pregnancy and Dysmorphia Checklist (Coles et al., 1985) ratings of physical characteristics related to prenatal alcohol exposure. The ratings were completed at follow-up evaluations at birth, 7 years, and mid-adolescence. Groups were defined as follows: 1) Exposed, positive for dysmorphia, (DYS: mother reported use of alcohol during pregnancy and the participant received a dysmorphia rating that was at least one standard deviation above the mean at one of the three evaluations); 2) Exposed, without dysmorphia (Non-DYS: mother reported use of alcohol during pregnancy and the participant received no dysmorphia ratings that were one standard deviation above the mean); and 3) Unexposed controls (mother reported no use of alcohol during pregnancy) from the same SES population. The mean ounces of absolute alcohol consumption per week of pregnancy for groups 1 and 2 were 13.8 (sd=13.4) and 7.7 (sd=13.3), respectively. Demographics information for the cohort is given in Table 2.1. A subset of subjects from Table 2.1 was used in the present study. Before imaging was done, potential participants who were left

57

handed or had some risk during the MRI procedure (e.g., due to pregnancy or metal in the body) were excluded. Additionally, certain subjects were excluded post-imaging from each analysis described below due to excessive head motion or artifact. As a result, the number of subjects in the final analyses were as follows: Resting-state analysis: DYS n=21, Non-DYS n=21, CON n=22; Functional (arithmetic) task analysis: DYS n=19, Non-DYS n=18, CON n=18; and DTI analysis: DYS n=27, Non-DYS n=29, CON n=26.

### 4.2.2   Experimental Design

All data, including DTI, resting state, and the arithmetic task, were collected in a single session. For the resting state scan, participants were asked only to gaze at a fixation cross. The arithmetic task (Connor, 2004) was block-design, involving alternating between a letter-matching control task (10 consecutive presentations) and a subtraction task (10 consecutive presentations). Five blocks of each task, with questions in random order in each block, were administered over 5 minutes. The task is described in further detail (Chapter 3) in our previous publication (Santhanam et al., 2009).

### 4.2.3   Image Acquisition

All images were acquired on a 3T Siemens Trio scanner (Siemens Medical Solutions, Erlangen, Germany). Both the functional and resting state scans used single-shot T2*-weighted echo planar imaging (EPI) sequences with the following parameters: functional run: 34 contiguous axial slices, 3 mm thickness, TR/TE/FA/FOV of 3000ms/32ms/90⁰/22cm, scan time of 5:06 min, 102 time points; resting state run: 10 contiguous axial slices, 5 mm thickness, TR/TE/FA/FOV 750ms/34ms/50⁰/22cm, scan t ime of 3:34 min, 280 time points. DTI data was acquired using a diffusion-weighted EPI sequence with the following

parameters: gradients applied in 12 directions (4 averages) with b-value of 1000 s/mm2, 34 contiguous axial slices, 2mm thickness, TR/TE/FOV of 7700ms/90ms/22cm, scan time of 7:08 min.

### 4.2.4    Image Analysis

*4.2.4.1 fMRI data*

FMRI analysis was done in AFNI (http://afni.nimh.nih.gov/afni, 09/2009). Preprocessing included slice timing correction, volume registration, band pass filtering (resting data only), signal normalization (functional data only), and 5mm FWHM Gaussian blur. Additionally, multiple linear regression of the resting state data was done to remove contributions from head motion (6 parameters: x, y, z displacements and roll, pitch, yaw rotations), white matter, cerebrospinal fluid, and whole brain signals (Fox et al., 2005b). Recently, the regression of whole brain signal from resting-state data has become controversial as it is thought to introduce anti-correlated networks into functional connectivity measures (Murphy et al., 2009). However, a recent report quantifying the effect of various pre-processing steps on connectivity measures determined that while using global signal regression does introduce anti-correlations, it also approximately doubles the sensitivity to positive correlations and is therefore recommended (Weissenbacher et al., 2009). Given the ongoing debate, we chose to analyze the data both with and without global regression.

In order to identify regions of deactivation during higher cognition, a general linear model was derived using the letter-matching task as the baseline and arithmetic task blocks as the stimulations. Convolution of the boxcar stimulation functions with a standard impulse response function ($y=t^b \times \exp(-t/c)$, where b and c are constants) produced the main

regressor (Cohen, 1997b). The 6 head motion parameters were used as additional regressors, and the output of the regression analysis (group activation maps) was generated by Talairach (Talairach and Tournoux, 1988b) transforming the functional data to common space and averaging across all subjects. To account for multiple comparisons, voxel-wise and cluster thresholding were applied. Monte Carlo simulation revealed that these thresholds corresponded to a false-positive discovery rate (alpha) of less than 1%.

Clusters of significant deactivation (with voxel-wise thresholding of $p<0.05$ and cluster thresholding of 10 contiguous voxels) at the MPFC and PCC were identified. While the DMN is comprised of several nodes, these two were chosen for subsequent resting-state analysis because they had the most robust deactivation clusters and were the most consistently included in slice coverage. Differences in deactivation between the letter matching and arithmetic tasks were determined by extracting and averaging the regression coefficients from the clusters identified as the MPFC and PCC, respectively. Deactivation differences in each ROI were examined independently given recent findings of unique functional specialization for each of these two DMN loci (Uddin et al., 2009). These clusters were chosen as their robust activity and connectivity within the DMN is well-established (Greicius et al., 2003b; Margulies et al., 2007). Difference maps were generated to visualize the differences in deactivation, masked over the MPFC and PCC regions, respectively, between controls and each PAE group (voxel-wise thresholding of $p<0.10$ and cluster thresholding of 4 contiguous voxels). Due to considerable head size differences in the PAE population, the deactivation clusters from the group activation map were masked and back-projected into native space for each subject for quantification of the deactivation difference. Average unthresholded regression coefficients were converted to percent signal change and compared between groups by t-test.

60

Using the deactivation clusters as masks, corresponding PCC regions in the resting state were extracted for each individual in native space, and correlation maps were derived. Voxel-wise thresholding of p<0.001 and cluster threshold of 8 contiguous voxels (corresponding to multiple comparisons correction of alpha<1% by Monte Carlo simulation) were used. Using the MPFC functionally deactivated region as a mask, a cluster of significant correlation with PCC in the resting state was found for each subject. For this correlated region of the DMN, the average correlation coefficient was extracted for each subject and compared between groups by t-test. Additionally, to examine whether differences exist in signal amplitude in the MPFC and PCC, mean signal intensity over the resting state run was compared between groups [*].

*4.2.4.2 DTI data*

Voxel-wise analysis of DTI data was performed using the tract-based spatial statistics (TBSS) program from FSL 4.0 (http://www.fmrib.ox.ac.uk/fsl/, 09/2009). TBSS offers the advantage of non-linear registration followed by projection onto an alignment-invariant white matter "skeleton." It was chosen because TBSS is less reliant on image registration between subjects for comparison (Smith et al., 2006) and was previously shown to elucidate differences between exposed and control groups from the same cohort in subregions of the corpus callosum (Li et al., 2009). Briefly, a fractional anisotropy (FA) template specific to the PAE population in this study was created from the FA images of all subjects. The average FA image was then eroded to form a mean FA skeleton to which the FA map of each individual is aligned. Details of the template creation, skeleton derivation, and alignment can be found in our previously published study (Li et al., 2009). Skeletons were derived in the same manner from FA, mean diffusivity (MD), axial diffusivity (AD), and radial diffusivity (RD) maps.

61

A permutation algorithm (Smith et al., 2006) that does not require a Gaussian distribution was used to run statistics on the group differences in DTI measures. Parameters were 5000 random permutations and comparisons were corrected to a family-wise (type I) error rate of less than 5%. Threshold-free cluster enhancement (TFCE: in FSL version 4.1) was used in place of voxel-wise or cluster thresholding. TFCE is a relatively new technique that allows for statistical analysis without an initial cluster-forming threshold. In this method, each voxel is given a value corresponding to the sum of the "scores" of its surrounding voxels; the score is determined by the height (increased incrementally from zero to the signal intensity of the given voxel) and extent of the cluster that contains the voxel. TFCE has been shown to improve sensitivity of signal detection, with an optimized height (H=2) and extent (E=0.5). Details of TFCE implementation and validation are provided by Smith and Nichols (2009). Skeleton-based region-of-interest (**ROI)** analysis of the bilateral cingulum bundles was then performed by defining the ROI as the intersection of the anatomical bilateral cingulum (as identified by a white matter atlas provided by FSL) and the FA skeleton. The ROI mask was used to extract average FA, MD, AD, and RD over this region. Statistical comparison of these DTI measures in exposed versus controls (t-test) was performed in SPSS 15.0 (SPSS Inc., Chicago, IL).

In order to examine the relationship between structural and functional connectivity of the DMN, correlation between DTI measures and functional synchrony (defined by average correlation coefficient over MPFC region in correlation map with PCC region) was determined. Statistical analysis was again performed in SPSS 15.0. Pearson's correlation coefficient was found for all subjects together, as well as within each exposure group individually (n=14 for control and dysmorphic groups; n=15 for non-dysmorphic PAE group).

62

**4.3 Results**

4.3.1    Functional and Resting-State Results

Figure 4.1 is a group average activation map indicating regions of DMN deactivation during the arithmetic task (using the letter-matching task as baseline). The most robust clusters of deactivation were found in the MPFC and PCC regions, identified in the figure. As difference maps in Figure 4.2 indicate, deactivation was significantly less in the dysmorphic PAE group as compared to controls, while the non-dysmorphic group had lower but not-significant deactivation compared to controls. This negative activation was quantified by extracting the unthresholded percent signal change in the MPFC and PCC, respectively (Table 2). The PCC cluster from Figure 4.1 was also used as a seeding region in the resting-state data to examine functional connectivity. Figure 4.3 shows the group correlation map using the PCC seed. Once again the most robust clusters are in the PCC and MPFC regions. Figures 4.3a and 4.3b indicated similar correlation extent and intensity (without introducing significant anti-correlation in the ROIs), regardless of global signal regression. Given the previously cited evidence that such regression increases sensitivity, resting-state data with the global signal removed was chosen for subsequent analysis. To compare the correlation with PCC between groups (as a measure of baseline DMN connectivity), difference maps over the MPFC region (identified in Figure 4.1) were rendered comparing the control group to both exposure groups (Figure 4.4). The control group appeared to have greater correlation in this region (positive difference). Correlation coefficients were extracted from the MPFC region in the resting-state using the deactivated MPFC cluster from Figure 4.1 as a mask (Table 4.1). Average correlation coefficients were significantly greater in the control group as compared to both exposure groups, and the two PAE groups had comparable correlation. Signal amplitude over the resting state time-course was found to be comparable between PAE

63

groups and controls (results not shown; p=0.36 for non-dysmorphic PAE group, p=0.23 for

dysmorphic PAE group).
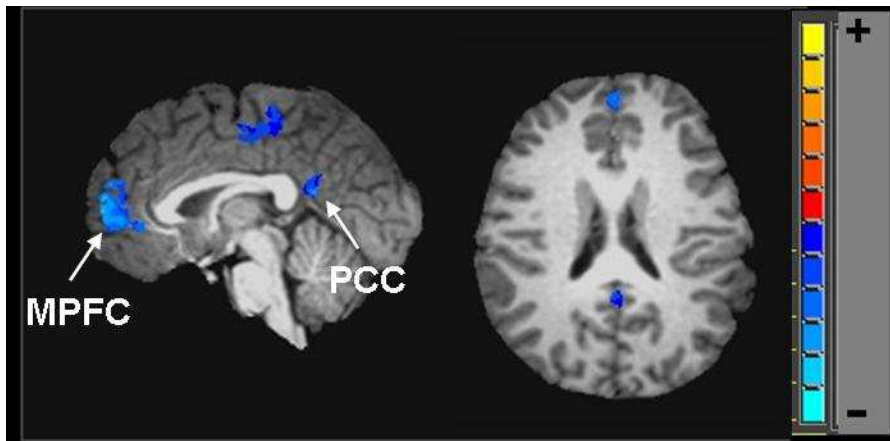


**Figure 4.1.** Regions of default mode deactivation during arithmetic task (using letter-matching task as baseline). MPFC and PCC clusters from these group average activation maps were used for subsequent resting-state analysis. Color bar indicates these regions are negatively activated.
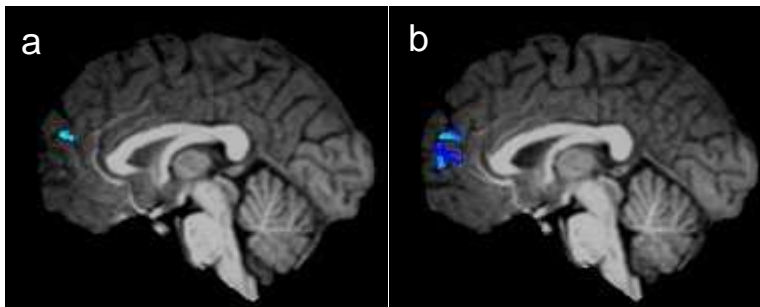


**Figure 4.2.** Difference map of default mode deactivation between a) control and non-dysmorphic PAE groups and b) control and dysmorphic PAE groups. Map is masked at the MPFC and PCC regions identified in Figure 4.1. Negative differences (blue shades) indicate less deactivation in the PAE group as compared to the control group.
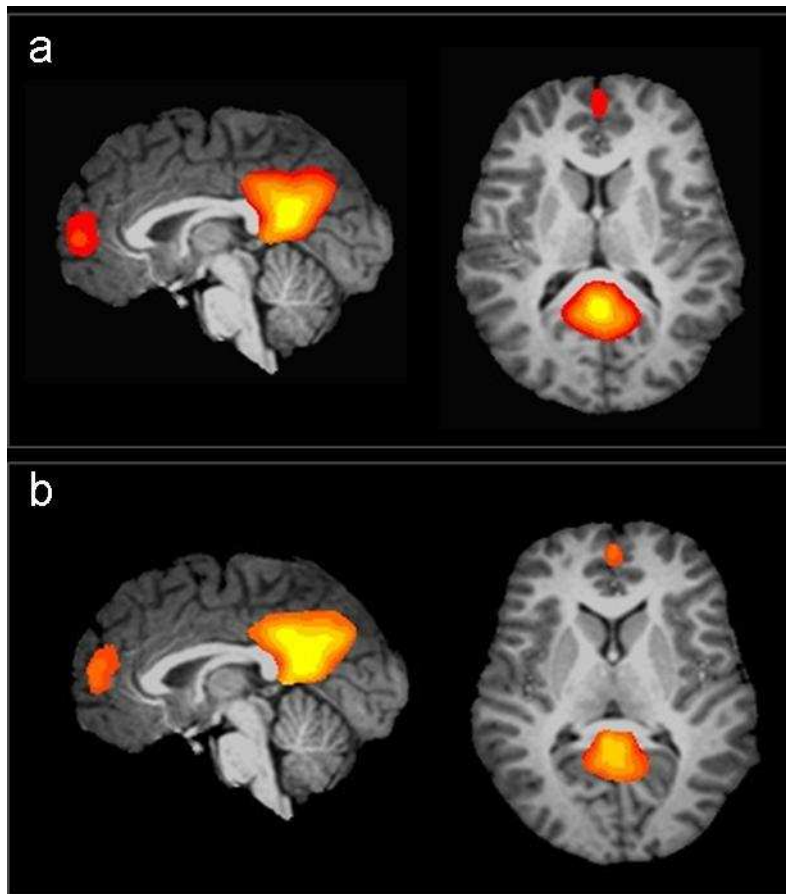
**Figure 4.3.** Resting-state functional connectivity (correlation) group maps (a) with and (b) without global signal regression. At threshold p<0.001, only positive correlation (red-yellow: see color bar in Figure 4.1) was noted with the seeding region regardless of regression method. Seeding was in the PCC region defined in Figure 4.1.
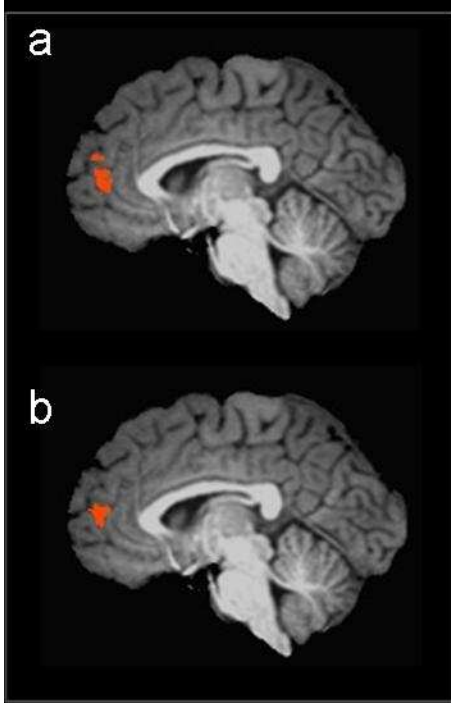
**Figure 4.4.** Difference correlation maps of (a) Control-Non Dysmorphic PAE and (b) Control-Dysmorphic PAE groups seeded at the PCC region and masked at MPFC region identified in Figure 1. Control groups had more correlation with the MPFC than either exposure group (red-yellow indicates positive difference). Threshold used was p<0.05 and 10 contiguous voxels (multiple comparison correction of alpha<1%).

**Table 4.1.** Comparison of resting-state DMN correlation and task-based DMN deactivation between control and PAE groups. * = significantly different from control group by t-test (p<0.05); SEM = standard error of the mean; GSR = global signal regression.

| Connectivity/Activation Measure | Control | Non-Dysmorphic PAE | Dysmorphic PAE |
|---|---|---|---|
| Percent Signal Change in MPFC (SEM) | -0.808 (0.087) | -0.789 (0.094) | -0.604* (0.098) |
| Percent Signal Change in PCC (SEM) | -0.265 (0.095) | -0.168 (0.060) | -0.174 (0.110) |
| Mean Correlation Coefficient in MPFC using PCC seed: with GSR (SEM) | 0.285 (0.030) | 0.190* (0.033) | 0.206* (0.027) |
| Mean Correlation Coefficient in MPFC using PCC seed: without GSR (SEM) | 0.428 (0.044) | 0.326* (0.023) | 0.343* (0.023) |

66

Figure 4.5 indicates the results of whole-brain TBSS. Differences in FA were detectable at the bilateral cingulum bundle between groups using a family-wise error of less than 5% (pFWE<0.05) and the TFCE method for cluster identification. However, in the subsequent regional skeleton-based ROI analysis (using bilateral cingulum bundles as the ROI), differences between groups in MD and RD were additionally detectable (Table 4.2). ROI extraction was done to compare differences in average FA, MD, AD, and RD between groups. Both PAE groups had lower FA and higher RD values as compared to controls and additionally the dysmorphic PAE group had a higher MD than controls.

To examine whether structural and functional connectivity were affected in a corresponding manner, correlation between the MPFC-PCC correlation coefficient and DTI measures was determined. A positive correlation was found (r=0.322, p=0.035) between functional connectivity and FA when considering all subjects together (Figure 4.6). No significant correlations were found for any other DTI measures. Correlation between MPFC-PCC connectivity and FA was further examined within each individual group, and a significant positive correlation was found for the control group (r=0.571, p=0.033), a nonsignificant negative trend for the non-dysmorphic PAE group, and a positive trend for the dysmorphic PAE group (r=0.404, p=0.092).
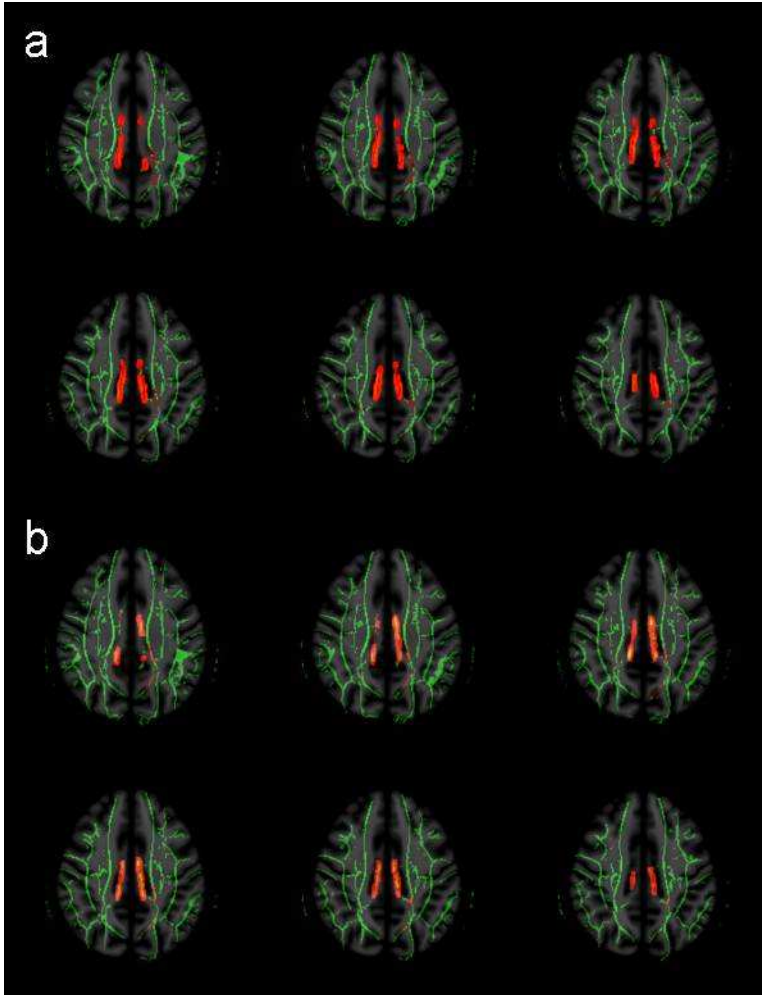
**Figure 4.5.** TBSS results for bilateral cingulum. ROI shows significant differences between (a) Control and Non Dysmorphic PAE groups and (b) Control and Dysmorphic PAE groups in FA. Green indicates mean FA skeleton and red indicates regions of significant difference between groups, with thickened red-yellow for the bilateral cingulum ROI. Axial slices shown are z=107 to z=112.

**Table 4.2.** Comparison of DTI measures between control and PAE groups by skeleton-based ROI analysis of bilateral cingulum. FA = fractional anisotropy; MD = mean diffusivity (x$10^{-3}$ mm$^2$/s); AD = axial diffusivity λ1 (x$10^{-3}$ mm$^2$/s); RD = radial diffusivity λ2+λ3/2 (x$10^{-3}$ mm$^2$/s); * = significantly different from control group by t-test (p<0.05); SEM = standard error of the mean.

| DTI Measure: Mean value over bilateral cingulum bundles | Control | Non-Dysmorphic PAE | Dysmorphic PAE |
| --- | --- | --- | --- |
| FA (SEM) | 0.570 (0.008) | 0.539* (0.007) | 0.546* (0.008) |
| MD (SEM) | 0.731 (0.006) | 0.741 (0.009) | 0.750* (0.008) |
| AD (SEM) | 1.265 (0.012) | 1.239 (0.015) | 1.272 (0.012) |
| RD (SEM) | 0.464 (0.008) | 0.492* (0.009) | 0.491* (0.011) |
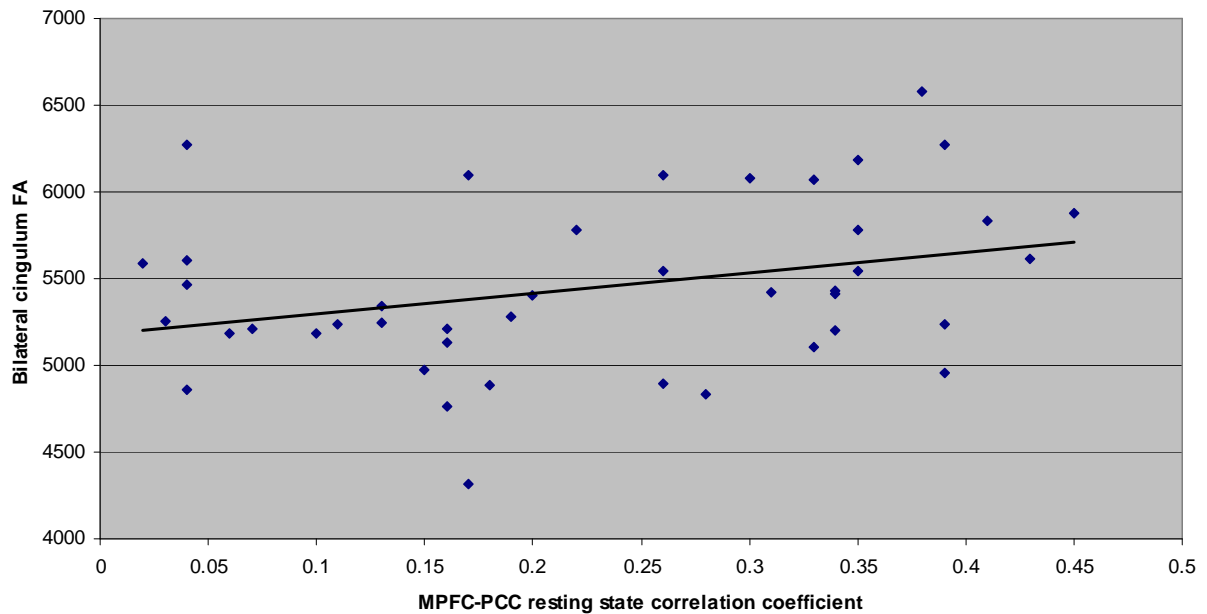


**Figure 4.6.** Scatterplot showing relationship between bilateral cingulum FA and MPFC-PCC resting state correlation for all subjects. Positive correlation is noted (r=0.322, p=0.035).

69

**4.4 Discussion**

4.4.1   <u>Summary</u>

Task-related deactivation, as well as structural and functional connectivity, of the DMN appears to be affected by PAE. Dysmorphic PAE individuals had significantly less deactivation in the MPFC and PCC during the arithmetic task as compared to controls. Structural connectivity and functional synchrony between PCC and MPFC regions were also lower for both PAE groups as compared to controls at rest, and these measures were additionally correlative.

4.4.2   <u>Context in Current Literature</u>

As previously mentioned, deactivation of the DMN has been observed to be altered in several clinical populations. In general, these studies agree that there exists a competition between an extrinsic (cognitive functioning) network and an intrinsic (default mode) network (Clare Kelly et al., 2008), and that this competition can be a point of dysfunction. Attentional modulation during the arithmetic task appears to be affected for the dysmorphic PAE group in this study, which can be related to their poorer task performance and lower activation in arithmetic centers (previously reported). It should be noted that even without the lowest scoring dysmorphic PAE participants, the reduced activation was still observed (previously reported), implying that the arithmetic centers are at least partially responsible for the lower performance. However, it is possible that the poorer performance is due to a combination of reduced activity in the regions required for arithmetic processing and an inability to control attention to the task.

70

Though the majority of literature on DMN functioning regards the network as homogenous, recently Uddin, et al. has investigated the possibility of unique functional specialization within the DMN (2009). They examined the positively and anti-correlated regions for the ventral medial PFC (vmPFC) and PCC regions, respectively, as these are the most robust nodes of the network. Findings included significant differences in networks anti-correlated with each node, with vmPFC activity anti-correlated with parietal visual spatial and temporal attention networks as compared to PCC activity, which was anti-correlated with motor control networks (Uddin et al., 2009). Granger causality results also suggested modulation of these loci upon the task-positive activity in these networks. Therefore, the authors conclude that activity in these two DMN loci may independently and uniquely influence task-positive activation in the networks with which they are anti-correlated. As the present study found significant DMN deactivation differences in the MPFC only (and not in the PCC region), it follows that arithmetic task activation would be affected, given the strong reliance on bilateral parietal visual spatial networks for arithmetic processing (Dehaene et al., 2004; Santhanam et al., 2009).

Both PAE groups had reduced structural and resting state functional connectivity between the MPFC and PCC. The cingulum bundles connecting these two nodes of the DMN had lower FA in both groups, and additionally increased RD in the dysmorphic PAE group. Furthermore, the resting state connectivity was reduced in both PAE groups, with comparable signal magnitude among groups confirming a dysfunction of synchrony specifically. The correlation between resting state DMN connectivity and FA of the cingulum bundles when all subjects were taken together implies a relationship between structural and functional damage in this part of the network. This positive correlation is consistent with previously mentioned studies of healthy subjects examining structural connectivity of the

71

DMN and its relation to functional connectivity (Greicius et al., 2003b), particularly in the case of the cingulum bundles (van den Heuvel et al., 2008). These results imply that PAE results in a "disconnection" between the MPFC and PCC nodes of the DMN, which may be a result of the underlying structural alterations.

### 4.4.3   Exposure-Dependent Effects

The non-dysmorphic PAE group had intermediate (but not significant from controls) deactivation of the DMN during the arithmetic task, which accompanies their previously reported intermediate task performance and activation. However, structural and baseline functional connectivity was significantly impaired in this group as compared to controls, with measures more comparable to the dysmorphic PAE group. Additionally, while the functional connectivity of control and dysmorphic PAE groups trended towards a positive correlation with FA, the non-dysmorphic PAE group reflected a non-significant negative correlation. One possible reason is that generally studies have shown stronger correlation between structural and functional connectivity when both measures are higher (stronger connectivity in each) (Damoiseaux and Greicius, 2009). Therefore, PAE affected groups may have less agreement due to reduction in both types of connectivity (which may also explain the lack of significance in the dysmorphic PAE group). It is difficult to interpret the trend towards negative correlation between cingulum bundle FA and functional connectivity between the PCC and ACC seen in the non-dysmorphic group, but it is likely that the overall PAE-induced damage is intermediate in this group, and so subjects may have varying degrees of structural or functional impairment in this network.

72

### 4.4.4  Technical Considerations

It should be noted that while the previous study on this cohort did not find diffusion-related differences at the cingulum when applying TBSS voxel-wise to the whole brain, the skeleton-based ROI findings can still be valid. It is possible that via the whole-brain method cingulum differences were masked by greater differences in the corpus callosum, but a more likely reason for the discrepancy is the use of the new TFCE statistical analysis versus the cluster-wise method applied in the previous study. TFCE is a newly developed alternative to voxel-wise and cluster thresholding that does not require an initial cluster-forming threshold. It has been validated for identifying clusters individually with less bias towards diffuse or focal signal shapes. The use of TFCE on the present dataset may have detected clusters more robustly than the previous study on the same cohort, which used a relatively strict threshold of pFWE<0.05 and cluster of t>2.5.

### 4.4.5  Future Considerations

This paper is the first to examine DMN activity in individuals with prenatal exposure to alcohol. Dysmorphic PAE individuals appear unable to sufficiently deactivate the DMN during cognitive tasks, which could contribute to lesser task-related positive activation and poorer task performance. Additionally, there appears to be a "disconnect" between the MPFC and PCC nodes of the network in individuals with PAE, which may be responsible for the reduced task-related deactivation. To our knowledge, this is the first paper to relate structural connectivity, functional connectivity, and task-related deactivation of the DMN in a clinical population. PAE appears to affect all these aspects of the network, implying a global effect on this resting state network and warranting further study. Examination of more structural and functional components of the DMN (e.g., bilateral parietal and medial

73

temporal regions) would aid in better understanding the effect of PAE on the network as a whole. Additionally, it would be interesting to note whether DMN deactivation is dependent on the task type and/or task performance. In the current study, we used an arithmetic task, which is highly cognitively demanding for individuals with PAE, and in our case task performance was lower in affected groups. However it is possible the deactivation patterns would differ with a less demanding task or when task performance is controlled. Finally, this study implies attentional modulation plays a role in cognitive deficit seen with PAE, but more studies controlling for specific types of attentional control and cognition are needed to elucidate the contribution of each to behavioral outcomes.

## 4.5 References

Broyd SJ, Demanuele C, Debener S, Helps SK, James CJ, Sonuga-Barke EJ (2009) Default-mode brain dysfunction in mental disorders: a systematic review. Neurosci Biobehav Rev 33(3):279-96.

Clare Kelly AM, Uddin LQ, Biswal BB, Castellanos FX, Milham MP (2008) Competition between functional brain networks mediates behavioral variability. Neuroimage 39(1):527-37.

Cohen MS (1997) Parametric analysis of fMRI data using linear systems methods. Neuroimage 6(2):93-103.

Coles CD, Platzman KA, Raskind-Hood CL, Brown RT, Falek A, Smith IE (1997) A comparison of children affected by prenatal alcohol exposure and attention deficit, hyperactivity disorder. Alcohol Clin Exp Res 21(1):150-61.

Coles CD, Smith I, Fernhoff PM, Falek A (1985) Neonatal neurobehavioral characteristics as correlates of maternal alcohol use during gestation. Alcohol Clin Exp Res 9(5):454-60.

Connor P (2004) Personal communication.

Conry J (1990) Neuropsychological deficits in fetal alcohol syndrome and fetal alcohol effects. Alcohol Clin Exp Res 14(5):650-5.

Damoiseaux JS, Greicius MD (2009) Greater than the sum of its parts: a review of studies combining structural connectivity and resting-state functional connectivity. Brain Struct Funct.

Dehaene S, Molko N, Cohen L, Wilson AJ (2004) Arithmetic and the brain. Curr Opin Neurobiol 14(2):218-24.

Fox MD, Snyder AZ, Vincent JL, Corbetta M, Van Essen DC, Raichle ME (2005) The human brain is intrinsically organized into dynamic, anticorrelated functional networks. Proc Natl Acad Sci U S A 102(27):9673-8.

Golland Y, Golland P, Bentin S, Malach R (2008) Data-driven clustering reveals a fundamental subdivision of the human cortex into two global systems. Neuropsychologia 46(2):540-53.

Greicius MD, Krasnow B, Reiss AL, Menon V (2003) Functional connectivity in the resting brain: a network analysis of the default mode hypothesis. Proc Natl Acad Sci U S A 100(1):253-8.

Greicius MD, Supekar K, Menon V, Dougherty RF (2009) Resting-state functional connectivity reflects structural connectivity in the default mode network. Cereb Cortex 19(1):72-8.

Guerri C, Bazinet A, Riley EP (2009) Foetal Alcohol Spectrum Disorders and alterations in brain and behaviour. Alcohol Alcohol 44(2):108-14.

Kennedy DP, Redcay E, Courchesne E (2006) Failing to deactivate: resting functional abnormalities in autism. Proc Natl Acad Sci U S A 103(21):8275-80.

Li L, Coles CD, Lynch ME, Hu X (2009) Voxelwise and skeleton-based region of interest analysis of fetal alcohol syndrome and fetal alcohol spectrum disorders in young adults. Hum Brain Mapp 30(10):3265-74.

Malisza KL, Allman AA, Shiloff D, Jakobson L, Longstaffe S, Chudley AE (2005) Evaluation of spatial working memory function in children and adults with fetal alcohol spectrum disorders: a functional magnetic resonance imaging study. Pediatr Res 58(6):1150-7.

Margulies DS, Kelly AM, Uddin LQ, Biswal BB, Castellanos FX, Milham MP (2007) Mapping the functional connectivity of anterior cingulate cortex. Neuroimage 37(2):579-88.

Mattson SN, Riley EP (1998) A review of the neurobehavioral deficits in children with fetal alcohol syndrome or prenatal exposure to alcohol. Alcohol Clin Exp Res 22(2):279-94.

Mattson SN, Riley EP, Gramling L, Delis DC, Jones KL (1998) Neuropsychological comparison of alcohol-exposed children with or without physical features of fetal alcohol syndrome. Neuropsychology 12(1):146-53.

McKiernan KA, D'Angelo BR, Kaufman JN, Binder JR (2006) Interrupting the "stream of consciousness": an fMRI investigation. Neuroimage 29(4):1185-91.

Murphy K, Birn RM, Handwerker DA, Jones TB, Bandettini PA (2009) The impact of global signal regression on resting state correlations: are anti-correlated networks introduced? Neuroimage 44(3):893-905.

Olson HC, Feldman JJ, Streissguth AP, Sampson PD, Bookstein FL (1998) Neuropsychological deficits in adolescents with fetal alcohol syndrome: clinical findings. Alcohol Clin Exp Res 22(9):1998-2012.

Persson J, Lustig C, Nelson JK, Reuter-Lorenz PA (2007) Age differences in deactivation: a link to cognitive control? J Cogn Neurosci 19(6):1021-32.

Pomarol-Clotet E, Salvador R, Sarro S, Gomar J, Vila F, Martinez A, Guerrero A, Ortiz-Gil J, Sans-Sansa B, Capdevila A, Cebamanos JM, McKenna PJ (2008) Failure to deactivate in the prefrontal cortex in schizophrenia: dysfunction of the default mode network? Psychol Med 38(8):1185-93.

Rombouts SA, Barkhof F, Goekoop R, Stam CJ, Scheltens P (2005) Altered resting state networks in mild cognitive impairment and mild Alzheimer's disease: an fMRI study. Hum Brain Mapp 26(4):231-9.

Santhanam P, Li Z, Hu X, Lynch ME, Coles CD (2009) Effects of Prenatal Alcohol Exposure on Brain Activation During an Arithmetic Task: An fMRI Study. Alcohol Clin Exp Res.

Shaywitz SE, Caparulo BK, Hodgson ES (1981) Developmental language disability as a consequence of prenatal exposure to ethanol. Pediatrics 68(6):850-5.

Simmons RW, Wass T, Thomas JD, Riley EP (2002) Fractionated simple and choice reaction time in children with prenatal exposure to alcohol. Alcohol Clin Exp Res 26(9):1412-9.

Singh KD, Fawcett IP (2008) Transient and linearly graded deactivation of the human default-mode network by a visual detection task. Neuroimage 41(1):100-12.

Smith IE, Coles CD, Lancaster J, Fernhoff PM, Falek A (1986) The effect of volume and duration of prenatal ethanol exposure on neonatal physical and behavioral development. Neurobehav Toxicol Teratol 8(4):375-81.

Smith SM, Jenkinson M, Johansen-Berg H, Rueckert D, Nichols TE, Mackay CE, Watkins KE, Ciccarelli O, Cader MZ, Matthews PM, Behrens TE (2006) Tract-based spatial statistics: voxelwise analysis of multi-subject diffusion data. Neuroimage 31(4):1487-505.

Smith SM, Nichols TE (2009) Threshold-free cluster enhancement: addressing problems of smoothing, threshold dependence and localisation in cluster inference. Neuroimage 44(1):83-98.

Sonuga-Barke EJ, Castellanos FX (2007) Spontaneous attentional fluctuations in impaired states and pathological conditions: a neurobiological hypothesis. Neurosci Biobehav Rev 31(7):977-86.

Sowell ER, Lu LH, O'Hare ED, McCourt ST, Mattson SN, O'Connor MJ, Bookheimer SY (2007) Functional magnetic resonance imaging of verbal learning in children with heavy prenatal alcohol exposure. Neuroreport 18(7):635-9.

Streissguth AP, Barr HM, Sampson PD, Parrish-Johnson JC, Kirchner GL, Martin DC (1986) Attention, distraction and reaction time at age 7 years and prenatal alcohol exposure. Neurobehav Toxicol Teratol 8(6):717-25.

Talairach J, Tournoux P (1988) Co-planar stereotaxic atlas of the human brain. New York: Thieme Medical Publishers, Inc.

Uddin LQ, Kelly AM, Biswal BB, Xavier Castellanos F, Milham MP (2009) Functional connectivity of default mode network components: correlation, anticorrelation, and causality. Hum Brain Mapp 30(2):625-37.

van den Heuvel M, Mandl R, Luigjes J, Hulshoff Pol H (2008) Microstructural organization of the cingulum tract and the level of default mode functional connectivity. J Neurosci 28(43):10844-51.

Weissenbacher A, Kasess C, Gerstl F, Lanzenberger R, Moser E, Windischberger C (2009) Correlations and anticorrelations in resting-state functional connectivity MRI: a quantitative comparison of preprocessing strategies. Neuroimage 47(4):1408-16.

Weissman DH, Roberts KC, Visscher KM, Woldorff MG (2006) The neural bases of momentary lapses in attention. Nat Neurosci 9(7):971-8.

Wilson SM, Molnar-Szakacs I, Iacoboni M (2008) Beyond superior temporal cortex: intersubject correlations in narrative speech comprehension. Cereb Cortex 18(1):230-42.

**CHAPTER 5**

**Part 1: Conclusions and Significance**

For decades it has been known that maternal alcohol consumption can lead to long-lasting behavioral problems in the offspring. Gross anatomical and structural imaging studies have revealed that significant physical brain damage can result from prenatal exposure to alcohol. Only recently has the advent of cognitive neuroimaging allowed us to bridge this gap between structural alterations and behavioral outcomes in the PAE population.

This thesis combines the study of task-positive and task-negative functional deficits in adults with PAE. Though the neuroimaging literature to date is limited, the studies that do exist have focused on task-positive brain activity. However, it is clear that brain functioning is a balance of excitatory and inhibitory activation, and that the interplay between these two network types is crucial to any behavioral outcome. We showed in these studies that the learning disability reported in individuals with PAE results from a combination of arithmetic processing deficit and default mode interference that leads to their poor performance. Although it is intuitive that any learning problem could be a combination of attentional modulation deficit and specific cognitive impairments, demonstration of this dual effect is a new finding for the PAE population and a relatively new concept in cognitive neuroimaging in general.

There are several strengths to the design of these studies that allow for a more comprehensive understanding of the spectrum of clinical disorders caused by PAE. Though behavioral deficits have been well-documented in children with PAE, their persistence to adulthood is assumed but not often investigated. Our examination of adults allows for a

78

clearly documented persistence of PAE-related learning problems to adulthood. Additionally, studying varying degrees of exposure gives insight into how severity of exposure affects specific brain functions. As shown in these studies, some types of neuronal alterations are observed in non-dysmorphic but exposed individuals (e.g., default mode structural and functional connectivity) while others are not. As the question of whether moderate PAE can cause significant brain damage is controversial, these studies elucidate some specific areas of dysfunction that appear to be more susceptible to prenatal exposure to alcohol.

Knowledge of specific loci of brain dysfunction in individuals with PAE can aid in adaptive measures for this population. At present, the main form of "treatment" for fetal alcohol syndrome is a specialized learning environment. Children with PAE need extra guidance in learning basic verbal and arithmetic skills; a better understanding of how brain regions involved in these subject areas are affected by exposure is useful to care-givers, social workers, and teachers involved with the special needs of this group of children.

Another result of these studies is evidence that structural and functional data from individuals with PAE, who have localized brain damage, can be improved with newer image registration methods. In terms of group comparison and anatomy-based inferences of imaging measures, it is crucial that images be accurately spatially normalized. Some structural alterations are already shown to be classifiers of PAE; it is evident that accurate inter-subject registration would be vital to this or any clinically diagnostic application.

The effects of prenatal exposure to alcohol on brain structure and function are part of a complicated process. This thesis contributes to a growing body of evidence that PAE causes severe and long-lasting neuronal impairments.

**PART 2**

**Structural and Functional Neuroimaging of Adolescents with**

**Prenatal Cocaine Exposure**

# CHAPTER 6

## Altered Prefrontal-Amygdala Functional Modulation and Structural Connectivity in Adolescents Prenatally Exposed to Cocaine

### 6.1 Background

#### 6.1.1  Prenatal Cocaine Exposure and Emotional Regulation

Prenatal cocaine exposure (PCE) is associated with problems of behavioral regulation and possibly some cognitive deficits (Bada et al., 2007; Frank et al., 2001; Jacobson et al., 1996). In particular, arousal dysregulation has been strongly linked to children with PCE (Mayes, 2002). PCE has been found to lead to disrupted emotional arousal regulation in children (Bendersky and Lewis, 1998b; Mayes, 2002), with suggestions that PCE creates a predisposition to decreased emotional and neurophysiological reactivity in infants and children (Dennis et al., 2006; Mayes et al., 1998b). Additional findings include increased response to negative affect and higher emotional reactivity when facing novel or stressful situations (Dennis et al., 2006; Mayes et al., 1998b).  The underlying neurodevelopmental causes for these behavioral outcomes are still not well understood. Functional MRI (fMRI) can be used to elucidate patterns of brain activity during cognitive and emotional stimulation in individuals with PCE, to further bridge the brain-behavior gap in this population.

### 6.1.2   Emotional Arousal and Dysfunction

A previous study of our PCE cohort has shown that individuals with PCE cannot effectively suppress amygdala activity in the presence of emotional distracters (during a working memory task), and that this distraction leads to disrupted activity in areas associated with working memory (Li et al., 2009). Since individuals with PCE exhibit deficiencies in both attentional and emotionally related arousal dysregulation, connections among regions responsible for these functions may be disrupted. That is, since connectivity between attentional regions and the emotional network modulates stable cognitive functioning, disruption in emotional regulation may contribute to decrements in cognitive processing. Involuntary emotional arousal inhibition during cognitive demand has been noted in healthy populations (Beauregard et al., 2001; Ochsner et al., 2002), but the relationship has only recently been examined in the PCE population.

### 6.1.3   Aims

It is known that the ventromedial prefrontal cortex (VMPFC) is functionally connected to and can deactivate the amygdala (Cohen et al., 2008; Urry et al., 2006). Given the attentional and arousal-related problems seen with PCE, it is possible that this functional suppression is altered in our PCE population. In the present study, using a working memory task with negatively emotive distractions, VMPFC activity was examined during emotional regulation in both a low and high-load cognitive condition in individuals with PCE. The expectation is that VMPFC activity will need to be increased to meet the higher cognitive demand and suppress amgydala-related distraction. Additionally, as VMPFC and bilateral amygdala regions have been shown to be structurally connected (Cohen et al., 2008), integrity of the white matter tracts connecting these regions was examined using diffusion tensor imaging

82

(DTI) and tractography. It was anticipated that during higher emotional distraction, control subjects would show an increase in VMPFC activity with increased cognitive load, while PCE subjects would not. Furthermore, decreased structural connectivity, in the form of reduced volume of tracts and fractional anisotropy (FA), between VMPFC and amygdala was expected in the PCE group as compared to healthy controls.

## 6.2 Methods

### 6.2.1 Participants

Participants were teenagers recruited from a longitudinal cohort, derived from a predominantly African-American, low socio-economic status (SES) population. They were first identified in the prenatal period between 1987 and 1989 (Brown et al., 1998a; Coles et al., 1999a). At the time of imaging, participants were aged 12-15. Upon explanation of the study procedures, assent forms were signed by participants under the age of 18, and informed consent was given by caregivers at the time of re-contact. From the cohort, two groups of participants were identified: 1) Exposed prenatally to cocaine and 2) Unexposed, healthy controls from the same SES population. For group 1, the average frequency of maternal drug use was 3-4 times a week for an average of 35 weeks of pregnancy. Demographics information for the cohort is shown in Tables 6.1 and 6.2. A subset of subjects from Tables 6.1 and 6.2 is included in the present study. Participants who were left handed or had some risk during the MRI procedure (e.g., due to pregnancy or metal in the body) were excluded. The number of subjects used in the resting state scan were: n=22 for controls, n=23 for PCE; for the DTI part of the study: n=16 for controls, n=30 for PCE.

83

**Table 6.1.** Characteristics of Teen at Follow-Up; a: If data for a variable are not available for some participants, the n used for the analysis is noted next to the variable name; b: Chi-square analyses completed for categorical variables; Independent sample t-tests completed for continuous variables.

| Variable | Control (n=23)[a] | | PCE (n=33)[a] | | P Value[b] |
|---|---|---|---|---|---|
| Age, M (SD) | 14.61 | (2.3) | 14.64 | (2.0) | .962 |
| Gender, No. (%) | | | | | .019 |
|   Female | 15 | (65.2) | 11 | (33.3) | |
|   Male | 8 | (34.8) | 22 | (66.7) | |
| Total monthly household income - $, M (SD) *n=53* | 1,898 | (1,284) | 1,221 | (922) | .030 |
| Handedness, No. (%) | | | | | .918 |
|   Right | 20 | (87.0) | 29 | (87.9) | |
|   Left | 3 | (13.0) | 4 | (12.1) | |
| Full-Scale IQ - WASI, M (SD) | 88.8 | (8.4) | 87.0 | (11.4) | .497 |
| Verbal IQ - WASI, M (SD) | 90.7 | (9.5) | 86.6 | (12.6) | .182 |
| Performance IQ - WASI, M (SD) | 89.3 | (9.5) | 89.8 | (11.2) | .855 |


**Table 6.2.** Ascertainment of maternal characteristics. a: If data for a variable are not available for some participants, the n used for the analysis is noted next to the variable name; b: Chi-square analyses completed for categorical variables; Independent sample t-tests completed for continuous variables.

| Variable | Control (n=23)[a] | | PCE (n=33)[a] | | P Value[b] |
|---|---|---|---|---|---|
| Age, M (SD) | 26.3 | (5.2) | 28.2 | (4.3) | .138 |
| Education, No. (%) *n=51* | | | | | .006 |
|   High school not completed | 2 | (9.1) | 13 | (44.8) | |
|   High school graduate or more | 20 | (90.9) | 16 | (55.2) | |
| Monthly income, No. (%) *n=51* | | | | | .773 |
|   ≤$600 | 20 | (90.9) | 27 | (93.1) | |
|   >$600 | 2 | (9.1) | 2 | (6.9) | |
| Marital status, No. (%) | | | | | .179 |
|   Married | 6 | (26.1) | 4 | (12.1) | |
|   Single, divorced, separated, widowed | 17 | (73.9) | 29 | (87.9) | |
| Other substance use in pregnancy, M (SD) | | | | | |
|   Tobacco - cigarettes/week *n=52* | 9.1 | (32.0) | 61.1 | (50.1) | .000 |
|   Alcohol - oz. of absolute alcohol/week *n=54* | 0.0 | (0.1) | 1.0 | (1.8) | .004 |
|   Marijuana - joints/week *n=54* | 0.0 | (0.0) | 1.3 | (2.9) | .016 |

84

## 6.2.2  Experimental Paradigm

For the resting state paradigm, participants were instructed to simply gaze at a fixation cross
and remain awake. For the functional imaging paradigm, participants were asked to perform
a working memory task by pressing a button either when "RR" was displayed (0-back
condition) or when the displaying letter pair matched the previous one (1-back condition).
Emotionally neutral or negative pictures (Lang et al., 1997) were placed to alternate with
memory stimuli, producing four different task blocks (neutral 0-back, NEU0; neutral 1-back,
NEU1; negative 0-back, NEG0; negative 1-back, NEG1). Figure 6.1 shows an example of
stimuli presented in the experiment. Paradigm presentation and response collection,
including accuracy and reaction time, were collected using Eprime software.
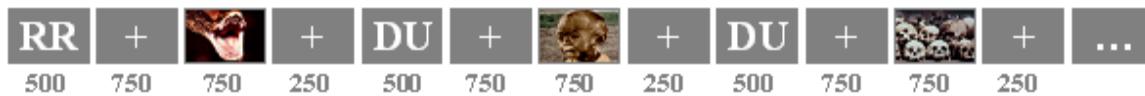


**Figure 6.1.** Example of working memory paradigm with emotive distracters. Duration shown
in milliseconds. One display cycle is letter-fixation-picture-fixation. Blocks were all "neutral"
or "negative" (only negative shown).

## 6.2.3  Image Acquisition

All fMRI data was acquired on a 3T Siemens Trio scanner. High-resolution, T1-weighted,
three-dimensional (3D) anatomical images were acquired with a 3D MPRAGE
(magnetization prepared rapid gradient echo) sequence for all participants. Sequence
parameters used were TR/TI/TE of 2300ms/1100ms/3.023ms, flip angle of 8°, field of view

of 256 mm, matrix of 256 × 224 × 176, corresponding to an isotropic resolution of 1mm. Scan duration was 6:56 minutes.

Resting state scan parameters were as follows: 210-volumes, matrix=64×64, 20 axial slices without gap, thickness=4 mm, TR/TE=2000 ms/30 ms, flip angle=90$^{o}$, FOV=192×192 cm$^{2}$. For the working memory task, two echo planar imaging blood oxygen level dependent (EPI-BOLD) scans were performed, lasting 6:06 minutes each, with 120 time points collected. Images consisted of 30 axial slices, with 3mm slice thickness. Sequence parameters were TR/TE/FA/FOV of 3000ms/30ms/90º/192cm.

DTI data was acquired with a diffusion-weighted, single-shot, spin-echo EPI sequence. A dual spin-echo technique combined with bipolar gradients were used to minimize the geometric distortion induced by eddy currents. Diffusion gradients were applied in 12 directions with a b value of 1000 sec/mm2. Thirty four contiguous axial slices were acquired with slice thickness of 2.5mm. The pulse sequence parameters were TR/TE/FOV of 6500ms/90ms/22cm, with a total scan time of 8:34 minutes.

6.2.4   Image Analysis

*6.2.4.1 Functional MRI Analysis*

AFNI (http://afni.nimh.nih.gov/afni, 09/2009) was used for resting and functional analysis. Subjects with head motion of more than one voxel (3.44mm) in any direction or with poor registration between EPI and T1-weighted images were excluded.

For the resting MRI analysis, preprocessing included slice timing correction, spatial registration, 0.08-0.01Hz band pass filtering and 5mm full-width half max (FWHM) Gaussian blur.

For the functional MRI analysis, preprocessing included slice timing correction, scan concatenation, volume registration, signal normalization, and blurring with a 5mm FWHM Gaussian filter. Average maps including all subjects were generated after transforming the dataset into the Talairach space (Talairach and Tournoux, 1988a) and normalizing the F values into z-scores. The bilateral amygdala was functionally localized using the negative versus neutral contrast, following general linear modeling. The amygdala regions were masked and this mask was applied to the resting state data as a seeding region. Cross-correlation analysis of low-frequency signal fluctuations (0.01-0.08Hz) revealed a cluster in VMPFC as functionally connected to the bilateral amygdala seed. This cluster was used to mask a region in the functional dataset, where regression coefficients (β-weights) representing the BOLD signal level for the 0-back and 1-back conditions, respectively, were derived for each subject using multiple regression analysis. Then a 2 (PCE vs. control) × 2 (0-back vs. 1-back) ANOVA was used to compare activation in the VMPFC, controlling for gender, alcohol and marijuana exposure as covariates.

*6.2.4.2 Diffusion MRI Analysis*

All diffusion MRI analysis was conducted in FSL (http://www.fmrib.ox.ac.uk/fsl/, 09/2009). Pre-processing consisted of correction for eddy-current distortin and brain extraction. Then FA maps were generated by fiting the data in each voxel to a diffusion tensor model. Visual examination was done to ensure the first eigenvector was oriented along white matter fibers for each individual. Then local diffusion directions were obtained using a function that executes Markov Chain Monte Carlo sampling and allows for modeling cross-fiber orientations within each voxel (Behrens et al., 2003). Briefly, this process involves repetitive sampling from distributions on voxel-wise principle diffusion directions to obtain an estimation for diffusion parameters at each voxel. The parameters used were the default based on Behrens, et al.(2007): number of fibers modeled per voxel=2; weight =1; number of iterations before sampling =1000.

87

Probabilistic tractography was used to identify white matter tracts connecting the VMPFC and bilateral amygdala. To derive seed and target regions, masks from the functional and resting state analysis described above were back-projected to native space for all subjects individually. The left and right amygdala, respectively, were used as seeding regions, and the VMPFC region was used as a target and a way-point mask, such that fibers originating in the amygdala seed mask and either terminating or passing through the VMPFC mask were included. The separation of the amygdala region of interest (ROI) into left and right was done because of known significant inter-hemispheric white matter asymmetries (Buchel et al., 2004; Yasmin et al., 2009). The output of the probabilistic tractography was a group of fibers representing the connectivity distribution between ROIs, along with the total number of fibers between them (i.e., waytotal). Upon visual inspection, subjects with incomplete or absent tracts in one hemisphere were excluded from quantification analysis (final subject number for tractography: RIGHT amygdala-VMPFC: n=12 for controls, n=22 for PCE; LEFT amygdala-VMPFC: n=14 for controls, n=29 for PCE).

Tractography between ROIs was quantified by waytotal, total tract volume, and FA along the non-zero tracts. For the volume and FA values, tractography results were obtained by dividing by waytotal (this value represents the probability of tract presence at each voxel) and thresholding this value at 0.01 and 0.1. To ensure the tracts were present and continuous at a range of thresholds, the thresholded tract data was examined visually. Differences in waytotal, total tract volume, and FA for tracts connecting left amygdala-VMPFC and right amygdala-VMPFC were determined between groups by t-test.

**6.3 Results**

Figure 6.2a indicates the localized bilateral amygdala from the neutral-negative contrast group average map. This region was used as the seeding region for subsequent resting

88

state correlation analysis. Figure 6.2b shows the correlation map for the seeding region, including VMPFC. The amount of activation in this region during low and high-cognitive load conditions is indicated for both groups in Figure 6.3. Higher working memory load caused an increase in VMPFC activity during emotional regulation (negative-neutral conditions) in the control group, but activity decreased in the PCE group with higher cognitive load.  This signifies a greater emotional suppression by controls but not by the PCE group. A significant memory by exposure interaction was found (p=0.0041).
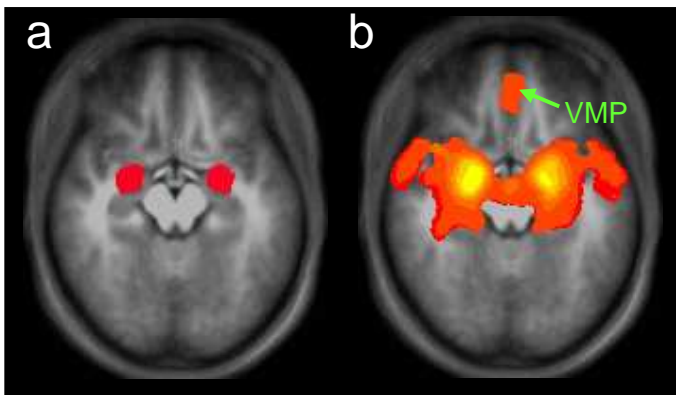


**Figure 6.2.** Group activation maps showing a) bilateral amygdala seeding region obtained from negative minus neutral contrast and b) correlation analysis with VMPFC cluster identified.  Figure reproduced with permission from Z. Li.
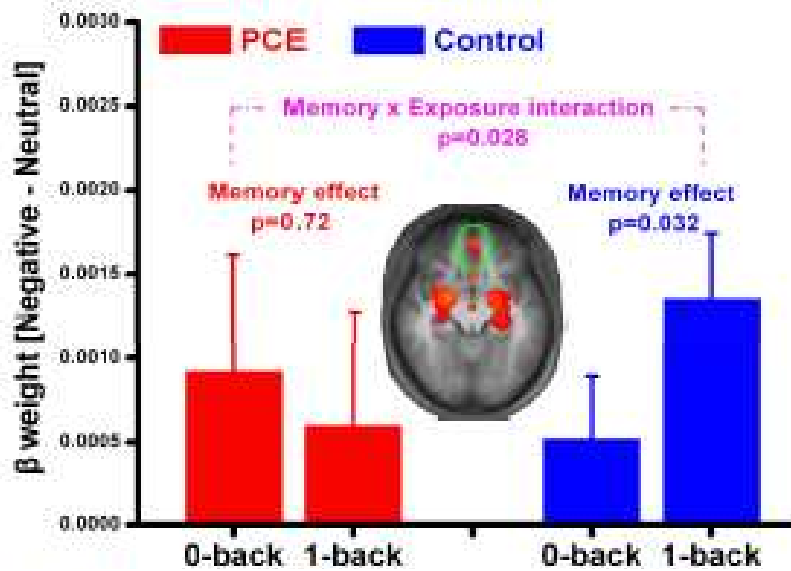
**Figure 6.3.** Emotional regulation associated VMPFC signal in different experimental conditions and exposure groups. Functional connectivity map shown in center (VMPFC circled). Error bars indicate standard error. Figure reproduced with permission from Z. Li.

Figure 6.4 indicates probabilistic tractography results from one representative individual in the study. Right and left amygdala were used as seeds, respectively, with VMPFC as the target region. The underlay for Figure 6.4 is the FA map for that individual. Structural connectivity between these regions was measured by waytotal, total tract volume, and FA along the tracts (Table 6.3). Left amygdala-VMPFC differences are notable in waytotal and FA at both thresholds, and right amygdala-VMPFC differences are seen in waytotal. No other measures showed significant differences between groups.
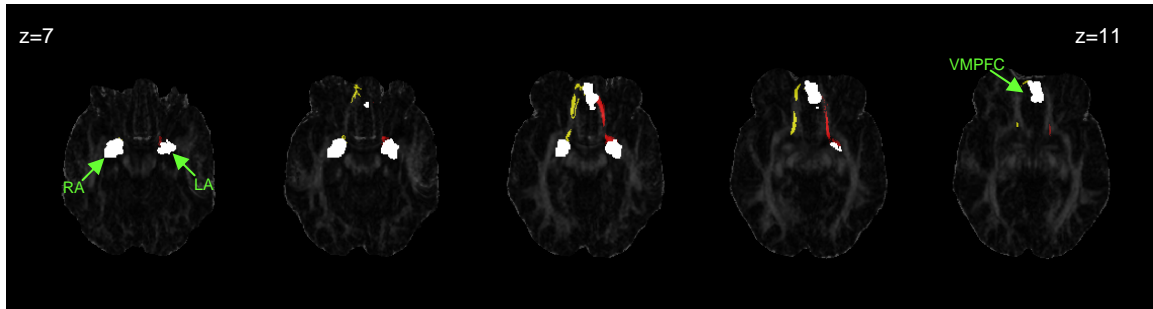
**Figure 6.4.** Results of probabilistic tractography in one representative subject from the PCE group. Serial axial slices are shown with white clusters indicating bilateral amygdala (seeding regions) and VMPFC (target region). Yellow tracts are right amygdala-VMPFC tracts; red tracts are left amygdala-VMPFC tracts. Underlay is the FA map.

**Table 6.3.** Tractography measures, including waytotal, tract volume, and FA values along tracts for right and left amygdala, respectively, connections with MPFC. SEM= standard error of mean;* = significantly different from control group (p<0.05).

| ROI network | | Tractography Measures (SEM) | | |
|---|---|---|---|---|
| | | Waytotal | Tract volume | FA |
| Left amydala-MPFC | Control | 2042.5 (888.4) | 1646.4 (236.8) | 0.338 (0.00870) |
| | PCE | 763.3* (276.6) | 1985.7 (205.0) | 0.313* (0.00636) |
| Right amygdala-MFC | Control | 685.3 (240.6) | 2023.6 (459.3) | 0.303 (0.0132) |
| | PCE | 169.7* (73.3) | 2259.0 (298.4) | 0.325 (0.00774) |

**6.4 Discussion**

6.4.1    <u>Summary</u>

The goal of this study was to examine a potential disconnection between VMPFC and bilateral amygdala in individuals with PCE, based on strong evidence of emotional arousal dysregulation in this population. Functional data revealed that, in the high emotional load condition, VMPFC activity increases in control subjects with increased cognitive demand, while VMPFC activity remains unchanged in PCE subjects. Furthermore, structural connectivity analysis showed that there is a significantly lower FA and total number of white matter tracts connecting the VMPFC and left amygdala.

6.4.2    <u>Context in Current Literature</u>

Several studies of behavioral outcomes in children with PCE have shown arousal and emotion-related dysregulation; however, there are limited findings from neuroimaging. One study by Hurt, et al. showed increased activation in prefrontal areas in adolescents with PCE during a working memory task (Hurt et al., 2008), and a separate study found response inhibition required more prefrontal activation in PCE children (Sheinkopf et al., 2009). The present study builds on previous findings from this cohort that adolescents with PCE cannot suppress emotion-related amygdala activity when facing higher cognitive load (Li et al., 2009). The current results give further evidence of a lack of coordination between prefrontal regions and the amygdala with PCE.

Functional connectivity between VMPFC and amygdala is known to be reciprocally modulated in healthy populations (Kilpatrick and Cahill, 2003; Urry et al., 2006). Furthermore, clinical studies have shown that this connectivity is associated with antisocial

92

behavior suppression (Hoptman MJ, 2008). Damage to VMPFC has been shown to cause increase aggression and hostility (Grafman et al., 1996), and a functional disconnection with amygdala has been observed in populations with post-traumatic stress disorder, bipolar disorder, and schizophrenia (Gilboa et al., 2004; Hoptman et al., 2009; Wang et al., 2009). These disorders are highly characterized by impulsivity and other behavioral dysregulations (Gilboa et al., 2004; Hoptman et al., 2009; Wang et al., 2009) similar to those seen in individuals with PCE.

### 6.4.3  Limitations

Probabilistic tractography revealed a decrease in structural connectivity between the VMPFC and left amygdala by lower FA and reduced number of tracts in the PCE group. However, connectivity between VMPFC and right amygdala did not appear to be different between groups. One possible reason for this hemispheric discrepancy is that a greater number of subjects had to be excluded for this connectivity measure because tracts were either incomplete or absent from the probabilistic tractography output (excluded: n=4 for controls; n=8 for PCE). There are several possible reasons for this incomplete tractography in the right hemisphere. It may be that the target mask (MPFC) is not evenly distributed between each hemisphere (shifted more to the left), limiting the number of tracts derived on the right side. As the MPFC cluster was generated by functional data, it appears to span both hemispheres due to spatial blurring, but is not likely evenly distributed in reality. By visual inspection the cluster does appear to be left-side shifted, but further analysis is needed to determine whether this methodological factor is responsible for the asymmetry. Another possible reason for the asymmetry is that the tracts are anatomically unevenly distributed between hemispheres. As hemispheric differences in these particular tracts are not well-characterized in the literature, it is unclear whether anatomical differences exist.

93

### 6.4.4   Future Considerations

The present study reveals more imaging evidence supporting the view that PCE has a long-term effect on arousal regulation. Given that the prefrontal region shown to be affected in our previous study was dorso-lateral PFC, as opposed to VMPFC, it appears that multiple subregions of the prefrontal cortex are affected by PCE. Further study of effective connectivity between these distinct prefrontal and emotion-related regions could reveal specific directional disconnects caused by PCE. Though the precise mechanism by which PCE results in arousal and emotional dysfunctions is unclear, the involvement of certain loci in behavioral regulation in these individuals is now better understood.

## 6.5 References

Archibald, S.L., Fennema-Notestine, C., Gamst, A., Riley, E.P., Mattson, S.N., and Jernigan, T.L. (2001). Brain dysmorphology in individuals with severe prenatal alcohol exposure. Developmental medicine and child neurology *43*, 148-154.

Ardekani, B.A., Bachman, A.H., Strother, S., Fujibayashi, Y., Yonekura, Y., (2004). Impact of inter-subject image registration on group analysis of fMRI data. Int. Congr. Ser., Elsevier 1265, 49-59.

Ashburner, J. (2007a). DARTEL guide. In http://www.fil.ion.ucl.ac.uk/~john/misc/dartel_guide.pdf. Accessed 09/2009.

Ashburner, J. (2007b). A fast diffeomorphic image registration algorithm. Neuroimage *38*, 95-113.

Bada, H.S., Das, A., Bauer, C.R., Shankaran, S., Lester, B., LaGasse, L., Hammond, J., Wright, L.L., and Higgins, R. (2007). Impact of prenatal cocaine exposure on child behavior problems through school age. Pediatrics *119*, e348-e359.

Baliki, M.N., Geha, P.Y., Apkarian, A.V., and Chialvo, D.R. (2008). Beyond feeling: chronic pain hurts the brain, disrupting the default-mode network dynamics. J Neurosci *28*, 1398-1403.

Bard, K.A., Coles, C.D., Platzman, K.A., and Lynch, M.E. (2000). The effects of prenatal drug exposure, term status, and caregiving on arousal and arousal modulation in 8-week-old infants. Dev Psychobiol *36*, 194-212.

Beauregard, M., Levesque, J., and Bourgouin, P. (2001). Neural correlates of conscious self-regulation of emotion. J Neurosci *21*, RC165.

Behrens, T.E., Berg, H.J., Jbabdi, S., Rushworth, M.F., and Woolrich, M.W. (2007). Probabilistic diffusion tractography with multiple fibre orientations: What can we gain? Neuroimage *34*, 144-155.

Behrens, T.E., Woolrich, M.W., Jenkinson, M., Johansen-Berg, H., Nunes, R.G., Clare, S., Matthews, P.M., Brady, J.M., and Smith, S.M. (2003). Characterization and propagation of uncertainty in diffusion-weighted MR imaging. Magn Reson Med *50*, 1077-1088.

Bendersky, M., and Lewis, M. (1998a). Arousal modulation in cocaine-exposed infants. Dev Psychol *34*, 555-564.

Bendersky, M., and Lewis, M. (1998b). Arousal modulation in cocaine-exposed infants. Dev Psychol *34*, 555-564.

Bergouignan, L., Chupin, M., Czechowska, Y., Kinkingnehun, S., Lemogne, C., Le Bastard, G., Lepage, M., Garnero, L., Colliot, O., and Fossati, P. (2009). Can voxel based morphometry, manual segmentation and automated segmentation equally detect hippocampal volume differences in acute depression? Neuroimage *45*, 29-37.

Blackston, R.D., Coles, C. D., Kable, J.A., & Seitz, R. (2004). Reliability and validity of the Dysmorphia Checklist: Relating severity of dysmorphia to cognitive and behavioral outcomes in children with prenatal alcohol exposure. In American Society of Human Genetics Annual Meeting, Toronto, Canada.

Bookheimer, S.Y., and Sowell, E.R. (2005). Brain imaging in FAS: commentary on the article by Malisza et al. Pediatric research *58*, 1148-1149.

Bookstein, F.L., Sampson, P.D., Connor, P.D., and Streissguth, A.P. (2002). Midline corpus callosum is a neuroanatomical focus of fetal alcohol damage. Anat Rec *269*, 162-174.

Bookstein, F.L., Sampson, P.D., Streissguth, A.P., and Connor, P.D. (2001). Geometric morphometrics of corpus callosum and subcortical structures in the fetal-alcohol-affected brain. Teratology *64*, 4-32.

Brown, J.V., Bakeman, R., Coles, C.D., Sexson, W.R., and Demi, A. (1998a). Maternal drug use, fetal growth and newborn behavior: Are preterms and fullterms affected differently? Developmental Psychology *34*, 540-554.

Brown, J.V., Bakeman, R., Coles, C.D., Sexson, W.R., and Demi, A.S. (1998b). Maternal drug use during pregnancy: are preterm and full-term infants affected differently? Dev Psychol *34*, 540-554.

Broyd, S.J., Demanuele, C., Debener, S., Helps, S.K., James, C.J., and Sonuga-Barke, E.J. (2009). Default-mode brain dysfunction in mental disorders: a systematic review. Neurosci Biobehav Rev *33*, 279-296.

Buchel, C., Raedler, T., Sommer, M., Sach, M., Weiller, C., and Koch, M.A. (2004). White matter asymmetry in the human brain: a diffusion tensor MRI study. Cereb Cortex *14*, 945-951.

Clare Kelly, A.M., Uddin, L.Q., Biswal, B.B., Castellanos, F.X., and Milham, M.P. (2008). Competition between functional brain networks mediates behavioral variability. Neuroimage *39*, 527-537.

Cohen, M.S. (1997a). Parametric analysis of fMRI data using linear systems methods. Neuroimage *6*, 93-103.

Cohen, M.S. (1997b). Parametric analysis of fMRI data using linear systems methods. Neuroimage *6*, 93-103.

Cohen, M.X., Elger, C.E., and Weber, B. (2008). Amygdala tractography predicts functional connectivity and learning during feedback-guided decision-making. Neuroimage *39*, 1396-1407.

Coles, C.D., Bard, K.A., Platzman, K.A., and Lynch, M.E. (1999a). Attentional response at eight weeks in prenatally drug-exposed and preterm infants. Neurotoxicology and teratology *21*, 527-537.

Coles, C.D., Bard, K.A., Platzman, K.A., and Lynch, M.E. (1999b). Attentional response at eight weeks in prenatally drug-exposed and preterm infants. Neurotoxicol Teratol *21*, 527-537.

Coles, C.D., Platzman, K.A., Raskind-Hood, C.L., Brown, R.T., Falek, A., and Smith, I.E. (1997). A comparison of children affected by prenatal alcohol exposure and attention deficit, hyperactivity disorder. Alcoholism, clinical and experimental research *21*, 150-161.

Coles, C.D., Platzman, K.A., Smith, I., James, M.E., and Falek, A. (1992). Effects of cocaine and alcohol use in pregnancy on neonatal growth and neurobehavioral status. Neurotoxicol Teratol *14*, 23-33.

Coles, C.D., Smith, I., Fernhoff, P.M., and Falek, A. (1985). Neonatal neurobehavioral characteristics as correlates of maternal alcohol use during gestation. Alcoholism, clinical and experimental research *9*, 454-460.

Connor, P. (2004). Personal communication.

Conry, J. (1990). Neuropsychological deficits in fetal alcohol syndrome and fetal alcohol effects. Alcoholism, clinical and experimental research *14*, 650-655.

Damasio, A.R. (1995). On some functions of the human prefrontal cortex. Ann N Y Acad Sci *769*, 241-252.

Damoiseaux, J.S., and Greicius, M.D. (2009). Greater than the sum of its parts: a review of studies combining structural connectivity and resting-state functional connectivity. Brain Struct Funct.

Dehaene, S., Molko, N., Cohen, L., and Wilson, A.J. (2004). Arithmetic and the brain. Curr Opin Neurobiol *14*, 218-224.

Delaney-Black, V., Covington, C., Templin, T., Ager, J., Martier, S., and Sokol, R. (1998). Prenatal cocaine exposure and child behavior. Pediatrics *102*, 945-950.

Dennis, T., Bendersky, M., Ramsay, D., and Lewis, M. (2006). Reactivity and regulation in children prenatally exposed to cocaine. Dev Psychobiol *42*, 688-697.

Dipietro, J.A., Suess, P.E., Wheeler, J.S., Smouse, P.H., and Newlin, D.B. (1995). Reactivity and regulation in cocaine-exposed neonates. Infant Behav Dev *18*, 407-414.

Dodge, N.C., Jacobson, J.L., Molteno, C.D., Meintjes, E.M., Bangalore, S., Diwadkar, V., Hoyme, E.H., Robinson, L.K., Khaole, N., Avison, M.J., and Jacobson, S.W. (2009). Prenatal alcohol exposure and interhemispheric transfer of tactile information: Detroit and Cape Town findings. Alcoholism, clinical and experimental research *33*, 1628-1637.

Fabri, M., Del Pesce, M., Paggi, A., Polonara, G., Bartolini, M., Salvolini, U., and Manzoni, T. (2005). Contribution of posterior corpus callosum to the interhemispheric transfer of tactile information. Brain Res Cogn Brain Res *24*, 73-80.

Fernhoff, P.M., Smith, I.E., and Falek, A. (1980). Dysmorphia Checklist. Document available through the Maternal Substance Abuse and Child Development Project, Department of Psychiatry and Behavioral Sciences, Emory University School of Medicine.

Fox, M.D., and Raichle, M.E. (2007). Spontaneous fluctuations in brain activity observed with functional magnetic resonance imaging. Nat Rev Neurosci *8*, 700-711.

Fox, M.D., Snyder, A.Z., Vincent, J.L., corbetta, M., Essen, D.C.V., and Raichle, M.E. (2005a). The human brain is intrinsically organized into dynamic, anticorrelated functional networks. Proc Natl Acad Sci U S A *102*, 9673-9678.

Fox, M.D., Snyder, A.Z., Vincent, J.L., Corbetta, M., Van Essen, D.C., and Raichle, M.E. (2005b). The human brain is intrinsically organized into dynamic, anticorrelated functional networks. Proc Natl Acad Sci U S A *102*, 9673-9678.

Frank, D.A., Augustyn, M., Knight, W.G., Pell, T., and Zuckerman, B. (2001). Growth, development, and behavior in early childhood following prenatal cocaine exposure. JAMA *285*, 1613-1625.

Garavan, H., Morgan, R.E., Mactutus, C.F., Levitsky, D.A., and Booze, R.M. (2000). Prenatal cocaine exposure impairs selective attention: evidence from serial reversal and extradimentional shift tasks. Behav Neurosci *114*, 725-738.

Garrity, A.G., Pearlson, G.D., McKiernan, K., Lloyd, D., Kiehl, K.A., and Calhoun, V.D. (2007). Aberrant "default mode" functional connectivity in schizophrenia. Am J Psychiatry *164*, 450-457.

Gilbert, S.J., Dumontheil, I., Simons, J.S., Frith, C.D., and Burgess, P.W. (2007). Comment on "wandering minds: the default network and stimulus-independent thought". Science *317*, 43b.

Gilboa, A., Shalev, A.Y., Laor, L., Lester, H., Louzoun, Y., Chisin, R., and Bonne, O. (2004). Functional connectivity of the prefrontal cortex and the amygdala in posttraumatic stress disorder. Biol Psychiatry *55*, 263-272.

Golland, Y., Golland, P., Bentin, S., and Malach, R. (2008). Data-driven clustering reveals a fundamental subdivision of the human cortex into two global systems. Neuropsychologia *46*, 540-553.

Grafman, J., Schwab, K., Warden, D., Pridgen, A., Brown, H.R., and Salazar, A.M. (1996). Frontal lobe injuries, violence, and aggression: a report of the Vietnam Head Injury Study. Neurology *46*, 1231-1238.

Greicius, M.D., Krasnow, B., Reiss, A.L., and Memon, V. (2003a). Functional connectivity in the resting brain: a network analysis of the default mode hypothesis. Proc Natl Acad Sci U S A *100*, 253-258.

Greicius, M.D., Krasnow, B., Reiss, A.L., and Menon, V. (2003b). Functional connectivity in the resting brain: a network analysis of the default mode hypothesis. Proc Natl Acad Sci U S A *100*, 253-258.

Greicius, M.D., Supekar, K., Menon, V., and Dougherty, R.F. (2009). Resting-state functional connectivity reflects structural connectivity in the default mode network. Cereb Cortex *19*, 72-78.

Guerri, C., Bazinet, A., and Riley, E.P. (2009). Foetal Alcohol Spectrum Disorders and alterations in brain and behaviour. Alcohol Alcohol *44*, 108-114.

Gusnard, D.A., Akbudak, E., Shulman, G.L., and Raichle, M.E. (2001). Medial prefrontal cortex and self-referential mental activity: relation to a default mode of brain function. Proc Natl Acad Sci U S A *98*, 4259-4264.

Gusnard, D.A., and Raichle, M.E. (2001). Searching for a baseline: functional imaging and the resting human brain. Nat Rev Neurosci *2*, 685-694.

Hahn, B., Ross, T.J., and Stein, E.A. (2007). Cingulate activation increases dynamically with response speed under stimulus unpredictability. Cereb Cortex *17*, 1664-1671.

Hoptman, M.J., D'Angelo, D., Catalano, D., Mauro, C.J., Shehzad, Z.E., Kelly, A.M., Castellanos, F.X., Javitt, D.C., and Milham, M.P. (2009). Amygdalofrontal Functional Disconnectivity and Aggression in Schizophrenia. Schizophr Bull.

Hoptman MJ, N.K. (2008). Schizophrenia. , 3rd edn (New York, NY: Springer).

98

Hurt, H., Giannetta, J., Korczykowski, M., Hoang, A., Tang, K., Betancourt, L., Brodsky, N., Shera, D., Farah, M., and Detre, J. (2008). Functional magnetic resonance imaging and working memory in adolescents with gestational cocaine exposure. J Pediatr *152*, 371-377.

Jacobson, S.W., Jacobson, J.L., Sokol, R.J., Martier, S.S., and Chiodo, L.M. (1996). New evidence for neurobehavioral effects of in utero cocaine exposure. J Pediatr *129*, 581-590.

Kable, J.A., Coles, C.D., Lynch, M.E., and Platzman, K. (2008). Physiological responses to social and cognitive challenges in 8-year-olds with a history of prenatal cocaine exposure. Dev Psychobiol *50*, 251-265.

Karmel, B.Z., and Gardner, J.M. (1996). Prenatal cocaine exposure effects on arousal-modulated attention during the neonatal period. Dev Psychobiol *29*, 463-480.

Kelley, W.M., Macrae, C.N., Wyland, C.L., Caglar, S., Inati, S., and Heatherton, T.F. (2002). Finding the self? An event-related fMRI study. J Cogn Neurosci *14*, 785-794.

Kennedy, D.P., Redcay, E., and Courchesne, E. (2006). Failing to deactivate: resting functional abnormalities in autism. Proc Natl Acad Sci U S A *103*, 8275-8280.

Kilpatrick, L., and Cahill, L. (2003). Amygdala modulation of parahippocampal and frontal regions during emotionally influenced memory storage. Neuroimage *20*, 2091-2099.

Klein, A., Andersson, J., Ardekani, B.A., Ashburner, J., Avants, B., Chiang, M.C., Christensen, G.E., Collins, D.L., Gee, J., Hellier, P.*, et al.* (2009). Evaluation of 14 nonlinear deformation algorithms applied to human brain MRI registration. Neuroimage *46*, 786-802.

Lang, P.J., Bradley, M.M., and Cuthbert, B.N. (1997). International affective picture system: technical manual and affective ratings. (Gainesville, FL, NIMH Center for the Study of Emotion and Attention).

Laufs, H., Hamandi, K., Salek-Haddadi, A., Kleinschmidt, A.K., Duncan, J.S., and Lemieux, L. (2007). Temporal lobe interictal epileptic discharges affect cerebral activity in "default mode" brain regions. Hum Brain Mapp *28*, 1023-1032.

Lebel, C., Rasmussen, C., Wyper, K., Walker, L., Andrew, G., Yager, J., and Beaulieu, C. (2008). Brain diffusion abnormalities in children with fetal alcohol spectrum disorder. Alcoholism, clinical and experimental research *32*, 1732-1740.

Li, Z., Coles, C.D., Lynch, M.E., Hamann, S., Peltier, S., LaConte, S., and Hu, X. (2009). Prenatal cocaine exposure alters emotional arousal regulation and its effects on working memory. Neurotoxicol Teratol *In press*.

Lum, C., McAndrews, M.P., Holodny, A.I., McManus, K.A., Crawley, A., Chakraborty, S., and Mikulis, D.J. (2009). Investigating Agenesis of the Corpus Callosum Using Functional MRI: A Study Examining Interhemispheric Coordination of Motor Control. J Neuroimaging.

Ma, X., Coles, C.D., Lynch, M.E., Laconte, S.M., Zurkiya, O., Wang, D., and Hu, X. (2005). Evaluation of corpus callosum anisotropy in young adults with fetal alcohol syndrome according to diffusion tensor imaging. Alcoholism, clinical and experimental research *29*, 1214-1222.

Malisza, K.L., Allman, A.A., Shiloff, D., Jakobson, L., Longstaffe, S., and Chudley, A.E. (2005). Evaluation of spatial working memory function in children and adults with fetal alcohol spectrum disorders: a functional magnetic resonance imaging study. Pediatric research *58*, 1150-1157.

Margulies, D.S., Kelly, A.M., Uddin, L.Q., Biswal, B.B., Castellanos, F.X., and Milham, M.P. (2007). Mapping the functional connectivity of anterior cingulate cortex. Neuroimage *37*, 579-588.

Mason, M.F., Norton, M.I., Horn, J.D.V., Wegner, D.M., Grafton, S.T., and Macrae, C.N. (2007). Wandering minds: the default network and stimulus-independent thought. Science *315*, 393-395.

Mattson, S.N., and Riley, E.P. (1998). A review of the neurobehavioral deficits in children with fetal alcohol syndrome or prenatal exposure to alcohol. Alcoholism, clinical and experimental research *22*, 279-294.

Mattson, S.N., Riley, E.P., Gramling, L., Delis, D.C., and Jones, K.L. (1998). Neuropsychological comparison of alcohol-exposed children with or without physical features of fetal alcohol syndrome. Neuropsychology *12*, 146-153.

Mayes, L.C. (2002). A behavioral teratogenic model of the impact of prenatal cocaine exposure on arousal regulatory systems. Neurotoxicol Teratol *24*, 385-395.

Mayes, L.C., Grillon, C., Granger, R., and Schottenfeld, R. (1998a). Regulation of arousal and attention in preschool children exposed to cocaine prenatally. Ann N Y Acad Sci *846*, 126-143.

Mayes, L.C., Grillon, C., Granger, R., and Schottenfeld, R. (1998b). Regulation of arousal and attention in preschool children exposed to cocaine prenatally. Ann N Y Acad Sci *846*, 126-143.

McKiernan, K.A., D'Angelo, B.R., Kaufman, J.N., and Binder, J.R. (2006). Interrupting the "stream of consciousness": an fMRI investigation. Neuroimage *29*, 1185-1191.

Muetzel, R.L., Collins, P.F., Mueller, B.A., A, M.S., Lim, K.O., and Luciana, M. (2008). The development of corpus callosum microstructure and associations with bimanual task performance in healthy adolescents. Neuroimage *39*, 1918-1925.

Murphy, K., Birn, R.M., Handwerker, D.A., Jones, T.B., and Bandettini, P.A. (2009). The impact of global signal regression on resting state correlations: are anti-correlated networks introduced? Neuroimage *44*, 893-905.

Nagai, Y., Critchley, H.D., Featherstone, E., trimble, M.R., and Dolan, R.J. (2004). Activity in ventromedial prefrontal cortex covaries with sympathetic skin conductance level: a physiological account of a "default mode" of brain function. Neuroimage *22*, 243-251.

Ochsner, K.N., Bunge, S.A., Gross, J.J., and Gabrieli, J.D. (2002). Rethinking feelings: an FMRI study of the cognitive regulation of emotion. J Cogn Neurosci *14*, 1215-1229.

Olson, H.C., Feldman, J.J., Streissguth, A.P., Sampson, P.D., and Bookstein, F.L. (1998). Neuropsychological deficits in adolescents with fetal alcohol syndrome: clinical findings. Alcoholism, clinical and experimental research *22*, 1998-2012.

Persson, J., Lustig, C., Nelson, J.K., and Reuter-Lorenz, P.A. (2007). Age differences in deactivation: a link to cognitive control? J Cogn Neurosci *19*, 1021-1032.

Platzman, K.A., Coles, C.D., Lynch, M.E., Bard, K.A., and Brown, J.V. (2001). Assessment of the caregiving environment and infant functioning in polydrug families: use of a structured clinical interview. Infant Ment Health J *22*, 351-373.

Pomarol-Clotet, E., Salvador, R., Sarro, S., Gomar, J., Vila, F., Martinez, A., Guerrero, A., Ortiz-Gil, J., Sans-Sansa, B., Capdevila, A*., et al.* (2008). Failure to deactivate in the prefrontal cortex in schizophrenia: dysfunction of the default mode network? Psychol Med *38*, 1185-1193.

Raichle, M.E., MacLeod, A.M., Snyder, A.Z., Powers, W.J., Gusnard, D.A., and Shulman, G.L. (2001). A default mode of brain function. Proc Natl Acad Sci U S A *98*, 676-682.

Raichle, M.E., and Mintun, M.A. (2006). Brain work and brain imaging. Annu Rev Neurosci *29*, 449-476.

Raichle, M.E., and Snyder, A.Z. (2007). A default mode of brain function: a brief history of an evolving idea. Neuroimage *37*, 1083-1090.

Rao, H., Wang, J., Giannetta, J., Korczykowski, M., Shera, D., Avants, B.B., Gee, J., Detre, J.A., and Hurt, H. (2007). Altered resting cerebral blood flow in adolescents with in utero cocaine exposure revealed by perfusion functional MRI. Pediatrics *120*, 1245-1254.

Riley, E.P., Mattson, S.N., Sowell, E.R., Jernigan, T.L., Sobel, D.F., and Jones, K.L. (1995). Abnormalities of the corpus callosum in children prenatally exposed to alcohol. Alcoholism, clinical and experimental research *19*, 1198-1202.

Riley, E.P., and McGee, C.L. (2005). Fetal alcohol spectrum disorders: an overview with emphasis on changes in brain and behavior. Experimental biology and medicine (Maywood, N.J *230*, 357-365.

Roebuck-Spencer, T.M., Mattson, S.N., Marion, S.D., Brown, W.S., and Riley, E.P. (2004). Bimanual coordination in alcohol-exposed children: role of the corpus callosum. J Int Neuropsychol Soc *10*, 536-548.

Roebuck, T.M., Mattson, S.N., and Riley, E.P. (1998). A review of the neuroanatomical findings in children with fetal alcohol syndrome or prenatal exposure to alcohol. Alcoholism, clinical and experimental research *22*, 339-344.

Romano, T.G., and Harvey, J.A. (1998). Prenatal cocaine exposure: long-term deficits in learning and motor performance. Ann N Y Acad Sci *846*, 89-108.

Rombouts, S.A., Barkhof, F., Goekoop, R., Stam, C.J., and Scheltens, P. (2005). Altered resting state networks in mild cognitive impairment and mild Alzheimer's disease: an fMRI study. Hum Brain Mapp *26*, 231-239.

Santhanam, P., Li, Z., Hu, X., Lynch, M.E., and Coles, C.D. (2009). Effects of Prenatal Alcohol Exposure on Brain Activation During an Arithmetic Task: An fMRI Study. Alcoholism, clinical and experimental research.

Shaywitz, S.E., Caparulo, B.K., and Hodgson, E.S. (1981). Developmental language disability as a consequence of prenatal exposure to ethanol. Pediatrics *68*, 850-855.

Sheinkopf, S.J., Lester, B.M., Sanes, J.N., Eliassen, J.C., Hutchison, E.R., Seifer, R., Lagasse, L.L., Durston, S., and Casey, B.J. (2009). Functional MRI and response inhibition in children exposed to cocaine in utero. Preliminary findings. Dev Neurosci *31*, 159-166.

Shulman, G.L., Fiez, J.A., Corbetta, M., Buckner, R.L., Miezin, F.M., Raichle, M.E., and Petersen, S.E. (1997). Common blood flow changes across visual tasks: II. Decreases in cerebral cortex. J Cogn Neurosci *9*, 648-663.

Simmons, R.W., Wass, T., Thomas, J.D., and Riley, E.P. (2002). Fractionated simple and choice reaction time in children with prenatal exposure to alcohol. Alcoholism, clinical and experimental research *26*, 1412-1419.

Singh, K.D., and Fawcett, I.P. (2008). Transient and linearly graded deactivation of the human default-mode network by a visual detection task. Neuroimage *41*, 100-112.

Smith, I.E., Coles, C.D., Lancaster, J., Fernhoff, P.M., and Falek, A. (1986). The effect of volume and duration of prenatal ethanol exposure on neonatal physical and behavioral development. Neurobehav Toxicol Teratol *8*, 375-381.

Smith, K.J., and Eckardt, M.J. (1991). The effects of prenatal alcohol on the central nervous system. Recent Dev Alcohol *9*, 151-164.

Smith, S.M., Jenkinson, M., Johansen-Berg, H., Rueckert, D., Nichols, T.E., Mackay, C.E., Watkins, K.E., Ciccarelli, O., Cader, M.Z., Matthews, P.M., and Behrens, T.E. (2006). Tract-based spatial statistics: voxelwise analysis of multi-subject diffusion data. Neuroimage *31*, 1487-1505.

Smith, S.M., and Nichols, T.E. (2009). Threshold-free cluster enhancement: addressing problems of smoothing, threshold dependence and localisation in cluster inference. Neuroimage *44*, 83-98.

Sonuga-Barke, E.J., and Castellanos, F.X. (2007). Spontaneous attentional fluctuations in impaired states and pathological conditions: a neurobiological hypothesis. Neurosci Biobehav Rev *31*, 977-986.

Sowell, E.R., Lu, L.H., O'Hare, E.D., McCourt, S.T., Mattson, S.N., O'Connor, M.J., and Bookheimer, S.Y. (2007). Functional magnetic resonance imaging of verbal learning in children with heavy prenatal alcohol exposure. Neuroreport *18*, 635-639.

www.manaraa.com

Sowell, E.R., Mattson, S.N., Thompson, P.M., Jernigan, T.L., Riley, E.P., and Toga, A.W. (2001). Mapping callosal morphology and cognitive correlates: effects of heavy prenatal alcohol exposure. Neurology *57*, 235-244.

Spadoni, A.D., McGee, C.L., Fryer, S.L., and Riley, E.P. (2007). Neuroimaging and fetal alcohol spectrum disorders. Neuroscience and biobehavioral reviews *31*, 239-245.

Streissguth, A.P., Barr, H.M., Sampson, P.D., Parrish-Johnson, J.C., Kirchner, G.L., and Martin, D.C. (1986). Attention, distraction and reaction time at age 7 years and prenatal alcohol exposure. Neurobehav Toxicol Teratol *8*, 717-725.

Talairach, J., and Tournoux, P. (1988a). Co-planar stereotaxic atlas of the human brain (New York: Thieme Medical Publishers, Inc.).

Talairach, J., and Tournoux, P. (1988b). Co-planar stereotaxic atlas of the human brain. New York: Thieme Medical Publishers, Inc.

Uddin, L.Q., Kelly, A.M., Biswal, B.B., Margulies, D.S., Shehzad, Z., Shaw, D., Ghaffari, M., Rotrosen, J., Adler, L.A., Castellanos, F.X., and Milham, M.P. (2008). Network homogeneity reveals decreased integrity of default-mode network in ADHD. J Neurosci Methods *169*, 249-254.

Uddin, L.Q., Kelly, A.M., Biswal, B.B., Xavier Castellanos, F., and Milham, M.P. (2009). Functional connectivity of default mode network components: correlation, anticorrelation, and causality. Hum Brain Mapp *30*, 625-637.

Urry, H.L., van Reekum, C.M., Johnstone, T., Kalin, N.H., Thurow, M.E., Schaefer, H.S., Jackson, C.A., Frye, C.J., Greischar, L.L., Alexander, A.L., and Davidson, R.J. (2006). Amygdala and ventromedial prefrontal cortex are inversely coupled during regulation of negative affect and predict the diurnal pattern of cortisol secretion among older adults. J Neurosci *26*, 4415-4425.

van den Heuvel, M., Mandl, R., Luigjes, J., and Hulshoff Pol, H. (2008). Microstructural organization of the cingulum tract and the level of default mode functional connectivity. J Neurosci *28*, 10844-10851.

Wahl, M., and Ziemann, U. (2008). The human motor corpus callosum. Rev Neurosci *19*, 451-466.

Wang, F., Kalmar, J.H., He, Y., Jackowski, M., Chepenik, L.G., Edmiston, E.E., Tie, K., Gong, G., Shah, M.P., Jones, M.*, et al.* (2009). Functional and structural connectivity between the perigenual anterior cingulate and amygdala in bipolar disorder. Biol Psychiatry *66*, 516-521.

Wang, S., Zhang, Z., Lu, G., and Luo, L. (2007). Localization of brain activity by temporal anti-correlation with the posterior

cingulate cortex. Conf Proc IEEE Eng Med Biol Soc. *2007*, 5227-5230.

Weissenbacher, A., Kasess, C., Gerstl, F., Lanzenberger, R., Moser, E., and Windischberger, C. (2009). Correlations and anticorrelations in resting-state

functional connectivity MRI: a quantitative comparison of preprocessing strategies. Neuroimage *47*, 1408-1416.

Weissman, D.H., Roberts, K.C., Visscher, K.M., and Woldorff, M.G. (2006). The neural bases of momentary lapses in attention. Nat Neurosci *9*, 971-978.

Wilson, S.M., Molnar-Szakacs, I., and Iacoboni, M. (2008). Beyond superior temporal cortex: intersubject correlations in narrative speech comprehension. Cereb Cortex *18*, 230-242.

Wozniak, J.R., Muetzel, R.L., Mueller, B.A., McGee, C.L., Freerks, M.A., Ward, E.E., Nelson, M.L., Chang, P.N., and Lim, K.O. (2009). Microstructural Corpus Callosum Anomalies in Children With Prenatal Alcohol Exposure: An Extension of Previous Diffusion Tensor Imaging Findings. Alcoholism, clinical and experimental research.

Yasmin, H., Aoki, S., Abe, O., Nakata, Y., Hayashi, N., Masutani, Y., Goto, M., and Ohtomo, K. (2009). Tract-specific analysis of white matter pathways in healthy subjects: a pilot study using diffusion tensor MRI. Neuroradiology.

Yassa, M.A., and Stark, C.E. (2009). A quantitative evaluation of cross-participant registration techniques for MRI studies of the medial temporal lobe. Neuroimage *44*, 319-327.

Zhang, L.J., Yang, G., Yin, J., Liu, Y., and Qi, J. (2007). Abnormal default-mode network activation in cirrhotic patients: a functional magnetic resonance imaging study. Acta Radiol *48*, 781-787.

Zhou, Y., Liang, M., Tian, L., Wang, K., Hao, Y., Liu, H., Liu, Z., and Jiang, T. (2007). Functional disintegration in paranoid schizophrenia using resting-state fMRI. Schizophr Res *97*, 194-205.

# CHAPTER 7

## Altered Default Mode Network Activity in Adolescents with

## Prenatal Cocaine Exposure

### 7.1 Background

7.1.1   Prenatal Cocaine Exposure and Arousal Dysregulation

Current literature on the developmental effects of prenatal cocaine exposure (PCE) indicates that while cognitive deficits are identifiable, the most common and potentially detrimental outcome may be arousal dysregulation (Mayes, 2002; Mayes et al., 1998a). Infants and children with PCE have been observed to show increased baseline arousal (Bard et al., 2000; Bendersky and Lewis, 1998a; Coles et al., 1999b; Dipietro et al., 1995; Karmel and Gardner, 1996) with persistence of such effects into adolescence and adulthood also reported (Bada et al., 2007; Dennis et al., 2006; Kable et al., 2008; Mayes et al., 1998a). Arousal dysregulation, described as being more easily distracted by salient but task-irrelevant stimuli, can also be noted in animal models of PCE (Garavan et al., 2000; Romano and Harvey, 1998); such studies are more capable of controlling for confounding factors often encountered in human PCE populations (e.g., prenatal care, dosage and timing of PCE).

Arousal regulation reflects the ability to adjust and allocate mental resources for distinct yet interactive streams of information processing (Damasio, 1995). This process regulates ongoing cognition and behavior through an excitatory/inhibitory balancing mechanism, and

the impact of PCE on such regulation could generate a general neuronal deficit, as opposed to specific cognitive deficits. With functional MRI, our previous study (Li et al., 2009) showed that PCE adolescents could not efficiently suppress amygdala activation when challenged by emotional arousal, which in turn affected prefrontal working memory activation. The present study further investigates the PCE impact on arousal regulation by examining the recently characterized default mode network (DMN).

## 7.1.2   Default Mode Network

A consistent "default mode" network of regions that are more active during resting periods than during cognitive demand has become the focus of many clinical neuroimaging studies (Greicius et al., 2003a; Gusnard and Raichle, 2001). The regions typically involved are medial prefrontal and posterior cinglulate cortices (Greicius et al., 2003a), and are identified as deactivated during increased task-oriented cognition and/or very low frequency synchronized fluctuations in the resting state (Gusnard and Raichle, 2001; Raichle et al., 2001). Though the physiological significance of default mode activity still remains to be fully understood, it is generally believed to reflect the intrinsic/spontaneous mental operations that are suspended during goal-oriented behaviors (Gusnard and Raichle, 2001; Raichle et al., 2001; Raichle and Snyder, 2007). DMN activity represents a lack of task focus (Mason et al., 2007), replaced by both stimulus-oriented and stimulus-independent thoughts (Gilbert et al., 2007; Gusnard et al., 2001; Gusnard and Raichle, 2001; Kelley et al., 2002). Given that PCE alters arousal regulation ability, which is closely associated with internal versus external attentional orientation (Nagai et al., 2004), it is hypothesized that DMN activity is altered by PCE.

### 7.1.3 Aims

DMN activity was assessed in adolescents with PCE and healthy controls by examining task-related deactivation and resting state functional connectivity. The functional task used was a working memory task containing neutral and negatively emotive distracters, to assess the effect of emotional regulation on DMN deactivation during task. Additionally, baseline functional connectivity was measured using a seeding-correlation approach between regions previously reported to comprise the network core. Given known increased arousal in individuals with PCE, it was expected that the PCE group would have increased DMN activity as compared to healthy controls, reflected in less task-related deactivation and higher baseline functional connectivity.

## 7.2 Methods

### 7.2.1 Participants

Participants were adolescents, aged 12-18, recruited from cohorts identified originally as part of two longitudinal studies of PCE on infant development (Brown et al., 1998b; Coles et al., 1992). Both cohorts were drawn from a low income, predominantly African-American population that was delivered at an urban hospital during 1987-1994. The PCE and control participants in the present study respectively comprised 33 and 23 participants with the adolescent and maternal characteristics shown in Tables 6.1 and 6.2.

Prenatal cocaine exposure was determined by maternal self-report and/or positive urine screen at recruitment post-partum and has been extensively described previously (Brown et al., 1998b; Coles et al., 1992). Before the imaging session, urine and blood specimens of the adolescents were tested to identify metabolites of 7 drugs (amphetamines, barbiturates, benzodiazepines, marijuana, cocaine, opiates, and phencyclidine) and problematic alcohol use. The majority was negative and no group differences were noted. Participating families were reconsented for the imaging study according to a protocol approved by Emory University's Institutional Review Board. Adolescents provided written assent and adults, including both teens and caregivers, informed consent, to participate.

### 7.2.2   Experimental Design

We used a verbal working memory task with two memory loads in the activation fMRI so that the signal difference between the memory loads could be used to identify default mode deactivations. The memory items were lists of letter pairs. In the low memory load condition, adolescents were instructed to press a button on seeing the letter pair "RR" (0-back task). In the high memory load condition, they were to press the button whenever the displaying letter pair exactly matched the last one displayed (1-back task). To introduce emotional distraction, neutral (arousal score $3.2\pm0.8$) and negative ($5.7\pm0.8$) pictures selected from the International Affective Picture System (Lang et al., 1997) were presented between the letter pairs. The fMRI paradigm was a factorial block-design with 4 different types of blocks (factorial combination of low or high memory loads with neutral or negative distraction) that were pseudo-randomly distributed across two data acquisition scans. Each fMRI scan run contained 12 blocks, each consisting of 12 trials, during which participants were instructed

108

to focus only on the memory task while ignoring the distracting pictures. A schematic diagram of the experimental paradigm is shown previously (Chapter 6).

During the resting-state fMRI scanning, participants did not perform a specific cognitive task but were instructed to simply fixate on a cross shown in the center of the screen. To minimize potential carryover of cognitive activity associated with the memory task or the emotional distracters, resting-state data were always acquired first, prior to the activation fMRI scan.

### 7.2.3  Image Acquisition

On a 3T MRI scanner (Siemens Medical Solutions, Malvern, PA), the activation and resting-state scans both were performed using a T2*-weighted echo-planar imaging sequence with the following parameters. Activation scan: 120-volumes, matrix=64×64, 30 axial slices without gap, thickness=3 mm, TR/TE=3000 ms/30 ms, flip angle=90o, FOV=192×192 cm2. Resting scan: 210-volumes, matrix=64×64, 20 axial slices without gap, thickness=4 mm, TR/TE=2000 ms/30 ms, flip angle=90o, FOV=192×192 cm2. Corresponding high resolution (256×256) 3D T1-weighted anatomical images were also collected from each subject.

### 7.2.4  Image Analysis

AFNI software package (http://afni.nimh.nih.gov, 09/2009) was used for imaging data analysis. For the activation fMRI, each subject's data were preprocessed with slice timing correction, volume registration, signal percent change normalization, scan concatenation, and 5 mm FWHM spatial smoothing. A multiple regression analysis was performed thereafter using regressors representing the 4 experimental conditions (low vs. high memory

109

load × neutral vs. negative emotion) and with head motion parameters included as nuisance covariates. The experimental condition regressors were generated by convolving respective boxcar stimulation functions with a impulse response function [$y=tb \times exp(-t/c)$, b and c are constants] (Cohen, 1997a). To assess the deactivation in the DMN, the "high load – low load" regression coefficients difference was calculated voxel by voxel for each subject. After transformation into the Talairach space (Talairach and Tournoux, 1988a), this difference, which corresponds to deactivation, was compared between the PCE and control subjects using a voxel-wise linear mixed-effects modeling analysis (http://afni.nimh.nih.gov/sscc/gangc/lme.html, 09/2009).

Instead of a simple group t-test, we used the linear mixed-effects modeling because the effects of prenatal cocaine exposure in humans are often confounded by other factors that are difficult to match between the PCE and control groups. For example, besides cocaine, PCE subjects are usually poly-drug (commonly tobacco, alcohol and marijuana) exposed. The linear mixed-effects modeling analysis can statistically control the confounding effects, thus ensuring that the final results are more specifically associated with the cocaine exposure. In the present data analysis, we included 3 nuisance variables in the model (in addition to EXPOSURE, which was the independent/interested variable): (i) GENDER (males and females may have different default mode and emotional responses and they are not evenly distributed in the two groups), (ii) ALCOHOL (ounces of absolute alcohol used weekly during pregnancy), and (iii) MARIJUANA~TOBACCO (amount used during pregnancy in units of joints/cigarette per week). The MARIJUANA ~TOBACCO was a joint variable derived by principle component factor reduction because their uses were highly correlated (Pearson correlation, $p=0.04$) in our sample. These nuisance controlling factors were determined by our preliminary analysis (data not shown) that revealed confounding effect on voxels in the DMN. Other factors (e.g. race, other drug use, preterm birth) that are

110

known to be related to cocaine effects were controlled via experimental design (Brown et al., 1998b; Coles et al., 1992).

Based on the deactivations during the working memory task, we defined a seeding area in the posterior cingulate region for the subsequent resting-state fMRI data analysis. Specifically, the regression coefficients for the 4 experimental conditions were analyzed by a 2 (high vs. low memory load) × 2 (neutral vs. negative emotion) repeated measures ANOVA, and a posterior cingulate voxel cluster (centroid coordinate = 3.6, 54.9, 16.9 mm, volume=175 mm$^3$) that showed a highly significant ($p<10^{-8}$) negative memory main effect (decreased fMRI signal in the 1-back condition than 0-back) was selected. We used equal number of participants (23 PCE and 23 control with 10 PCE subjects randomly dropped) in this process so that the resultant seeding region would not be biased by deactivation of either group.

The resting-state data processing steps were similar to those used by Fox and colleagues for characterizing the intrinsic resting functional networks (Fox et al., 2005a). After preprocessing (slice timing correction, rigid body registration, 0.009 Hz < f < 0.08 Hz band-pass filtering, and 5 mm FWHM Gaussian smoothing), cross-correlation between the time courses of posterior cingulate seeding area and every brain voxel was calculated for each subject. Spurious contributions from the white matter and cerebrospinal fluid as well as the head motion parameters were removed in this cross-correlation analysis through multiple linear regression. Another variable often included in this regression as a nuisance effects is the global brain signal. However, Murphy and colleagues have recently demonstrated that using global signal regression can bias connectivity measures by introducing anti-correlations (Murphy et al., 2009). As it is unclear whether using global signal regression would significantly affect connectivity group differences, we performed the analysis with and

111

without removing the global signal regression. In order to combine/compare correlation results within/between groups, correlation coefficients for each subject were converted to z-scores and then transformed into the Talairach space. The same as in the activation data processing, a linear mixed-effect modeling analysis was applied to contrast the resultant correlation z-score maps between the PCE and control groups.

**7.3 Results**

7.3.1   Task Performance

The behavioral measures of the working memory task were described in detail in our previous report (Li et al., 2009). Briefly, the overall memory performance was decreased with higher memory load (as compared to low load) and negative emotional distraction (as compared to neutral). However, because the task paradigm was deliberately designed to minimize behavioral group difference (Li et al., 2009), there were no significant group differences in task performance related to cocaine exposure.

7.3.2   Resting-State Results

The results of group comparison of resting-state data are shown in representative mid-sagittal slices in Figure 7.1. Consistent with the reports of Murphy and colleagues, using global signal regression introduced more negative correlation in the results (which therefore reduced the positive correlation areas); however, significant positive correlations in the DMN could be observed regardless of whether the global signal regression was used. Though the group difference maps obtained with and without the use of global signal regression are not exactly the same, Figure 7.1 shows that the DMN positive correlation of the PCE group was

112

generally higher in both cases. By performing a "logical AND" between group difference

maps with and without global regression, the common areas that have a higher DMN

correlation in the PCE group were obtained. These areas, listed in Table 7.1, including

medial prefrontal cortex, parahippocampal and cingulate regions, as well as the inferior

parietal cortex, are all prominent nodes in DMN. In contrast, the group comparison identified

no brain region exhibiting a significantly higher DMN correlation in the control group.

**Table 7.1.** Brain regions with significant PCE > CON DMN signal correlation regardless global regression. Significant means $p<0.05$/voxel plus 18 mm$^3$ cluster, multiple comparison corrected $p<0.01$; PCE: prenatal cocaine exposure; CON: control; DMN: default mode network.

| Brain Regions | Volume (mm³) | Coordinates (mm) | | |
|---|---|---|---|---|
| | | X | Y | Z |
| Left medial frontal cortex (BA 9 / 10) | 545 | 11.9 | -52.9 | 19.3 |
| Left cingulate gyrus (BA 31) | 136 | 2.8 | 30.4 | 38.9 |
| Right posterior cingulate area (BA 23) | 130 | -2.2 | 55.3 | 15.6 |
| Right parahippocampal / posterior cingulate area (BA 30) | 69 | -11.3 | 41.0 | 4.2 |
| Left parahippocampal / amygdala area (BA 28) | 68 | 20.6 | 12.9 | -9.4 |
| Left precuneus / posterior cingulate area (BA 7 / 31) | 45 | 6.3 | 54.7 | 37.2 |
| Right inferior parietal cortex (BA 19 / 39) | 44 | -40.5 | 69.9 | 39.6 |
| Left parahippocampal / posterior cingulate area (BA 30) | 33 | 17.0 | 44.3 | 7.6 |
| Left inferior parietal / middle temporal cortex (BA 39) | 18 | 41.4 | 71.3 | 16.9 |

113

**Figure 7.1.** Group comparison of resting-state DMN signal correlation with global regression included (pink frame) and excluded (green frame) in the data analysis. The seeding region of the correlation analysis is marked by a purple arrow in the slices marked with an "S". All the other slices are to the left (up) and right (down) of the seeding region in steps of 2 mm. In the group correlation maps, positive (red/yellow) and negative (blue/azury) correlations are displayed at a threshold level of p<0.01/voxel plus 683 mm$^3$ cluster (multiple comparison corrected p<0.01); in the group difference maps, because the comparison only restricted in positive correlation regions, the displaying threshold changed to p<0.05/voxel plus 18 mm$^3$ cluster (multiple comparison corrected p<0.01). CON: control, PCE: prenatal cocaine exposure. Figure reproduced with permission from Z. Li.

### 7.3.3 Functional Task-Related Results

Group differences of default mode activity were also observed in the working memory fMRI data (Figure 7.2). Compared to the low memory load condition, both the PCE and control subjects exhibited a decreased BOLD signal in the DMN during the high memory load condition. However, the magnitude of these signal reductions was significantly higher in the controls; in other words, the signal of PCE subjects did not decrease as much as that of the controls. As shown in Table 7.2, this group difference was observed in a number of DMN areas including medial prefrontal cortex, posterior cingulate area and inferior parietal cortex.

To further examine the emotional arousal effect on DMN fMRI signal, we defined two regions of interest (ROIs) based on the group difference of the deactivation. They are one anterior (centroid coordinate = 4.1, -51.6, 23.3 mm, volume=442 mm3) and one posterior (centroid coordinate = 11.3, 48.6, 9.6 mm, volume=752 mm3) cingulate clusters that showed a significant group difference on fMRI deactivation (Figure 7.2, the red regions). Examining the 4 condition regression coefficients of these two ROIs, a 2 (PCE vs. control group) × 2 (negative vs. neutral emotion) × 2 (1-back vs. 0-back memory load) × 2 (medial prefrontal vs. posterior cingulate location) ANOVA (with gender and multidrug exposure as nuisance factors) showed a significant memory × exposure (p=0.03) and emotion × exposure (p=0.01) effect. With the signal regression coefficients shown in Figure 7.2 (the red frame), the memory × exposure effect was evident as these ROIs were defined on the group difference map of default mode deactivation. This ROI data simply replicated the voxel-wise group comparison observation that PCE adolescents could not decrease the signal as much as the controls during the high memory load task. However, the emotion × exposure effect in these two ROIs was a new observation. Compared to the neutral distracters, the negative

115

distracters generally increased the DMN signal level and this increase was greater in the

PCE group as compared to controls.

**Table 7.2.** Brain regions with significant CON > PCE deactivation in the working memory task. Significant means a $p<0.05$/voxel plus 18 mm$^3$ cluster, multiple comparison corrected $p<0.01$; PCE: prenatal cocaine exposure; CON: control.

| Brain Regions | Volume (mm³) | Coordinates (mm) | | |
|---|---|---|---|---|
| | | X | Y | Z |
| Left posterior cingulate area (BA 29) | 694 | 11.3 | 48.5 | 9.6 |
| Left inferior parietal / middle temporal cortex (BA 39) | 500 | 39.5 | 62.0 | 18.2 |
| Left cingulate gyrus (BA 31) | 477 | 6.2 | 41.9 | 38.8 |
| Left medial frontal cortex (BA 9) | 406 | 4.2 | -51.6 | 23.3 |
| Right posterior cingulate area (BA 29) | 30 | -4.3 | 42.1 | 8.3 |
| Right posterior cingulate area (BA 30) | 27 | -0.6 | 43.6 | 23.1 |
| Right anterior cingulate area (BA 24) | 24 | -5.3 | -28.9 | -0.3 |
| Left posterior cingulate area (BA 30 / 31) | 24 | 9.1 | 50.4 | 21.7 |
| Left middle frontal gyrus (BA 9) | 19 | 20.1 | -36.3 | 32.5 |

116
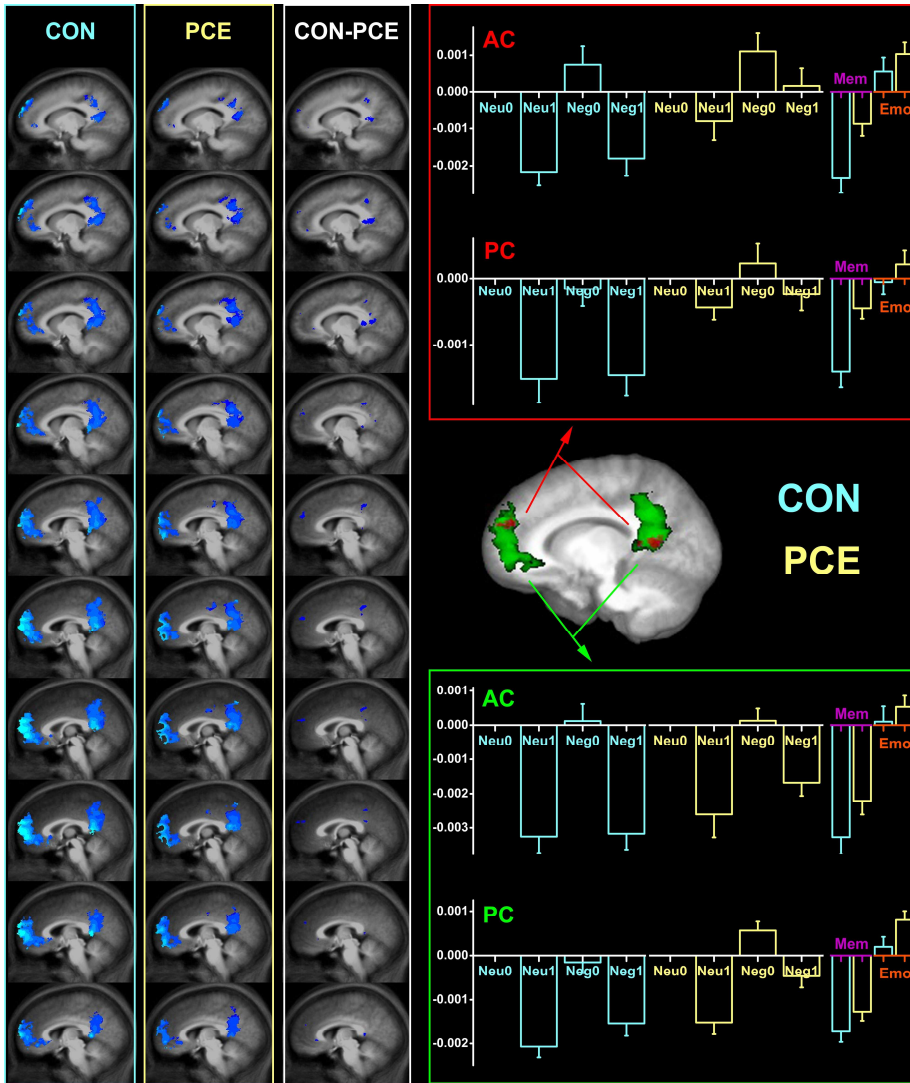
**Figure 7.2.** Voxel-wise (left) and ROI level (right) group comparisons of task-state DMN activity. The voxel-wise comparisons are shown in successive sagittal slices that have exactly the same location and threshold as those in Fig.2. The shallow to deep signal decreases are coded by the blue to cyan color gradient. The group-difference (red) and group-common (green) ROIs are shown on the right with the corresponding ROI regression coefficients plotted above (red frame) and below (green frame). These regression coefficient plots used the "Neutral, 0-back" condition as the baseline. For easy visualization purpose, the group comparisons of the memory and emotion effects are put at the right end of these plots. CON: control; PCE: prenatal cocaine exposure; AC: anterior cingulate; PC: posterior cingulate; Neu: neutral; Neg: negative; 0: 0-back; 1: 1-back; Mem: memory effect (Neu1+Neg1-Neu0-Neg0); Emo: emotion effect (Neg0+Neg1-Neu0-Neu1). Figure reproduced with permission from Z. Li.

These memory and emotion effects were based on ROIs defined by group difference in deactivations. To examine whether these results could represent the group differences in a larger extent of the DMN, we defined two alternative ROIs also in the anterior (centroid coordinate = 0.9, -49.8, 10.8 mm, volume=7356 mm$^3$) and posterior (centroid coordinate = 2.9, 49.9, 23.7 mm, volume=9082 mm3) cingulate cortices (Figure 7.2, the green regions). Instead of group difference, these two new ROIs were defined based on the common deactivation map of both groups (PCE and control deactivation maps averaged together). Similar to the seeding area localization in the resting data analysis, this across-group average included equal numbers of PCE and control subjects (23 vs. 23) to avoid potential group bias. The regression coefficients of these common deactivation ROIs are presented in Figure 7.2 (the green frame) and they were analyzed by the same emotion × memory × group × location ANOVA mentioned above. The results of these group-common ROIs are generally the same as those of the group-difference ROIs. Specifically, the PCE group exhibited reduced DMN deactivation magnitude and increased DMN response to emotional arousal. However, while the group × emotion effect was still statistically significant (p=0.02), the group × memory effect, because many more "group-common" voxels were involved, did not reach statistical significance (p=0.4).

## 7.4 Discussion

7.4.1 <u>Summary</u>

The present study examined the effect of PCE on DMN functioning, as it relates to arousal dysfunction. The PCE group had less DMN deactivation during a working memory task as compared to controls, and even less deactivation in the presence of emotional distracters.

118

Given the propensity of the PCE group for distractibility, particularly with emotional arousal, results suggest that inefficient DMN deactivation represents an inability in those with PCE to down-regulate task-unrelated stimuli. Additionally, resting state functional connectivity in the network was higher in PCE group than in controls, implying a higher baseline arousal level in exposed populations.

### 7.4.2    Context in Current Literature

Altered DMN activity been associated with several clinical disorders, including schizophrenia, epilepsy, chronic pain, anxiety disorder, Alzheimer's disease, and attention deficit hyperactivity disorder (ADHD) (Baliki et al., 2008; Garrity et al., 2007; Laufs et al., 2007; Uddin et al., 2008; Wang et al., 2007; Zhang et al., 2007; Zhou et al., 2007). With the observation of increased default mode activity in the adolescents prenatally exposed to cocaine, namely increased functional connectivity during rest and less suppressed activation during task, the present study extends the scope of reported alterations in default mode functionality to the domain of prenatal influences of drug exposure on cognition. As intrinsic brain activity reflects basic neuronal organization and comprises a high percentage of total brain energy used (Fox and Raichle, 2007; Raichle and Snyder, 2007), the significance of DMN activity in PCE is of interest as much as PCE-induced cognitive deficits.

The default mode function has often been interpreted as representing either internal self-reflective thoughts (Gusnard et al., 2001; Kelley et al., 2002) or external environment monitoring (Hahn et al., 2007; Shulman et al., 1997). The increased default mode activity observed in our PCE adolescents could represent contributions from both of these aspects of non-task oriented thought. With respect to the external monitoring, PCE subjects are reported to be more sensitive to salient stimuli in the environment (Garavan et al., 2000;

119

Romano and Harvey, 1998), and their sleep was found to be more easily disturbed (Platzman et al., 2001). Related to the internal thoughts, PCE children were found to have a higher daydreaming score, which was deemed problematic behavior by their teachers (Delaney-Black et al., 1998).

Recent studies on the default mode function speculate that the intrinsic brain activity of DMN may represent a "balance" between the excitatory and inhibitory neural responses (Raichle and Mintun, 2006; Raichle and Snyder, 2007); namely, a neural mechanism that controls brain responsiveness to various inputs. Our previous report showed that PCE alters the excitatory and inhibitory "balance" between the emotion and working memory systems (Li et al., 2009). Here, a similar PCE effect is demonstrated from the view point of default mode function. A notable common outcome of these two studies is that PCE adolescents are more vulnerable to task irrelevant emotional arousal challenge (as indicated by their stronger emotion responses in both the amygdala and DMN). Group differences in balancing different streams of information processing suggest that prenatal cocaine exposure may affect the brain in a fundamental level that could underlie a variety of cognitive functions.

The present findings based on blood oxygen level dependent (BOLD) signals are also consistent with previous neuroimaging observations based on cerebral blood flow (CBF) measurements (Rao et al., 2007). Rao and colleagues recently reported that PCE could increase the relative cerebral blood flow in the cingulate, insular and parietal cortices as well as in the amygdala area. These brain regions are largely the important nodes in the DMN, and higher proportion of blood supply to these regions could underlie the increased default mode activity in the PCEs. Rao et al. also observed that PCE was associated with a higher gray matter volume in the amygdala area. This result is also in accordance with both our

120

present and previous (Li et al., 2009) findings that showed an increased emotional arousal level in the PCE subjects.

### 7.4.3    Future Considerations

The interaction between prenatal cocaine exposure and neural development is a complicated process. Specifically, the interactions between emotional regulation and DMN functioning, which are likely strongly linked based on previous behavioral studies and the present study, could use more detailed examination. For example, recent findings indicate that the DMN functional connectivity reflects its underlying structural connectivity (Greicius et al., 2009; van den Heuvel et al., 2008); thus the presence or absence of alterations in DMN structure in individuals with PCE could further elucidate the neurobiological mechanisms behind behavioral outcomes.  Future studies that combine multi-modal neuroimaging approaches like functional, structural, and diffusion tensor imaging could lead us to a greater understanding of the teratogenic effects of PCE and of ways in which the brain responds to such challenges.

## 7.5 References

Bada HS, Das A, Bauer CR, Shankaran S, Lester B, LaGasse L, Hammond J, Wright LL, Higgins R. 2007. Impact of prenatal cocaine exposure on child behavior problems through school age. Pediatrics 119:e348-e359.

Baliki MN, Geha PY, Apkarian AV, Chialvo DR. 2008. Beyond feeling: chronic pain hurts the brain, disrupting the default-mode network dynamics. J Neurosci 28(6):1398-403.

Bard KA, Coles CD, Platzman KA, Lynch ME. 2000. The effects of prenatal drug exposure, term status, and caregiving on arousal and arousal modulation in 8-week-old infants. Dev Psychobiol 36:194-212.

Bendersky M, Lewis M. 1998. Arousal modulation in cocaine-exposed infants. Dev Psychol 34(3):555-564.

Brown JV, Bakeman R, Coles CD, Sexson WR, Demi AS. 1998. Maternal drug use during pregnancy: are preterm and full-term infants affected differently? Dev Psychol 34(3):540-554.

Cohen MS. 1997. Parametric analysis of fMRI data using linear systems methods. Neuroimage 6:93-103.

Coles CD, Bard KA, Platzman KA, Lynch ME. 1999. Attentional response at eight weeks in prenatally drug-exposed and preterm infants. Neurotoxicol Teratol 21(5):527-537.

Coles CD, Platzman KA, Smith I, James ME, Falek A. 1992. Effects of cocaine and alcohol use in pregnancy on neonatal growth and neurobehavioral status. Neurotoxicol Teratol 14:23-33.

Damasio AR. 1995. On some functions of the human prefrontal cortex. Ann N Y Acad Sci 769(1):241-252.

Delaney-Black V, Covington C, Templin T, Ager J, Martier S, Sokol R. 1998. Prenatal cocaine exposure and child behavior. Pediatrics 102(4):945-950.

Dennis T, Bendersky M, Ramsay D, Lewis M. 2006. Reactivity and regulation in children prenatally exposed to cocaine. Dev Psychobiol 42(4):688-697.

Dipietro JA, Suess PE, Wheeler JS, Smouse PH, Newlin DB. 1995. Reactivity and regulation in cocaine-exposed neonates. Infant Behav Dev 18:407-414.

Fox MD, Raichle ME. 2007. Spontaneous fluctuations in brain activity observed with functional magnetic resonance imaging. Nat Rev Neurosci 8:700-711.

Fox MD, Snyder AZ, Vincent JL, corbetta M, Essen DCV, Raichle ME. 2005. The human brain is intrinsically organized into dynamic, anticorrelated functional networks. Proc Natl Acad Sci U S A 102(27):9673-9678.

Garavan H, Morgan RE, Mactutus CF, Levitsky DA, Booze RM. 2000. Prenatal cocaine exposure impairs selective attention: evidence from serial reversal and extradimentional shift tasks. Behav Neurosci 114(4):725-738.

Garrity AG, Pearlson GD, McKiernan K, Lloyd D, Kiehl KA, Calhoun VD. 2007. Aberrant "default mode" functional connectivity in schizophrenia. Am J Psychiatry 164(3):450-7.

Gilbert SJ, Dumontheil I, Simons JS, Frith CD, Burgess PW. 2007. Comment on "wandering minds: the default network and stimulus-independent thought". Science 317:43b.

Greicius MD, Krasnow B, Reiss AL, Memon V. 2003. Functional connectivity in the resting brain: a network analysis of the default mode hypothesis. Proc Natl Acad Sci U S A 100(1):253-258.

122

Greicius MD, Supekar K, Menon V, Dougherty RF. 2009. Resting-state functional connectivity reflects structural connectivity in the default mode network. Cereb Cortex 19(1):72-8.

Gusnard DA, Akbudak E, Shulman GL, Raichle ME. 2001. Medial prefrontal cortex and self-referential mental activity: relation to a default mode of brain function. Proc Natl Acad Sci U S A 98(7):4259-4264.

Gusnard DA, Raichle ME. 2001. Searching for a baseline: functional imaging and the resting human brain. Nat Rev Neurosci 2:685-694.

Hahn B, Ross TJ, Stein EA. 2007. Cingulate activation increases dynamically with response speed under stimulus unpredictability. Cereb Cortex 17:1664-1671.

Kable JA, Coles CD, Lynch ME, Platzman K. 2008. Physiological responses to social and cognitive challenges in 8-year-olds with a history of prenatal cocaine exposure. Dev Psychobiol 50(3):251-265.

Karmel BZ, Gardner JM. 1996. Prenatal cocaine exposure effects on arousal-modulated attention during the neonatal period. Dev Psychobiol 29(5):463-480.

Kelley WM, Macrae CN, Wyland CL, Caglar S, Inati S, Heatherton TF. 2002. Finding the self? An event-related fMRI study. J Cogn Neurosci 14(5):785-794.

Lang PJ, Bradley MM, Cuthbert BN. 1997. International affective picture system: technical manual and affective ratings. Gainesville, FL: NIMH Center for the Study of Emotion and Attention.

Laufs H, Hamandi K, Salek-Haddadi A, Kleinschmidt AK, Duncan JS, Lemieux L. 2007. Temporal lobe interictal epileptic discharges affect cerebral activity in "default mode" brain regions. Hum Brain Mapp 28(10):1023-32.

Li Z, Coles CD, Lynch ME, Hamann S, Peltier S, LaConte S, Hu X. 2009. Prenatal cocaine exposure alters emotional arousal regulation and its effects on working memory. Neurotoxicol Teratol In press.

Mason MF, Norton MI, Horn JDV, Wegner DM, Grafton ST, Macrae CN. 2007. Wandering minds: the default network and stimulus-independent thought. Science 315:393-395.

Mayes LC. 2002. A behavioral teratogenic model of the impact of prenatal cocaine exposure on arousal regulatory systems. Neurotoxicol Teratol 24:385-395.

Mayes LC, Grillon C, Granger R, Schottenfeld R. 1998. Regulation of arousal and attention in preschool children exposed to cocaine prenatally. Ann N Y Acad Sci 846:126-143.

Murphy K, Birn RM, Handwerker DA, Jones TB, Bandettini PA. 2009. The impact of global signal regression on resting state correlations: are anti-correlated networks introduced? Neuroimage 44(3):893-905.

Nagai Y, Critchley HD, Featherstone E, trimble MR, Dolan RJ. 2004. Activity in ventromedial prefrontal cortex covaries with sympathetic skin conductance level: a physiological account of a "default mode" of brain function. Neuroimage 22:243-251.

Platzman KA, Coles CD, Lynch ME, Bard KA, Brown JV. 2001. Assessment of the caregiving environment and infant functioning in polydrug families: use of a structured clinical interview. Infant Ment Health J 22(3):351-373.

Raichle ME, MacLeod AM, Snyder AZ, Powers WJ, Gusnard DA, Shulman GL. 2001. A default mode of brain function. Proc Natl Acad Sci U S A 98(2):676-682.

Raichle ME, Mintun MA. 2006. Brain work and brain imaging. Annu Rev Neurosci 29:449-476.

Raichle ME, Snyder AZ. 2007. A default mode of brain function: a brief history of an evolving idea. Neuroimage 37:1083-1090.

Rao H, Wang J, Giannetta J, Korczykowski M, Shera D, Avants BB, Gee J, Detre JA, Hurt H. 2007. Altered resting cerebral blood flow in adolescents with in utero cocaine exposure revealed by perfusion functional MRI. Pediatrics 120(5):1245-1254.

Romano TG, Harvey JA. 1998. Prenatal cocaine exposure: long-term deficits in learning and motor performance. Ann N Y Acad Sci 846:89-108.

Shulman GL, Fiez JA, Corbetta M, Buckner RL, Miezin FM, Raichle ME, Petersen SE. 1997. Common blood flow changes across visual tasks: II. Decreases in cerebral cortex. J Cogn Neurosci 9(5):648-663.

Talairach J, Tournoux P. 1988. Co-planar stereotaxic atlas of the human brain. Rayport M, translator. New York: Thieme Medical Publishers, Inc.

Uddin LQ, Kelly AM, Biswal BB, Margulies DS, Shehzad Z, Shaw D, Ghaffari M, Rotrosen J, Adler LA, Castellanos FX and others. 2008. Network homogeneity reveals decreased integrity of default-mode network in ADHD. J Neurosci Methods 169(1):249-54.

van den Heuvel M, Mandl R, Luigjes J, Hulshoff Pol H. 2008. Microstructural organization of the cingulum tract and the level of default mode functional connectivity. J Neurosci 28(43):10844-51.

Wang S, Zhang Z, Lu G, Luo L. 2007. Localization of brain activity by temporal anti-correlation with the posterior

cingulate cortex. Conf Proc IEEE Eng Med Biol Soc. 2007:5227-30.

Zhang LJ, Yang G, Yin J, Liu Y, Qi J. 2007. Abnormal default-mode network activation in cirrhotic patients: a functional magnetic resonance imaging study. Acta Radiol 48(7):781-7.

Zhou Y, Liang M, Tian L, Wang K, Hao Y, Liu H, Liu Z, Jiang T. 2007. Functional disintegration in paranoid schizophrenia using resting-state fMRI. Schizophr Res 97(1-3):194-205.

124

## CHAPTER 8

## Part 2: Conclusions and Significance

Since the cocaine-abuse epidemic of the 1980s, prenatal cocaine exposure has been a major public health concern. In the time shortly after the epidemic, there was great concern that so-called "crack babies" would have severe and irreversible cognitive impairments. However, behavioral and neuroimaging evidence shows relatively little cognitive deficit, but rather a general arousal dysfunction that affects behavior in a global manner.

As the most documented behavioral problems in children with PCE are related to arousal and emotional regulation, the present thesis examined neuronal functioning in areas specifically related to such regulation. Two prominent networks involved in arousal and emotional regulation are the prefrontal-amygdala network and default mode network. Our results show significantly higher activity in the DMN, characteristic of increased baseline arousal, and a disconnect between prefrontal and amygdala areas, a deficit known to lead to problems of executive functioning due to an inability to down-regulate emotional arousal. Our study of the neurological basis of PCE additionally benefits from comparative study with the slew of other clinical disorders that manifest as socioemotional dysfunction.

There are a number of strengths to the present study design that allow for a more comprehensive understanding of the spectrum of clinical disorders resulting from prenatal cocaine exposure. As multi-drug effects are an unavoidable confound in PCE studies in humans, documentation of all types of maternal drug abuse enabled us to control for these nuisance variables. Additionally, in the study of prefrontal-amygdala interactions, a

125

combination of structural and functional disconnection was found, supporting the growing opinion in the neuroimaging field that structure and function are closely linked and are best studied together.

The overall goal of this part of the thesis was to apply emerging neuroimaging methods to the study of neuronal effects of PCE on adolescence-related development. Social and emotional arousal dysregulation is particularly noted at the adolescent age in this population, and is correlated with lower quality of life in adulthood. Though the process by which PCE causes brain damage is complex, the current findings contribute significantly to elucidating the neurobiological basis of the effect of PCE. Such knowledge can in turn be applied to awareness and interventional efforts.